ELUCIDATING THE INTERACTION OF *BORRELIA BURGDORFERI* OSPC WITH

PHAGOCYTES IN THE ESTABLISHMENT OF LYME BORRELIOSIS

Sebastian Eduardo Carrasco

Accepted by the Graduate Faculty, of Indiana University, in partial
fulfillment of the requirements for the degree of Doctor of Philosophy.

_____

X. Frank Yang, Ph.D. - Chair

_____

Janice S. Blum, Ph.D.

Doctoral Committee

_____

C. Henrique Serezani, Ph.D.

March 20, 2015

_____

Raymond M. Johnson, M.D., Ph.D.

_____

Margaret E. Bauer, Ph.D.

ii

DEDICATION

This dissertation is dedicated to my wife Maria Faricelli and son Juan Martin

Carrasco for all of their love, encouragement, and unconditional support throughout this

process. This dissertation would not have been possible without them.

Sebastian Eduardo Carrasco

ELUCIDATING THE INTERACTION OF *BORRELIA BURGDORFERI* OSPC WITH

PHAGOCYTES IN THE ESTABLISHMENT OF LYME BORRELIOSIS

Lyme disease, the most prevalent vector-borne illness in the United States, is a multisystem inflammatory disorder caused by infection with the spirochete *Borrelia burgdorferi* (*Bb*). This spirochete is maintained in nature through an enzootic cycle involving ticks and small mammals. The *Bb* genome encodes a large number of surface lipoproteins, many of which are expressed during mammalian infection. One of these lipoproteins is the major outer surface protein C (OspC) whose production is induced during transmission as spirochetes transition from ticks to mammals. OspC is required for *Bb* to establish infection in mice and has been proposed to facilitate evasion of innate immunity. However, the exact biological function of OspC remains elusive. Our studies show the *ospC*-deficient spirochete could not establish infection in NOD-*scid IL2rγ^{null}* mice that lack B cells, T cells, NK cells, and lytic complement, whereas the wild-type spirochete was fully infectious in these mice. The *ospC* mutant also could not establish infection in SCID and C3H mice that were transiently neutropenic during the first 48 h post-challenge. However, depletion of F4/80^{+} phagocytes at the skin-site of inoculation in SCID mice allowed the *ospC* mutant to establish infection *in vivo*. In phagocyte-depleted SCID mice, the *ospC* mutant was capable to colonize the joints and triggered neutrophilia during dissemination in a similar pattern as wild-type bacteria. We then constructed GFP-expressing *Bb* strains to evaluate the interaction of the *ospC* mutant with phagocytes. Using

flow cytometry and fluorometric assay for phagocytosis, we found that phagocytosis of GFP-expressing *ospC* mutant spirochetes by murine peritoneal macrophages and human THP-1 cells was significantly higher than parental wild-type *Bb* strains, suggesting that OspC has an anti-phagocytic property. This enhancement in phagocytosis was not mediated by MARCO and CD36 scavenger receptors and was not associated with changes in mRNA levels of TNFα, IL-1β, and IL-10. Phagocytosis assays with HL60 neutrophil-like cells showed that uptake of *Bb* strains was independent to OspC. Together, our findings reveal that F4/80[+] phagocytes are important for clearance of the *ospC* mutant, and suggest that OspC promotes spirochetes' evasion of macrophages in the skin of mice during early Lyme borreliosis.

X. Frank Yang, Ph.D. - Chair

TABLE OF CONTENTS

LIST OF TABLES

LIST OF FIGURES

LIST OF ABBREVIATIONS

ABC   ATP binding cassette transporters

Arp   Actin-related protein

bb   *Borrelia burgdorferi* gene number

BB   *Borrelia burgdorferi* protein number

BBK32   *Borrelia burgdorferi* fibronectin-binding protein

Bgp   *Borrelia burgdorferi* glycosaminoglycan-binding protein

BPI   Bactericidal/permeability-increasing protein

BMDM   Bone marrow-derived macrophages

BosR   *Borrelia burgdorferi* oxidative stress regulator

BSK   Barbour-Stoenner-Kelly

BSA   Bovine serum albumin

C   Complement proteins

˚C   Degrees Celsius

CCL   C-C chemokine ligand

CD   Cluster of differentiation

CDC   Center for Disease Control and Prevention

CDC42   Cell division control protein 42

CASR   Class-A scavenger receptor family

CHO	Chinese hamster ovary cells
CRASP	Complement regulator acquiring surface proteins
CO_2	Carbon dioxide
cp	Circular plasmid
csf1r	Macrophage colony-stimulating factor 1 receptor
CR3	Complement receptor 3
Daam1	Dishevelled associated activator of morphogenesis 1
DbpAB	Decorin-binding proteins A and B
DCs	Dendritic cells
DMSO	Dimethylsulphoxide
DMEM	Dulbecco's Modified Eagle's Medium
DNA	Deoxyribonucleic acid
DTT	Dithiothreitol
ECM	Extracellular matrix
EDTA	Ethylenediaminetetraacetic acid
EF-Tu	Elongation factor Tu
ELISA	Enzyme-linked immunosorbent assay
Erp	*Borrelia burgdorferi* Erp proteins
FBS	Fetal bovine serum
FACS	Fluorescence-activated cell sorting

Fl	*Borrelia burgdorferi* flagellar proteins
FMNL1	Formin-like protein 1
F4/80	Macrophage specific glycoprotein molecule F4/80
GFP	Green fluorescent protein
Gp91phox	Heme-binding membrane glycoprotein gp91phox
h	hour
H&E	Hematoxylin and eosin
HL60	Human promyelocitic cell line
ICAMs	Intercellular Adhesion Molecules
IFA	Immunofluorescence assay
IPTG	Isopropyl-β-d-thiogalactopyranoside
M-CSF	Macrophage colony-stimulating factor
IFN	Interferon
IRF	Interferon Regulatory Factor
Ig	Immunoglobulin
IL	Interleukin
iNOS	Inducible nitric oxide synthase
LCs	Langerhans cells
LL-37	Cathelicidin
L-NMMA	L-N^{G}-monomethyl Arginine citrate
LPS	Lipopolysaccharide
Ly6G	Lymphocyte antigen 6 complex - locus G
MARCO	Macrophage Receptor with Collagenous Structure

mDia1	Diaphanous-related formin-1
MHC	Major histocompatibility complex
MOI	Multiplicity of infection
MyD88	Myeloid differentiation primary response 88
mRNA	messenger ribonucleic acid
NaCl	Sodium chloride
NADPH	Nicotinamide adenine dinucleotide phosphate-oxidase
NaH_2PO_4	Monosodium phosphate
Ncf1	Neutrophil cytosolic factor-1
NF-κB	Nuclear transcription factor kappa-B
NK	Natural killer
NKT	Natural killer T
NLR	Nucleotide Oligomerization Domain-like receptor
NLRP3	NLR family, pyrin domain containing 3
NOD	Non-obese diabetic
Nod	Nucleotide-binding oligomerization domain
OMVs	Outer membrane vesicles
Osp	Outer surface lipoprotein
P66	αIIbβ3 integrin binding protein
PBMCs	Peripheral blood mononuclear cells
PBS	Phosphate buffered saline
PC	Protoplasmic cylinders
PCR	Polymerase chain reaction

PI3K	Phosphatidylinositol 3-kinase
Plac8	Placenta-specific 8
Poly C	Polycytidylic acid
Poly I	Polyinosinic acid
PM	Peritoneal macrophages
PMA	Phorbol 12-myristake 13-acetate
PMN	Polymorphonuclear leukocytes
PMSF	Phenylmethylsulfonyl fluoride
PRRs	Pattern recognition receptors
PTS	Phosphotransferase system
qPCR	Quantitative Polymerase chain reaction
Rac1	RAS-related C3 botulinum substrate 1
RevA/B	Fibronectin-binding proteins RevA and B
RFU	Relative fluorescence units
Rho	Rhodopsin
RT-PCR	Reverse transcriptase Polymerase chain reaction
RNA	Ribonucleic acid
RpoS	Sigma factor S regulator
Rrp	Response regulator protein

Salp15   Tick salivary protein 15

SCID   Severe combined immunodeficiency

SDS-PAGE   Sodium dodecyl sulfate polyacrylamide gel electrophoresis

siRNA   small interfering RNA

SRAI/II   Scavenger receptor A I/II

STAT3   Signal transducer and activator of transcription 3

THP-1   Human monocytic cell line

TLR   Toll-like receptor

TNF   Tumor necrosis factor

TSLP1   Tick salivary protein 1

VlsE   Vmp-like sequence protein E

WASP   Wiskott-Aldrich syndrome protein

CHAPTER I: INTRODUCTION

Lyme disease

History and epidemiology of Lyme disease

Lyme disease was first reported in the United States in 1975 when Drs. Allen

Steere and Stephen Malawista described an unusually high incidence of acute arthritis

among children in Old Lyme, Connecticut (1). A skin rash with an expanding bull's-eye

pattern was also reported to precede the onset of arthritic symptoms in 25% of these cases

(1). Clinical, temporal and spatial findings from this disease outbreak investigation

allowed Dr. Steere and coworkers to postulate that an infectious agent was responsible

for this unusually high onset of Lyme arthritis in children. They suspected that this

infectious agent was transmitted by an unidentified arthropod vector since most cases

occurred in rural communities near wooded areas with the onset peaking in summer and

early fall (1). In 1982, Dr. Burgdorfer and colleagues detected and isolated spirochetes

belonging to the genus *Borrelia* spp. from the mid-guts of *Ixodes* ticks (2). This

spirochetal bacterium was later named *Borrelia burgdorferi* (3). To date, there are three

Borrelia species that are known to cause Lyme disease that are transmitted by the hard

tick *Ixodes*. *B. burgdorferi sensu stricto* is the sole agent of Lyme disease in the United

States while the other two *Borrelia* species (*B. garini* and *B. afzelii*) are found only in

Europe and parts of Asia (4, 5).

Lyme disease became a reportable illness in 1991 and is the most common

arthropod-borne disease in the United States, with almost 30,000 confirmed cases

reported each year to the Center for Disease Control and Prevention (CDC) (6). Recently,

the CDC have estimated that the number of probable infections is around 300,000

reported cases annually (7). In terms of its geographic distribution, Lyme disease is endemic in the northeastern and northcentral (upper Midwest) region of the United States (**Figure 1**) (6). In 2013, the CDC estimated that 95% of reported and confirmed Lyme disease cases were from 14 states, including Connecticut, Maine, Maryland, Massachusetts, Minnesota, New Hampshire, New Jersey, New York, Pennsylvania, Rhode Island, Vermont, Virginia, and Wisconsin.

1 dot placed randomly within county of residence for each confirmed case
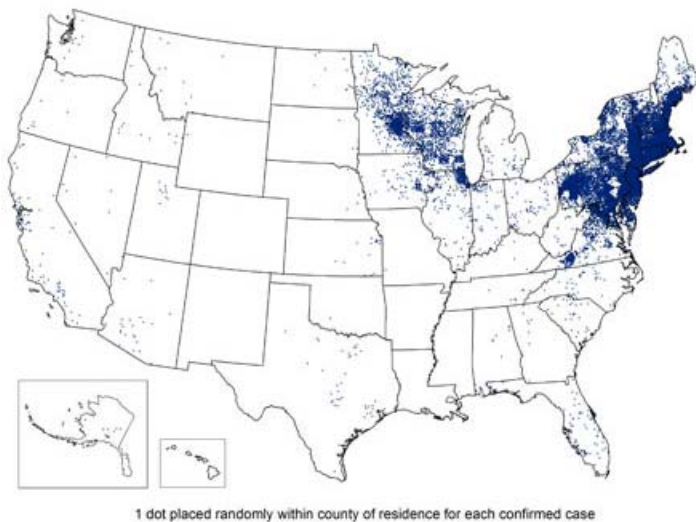
Figure 1. Reported Cases of Lyme Disease in the United States, 2013 (CDC Division of Vector-borne Infectious Diseases - last accessed February 5, 2015) (8). For each case of Lyme disease confirmed by the State Health Departments, one dot is placed randomly within the county of the patient's residence. Cases have been reported in nearly every state, but the county of residence is not necessarily the county in which the infection was acquired. The greatest number of cases was reported in the northeastern and the upper midwestern states.

The enzootic life cycle of *B. burgdorferi*

   B. burgdorferi circulates in natural enzootic cycles involving *Ixodes* ticks and a wide range of vertebrate hosts. *Ixodes scapularis*, commonly known as the deer tick or Eastern black-legged tick, is the principal arthropod vector responsible for transmitting *B. burgdorferi* to mammals in northeastern and northcentral regions of the United States (3). In addition, *Ixodes pacificus*, the Western black-legged tick, has been reported to maintain *B. burgdorferi* in nature in western areas of United States such as northern California, Oregon, and Washington State (9-11). These *Ixodes* species are considered to be three-host ticks since they feed once at each of the three life stages: larvae, nymphs, and adults (12). The *Ixodes* ticks have a 2-year life cycle which begins when adult female ticks lay eggs during early spring. After these eggs hatch into larvae during summer, they take their first blood meal by feeding on an infectious vertebrate host such as the white-footed mouse (*Peromyscus leucopus*), a common natural reservoir for *B. burgdorferi* in the United States (13, 14). After feeding for at least 72 h, engorged larvae drop from the host to the ground and become dormant for winter months. In the following late spring or early summer, the larvae molt into nymphs, which can then take their second blood meal on a competent reservoir host, such as small rodents. After feeding for at least 72 h, engorged nymphs detach and drop to the ground and molt into the adult ticks during the fall. At this time, adult ticks feed for the final time on a larger mammal such as a white tailed deer (*Odocoileus virginianus*), which are considered incompetent hosts for *B. burgdorferi*. However, deer play an important role in the maintenance of the tick population because adult ticks mate on these animals (15). After mating, the adult female ticks fall off the deer and lay eggs prior to dying in the late fall or early spring (13, 16,

17). Humans and dogs are considered accidental dead-end hosts within the *B. burdorferi* life cycle and can develop clinical manifestations of disease. Although *Ixodes* ticks can feed on humans in any of the three developmental stages, the nymphal stage is when infected ticks are most likely to transmit *B. burgdorferi* to humans (13, 14).

Clinical manifestations of Lyme disease

The clinical manifestations of Lyme disease in humans are divided in three separate stages: early localized infection at the skin (stage 1), disseminated infection (stage 2), and late persistent infection (stage 3) (18). Infection with *B. burgdorferi* can result in dermatologic, musculoskeletal, cardiac, neurologic and/or ocular abnormalities (18). Early localized infection develops within the first 30 days after a tick bite and is characterized by a cutaneous lesion, called *erythema migrans* (**Figure 2**), which is reported in 70-80% of infected individuals (19). This cutaneous lesion is accompanied by arthralgia, myalgia and/or swollen lymph nodes. Dissemination of spirochetes occurs within days to weeks and could be accompanied by different clinical manifestations, including secondary annular skin lesions, acute lymphocytic meningitis, cranial neuropathy, radiculoneuritis, atrioventricular nodal block, musculoskeletal pain in joint and adjacent tissues, and ocular pain and photophobia (18). Chronic or persistent clinical manifestations can occur months or years after the infection in untreated individuals or in 10% of infected individuals that fail to respond to antibiotic therapy. The most common manifestation of late infection is monoarticular or oligoarticular arthritis (20). Other reported clinical manifestations of persistent infection are peripheral and central nervous system abnormalities (e.g. encephalomyelitis, encephalopathy, and axonal

4

polyneuropathy) and cardiac abnormalities (e.g. atrioventricular blocks and myopericarditis) (21, 22).
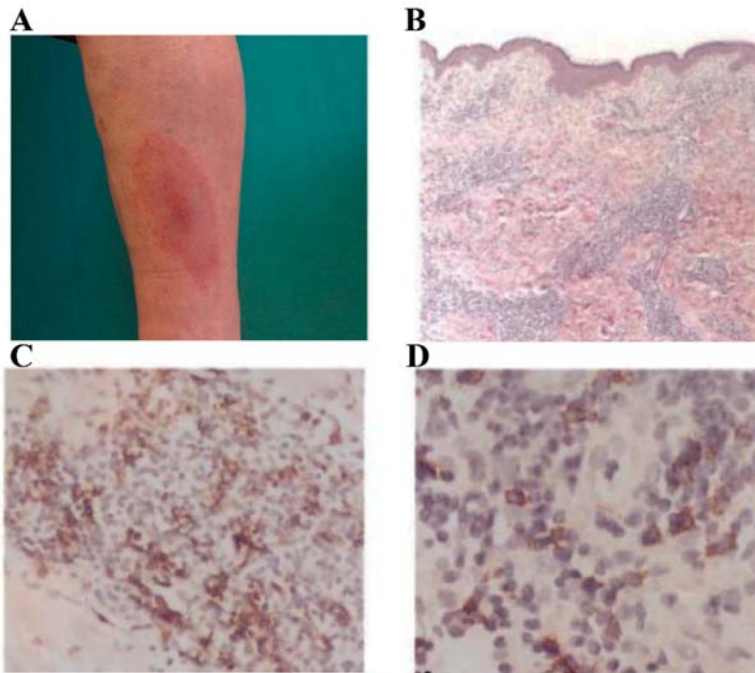
Figure 2. Macroscopic and microscopic features of *erythema migrans* of patients exposed to or infected with *B. burgdorferi*. **A)** Representative example of *erythema migrans* (EM) lesion on patient arm characterized by red "bull's-eye" macule (photograph was reproduced from (23)). **B)** Biopsy specimen of EM lesion characterized by perivascular infiltrates of mononuclear cells (blue color using H&E staining) are observed throughout the dermis. **C)** Immunohischemical staining of skin biopsy specimen that shows large numbers of CD68^{+} macrophages (brown staining) and moderate numbers of CD3^{+} T cells (D, brown staining) in perivascular infiltrate (photomicrographs were reproduced from (24)).

Diagnosis of Lyme disease

Currently, the CDC recommends that practitioners diagnose Lyme disease based on clinical evidence of EM lesion, late clinical manifestations involving the musculoskeletal, nervous or cardiovascular system, laboratory evidence of infection, and known exposure to potential tick habitats in an endemic Lyme disease region (within 30 days before onset of EM). Laboratory assays recommended by the CDC that are used to define a Lyme disease case include a positive culture for *B. burgdorferi* or a positive serology for evidence of antibodies against this spirochete (25). Although cultivation of *B. burgdorferi* has been reported from various clinical specimens, including skin biopsies, blood, plasma, sera, and other fluids (26-29), this method is not sensitive for isolation of spirochetes in patients with disseminated and persistent infection due to the sparseness of organisms in tissues or technical limitations associated with laboratory contamination of patient samples (26, 27). However, culture can be a highly sensitive tool for detection of *B. burgdorferi* from skin biopsies collected from patients with acute EM whose diagnosis was based mostly on the clinical recognition of this lesion (26, 30).

Detection of antibodies to *B. burgdorferi* by ELISA and immunoblot are currently the only standardized tools for laboratory diagnosis of Lyme disease in humans. The CDC recommends a two-step process when testing blood from individual Lyme disease patients and conducting epidemiological surveillance of Lyme disease (25). The ELISA assays use whole cell lysates or purified recombinant *B.burgdorferi* antigens as sources of substrate for detection of IgM and IgG antibodies individually or in combination (25, 26). If the result from ELISA is positive or intermediate (weak positive), then immunoblotting is used as a confirmatory assay. The second step uses an immunoblot

assay that allows the assessment of antibodies against specific *B. burgdorferi* antigens (**Table 1**). This assay has contributed to determining which antigens of *B. burgdorferi* are immunodominant at different stages of infection. For example, OspC is an immunodominant antigen that elicits a strong IgM reactivity during early stages of infection while most responses to *B. burgdorferi* immunodominant antigens develop at different time points during later stages of disease (26). Although serology is the method of choice for laboratory diagnosis of Lyme disease, other methods such as PCR have been developed for detection of *B. burgdorferi* DNA from samples and are employed in research settings and reference laboratories (25).

Table 1. *Borrelia burgdorferi* antigens of diagnostic significance

Antigen	Other designation	Molecular size (kDa)	Gene location
93	P63/100	93	Chromosome
66	P66, αIIbβ3 integrin binding protein	66	Chromosome
58		58	Chromosome
BBK32	P47, Fibronectin binding protein	47	lp36
45		45	Chromosome
VlsE	Antigenic variation protein	35-43	lp28-1
41	FlaB, Flagellin	41	Chromosome
39	BmpA, Laminin binding protein	39	Chromosome
34	OspB	34	lp54
31	OspA	31	lp54
28	OspD	28	lp38
23	OspC	21-25	cp26
DbpA	P17, Decoring binding protein A	17-18	lp54
17	RevA, Fibronectin binding protein	17	cp32
ErpA	OspE related protein	17	cp32

Although this two-step serology approach is highly sensitive and specific for detection of antibodies to *B. burgdorferi* after the first 3-4 weeks of infection in Lyme disease patients, this approach is not sensitive for detection of *B. burgdorferi*-specific antibodies within the first 2-3 weeks after infection in patients with acute EM and/or early neurological

manifestations (25, 26). These serological assays are not going to test positive until an infected individual has had time to develop antibodies against most *B. burgdorferi* antigens used for the serodiagnosis of Lyme disease (25, 26). In addition, the use of *B. burgdorferi* antigens for the early serodiagnosis of Lyme disease has been a subject of considerable debate as some of these antigens are either highly heterogenous among strains such as OspC or crossreactive with other bacterial antigens such as flagellar proteins (26). Therefore, research efforts have focused on developing serological assays against new recombinant antigens and synthetic peptides to improve the detection of *B. burgdorferi*-specific antibodies during early infection (25). Serodiagnosis of early Lyme borreliosis is important in the management of disease progression as infected individuals at this disease stage are completely cured after antibiotic treatment (18). Our findings in part II of this dissertation discuss the potential use of *B. burgdorferi* EF-Tu as an early serodiagnostic marker of Lyme borreliosis.

The murine model of Lyme disease

The use of laboratory inbred mouse strains has been extremely useful for understanding many features of the immune response and pathogenesis of human Lyme arthritis and carditis (31-33). This mouse model also recapitulates other clinical manifestations of Lyme disease, including vasculitis, myositis, and peripheral neuritis (31, 33, 34). However, mice do not manifest the EM lesion that is observed in most infected individuals or develop central nervous system disease and chronic Lyme arthritis that may occur in some human patients (34).

To establish this mouse model several host and bacterial factors were initially tested. Early studies into the host-pathogen interaction of *B. burgdorferi* showed that disease severity in mice is influenced by genotype, immune status, age, *B. burgdorferi*

isolate and passage history, infectious dose and route of inoculation, and site of inoculation (35). To date, it is well-accepted that inbred mouse strains are equally susceptible to *B. burgdorferi* infection, but the susceptibility of arthritis and carditis is dependent on the mouse genotype (31, 36). The C3H/HeN and C3H/HeJ mice are the primary strains to study the pathological changes in the heart and joints since they develop severe carditis and arthritis in the tibio-tarsal joints by 2-3 weeks after *B. burgdorferi* infection. Other mouse strains such as Balb/c develop severe carditis but mild arthritis, and C57BL/6 develop milder carditis and arthritis (33, 35, 37).

Multiple transgenic mouse models have been used to delineate the contribution of innate and adaptive immune factors in the development of Lyme borreliosis (35). The importance of innate host defense against *B. burgdorferi* has been demonstrated by the use of TLR2$^{-/-}$ and MyD88$^{-/-}$ mouse models as they displayed a severe defect in controlling the spirochetal burden in blood and tissues. However, these innate factors were not required for disease resolution as these mouse strains showed severe arthritis at 2 - 4 weeks after *B. burgdorferi* infection (38-41). The importance of adaptive immune responses in Lyme disease pathogenesis has been demonstrated in mouse strains deficient in B cells and B and T cells (e.g. µMT$^{-/-}$ and *igh*$^{-/-}$, lack B cells but bear T cells; SCID and *rag1*$^{-/-}$, lack B and T cells). Early studies using these immundeficient mouse strains showed that they developed persistent arthritis and carditis and exhibited an elevated spirochetal burden in blood and tissues after *B. burgdorferi* infection for 4 - 8 weeks (42-45). These studies also showed that spirochetal burden and disease progression can be effectively reduced by adoptive transfer of immune mouse serum and B cells, indicating

that humoral immunity plays an important role in the control of Lyme borreliosis (43, 45).

Early studies also reported that severity of arthritis decreased overtime as mice become adults. For example, C3H mice at age 3 weeks developed more severe arthritis than adult mice (12 weeks) (33, 34). Although all laboratory mice, regardless of the age, are susceptible to *B. burgdorferi* infection, another important factor to take into consideration is the plasmid content of the *B. burgdorferi* isolate used to inoculate those mice. Comparison of the plasmid profiles of 19 *B. burgdorferi* clonal isolates showed that the lp25 and lp28-1 were essential to infect mice (46). Plasmid loss after *in vitro* passages of *B. burgdorferi* is also associated with decreased virulence in mice (35, 46, 47). Laboratory mice can be infected by *B. burgdorferi* strains by tick bite and a variety routes of inoculation, including the intradermal, intraperitoneal, and intravenous routes (48-50). Naïve mice are readily infected by the bite of infected ticks (51, 52); however, the infectious dose for needle-challenged mice appears to be different among these routes. For example, mice can be infected with a dose of 10 or fewer spirochetes per mouse via the intradermal route whereas one hundred-fold more spirochetes are needed to infect mice via the intraperitoneal route (35, 48). In addition, disease severity has been shown to be influenced by the site of inoculation in the skin as mice inoculated in the footpad developed higher arthritis and carditis than mice inoculated in the shoulder (53). Thus, the use of laboratory mice has provided a useful system for studying Lyme disease pathogenesis.

Biology of *B. burgdorferi*

***B. burgdorferi* architecture and genome**

      B. burgdorferi is a Gram-negative bacterium belonging to the genus of *Borrelia* species within the phylum of *Spirochaetes*. These organisms, 20-30 μm in length and 0.2-0.3 μm in width, have a characteristic wave-like cell morphology with an outer and inner membrane surrounding the periplasmic endoflagella (**Figure 3**) (14). This endoflagella also provides a unique mode of motility with both rotational and translational movements that allows the spirochete to migrate through host tissues (14, 54). The outer membrane is a fluid and fragile bilayer that does not contain LPS. The major lipid constituents in the membrane are phosphatidylcholine, phosphatidylglycerol, and cholesterol-glycolipid-rich lipid rafts (55, 56). The outer membrane also contains numerous outer-surface lipoproteins and few β-barrel outer membrane spanning proteins. The inner membrane is rich in integral membrane proteins and different types of specialized transporters (e.g. electrochemical, PTS sugar transport system, and ABC transporters) and sits underneath a thin peptidoglycan layer (**Figure 3**) (14).
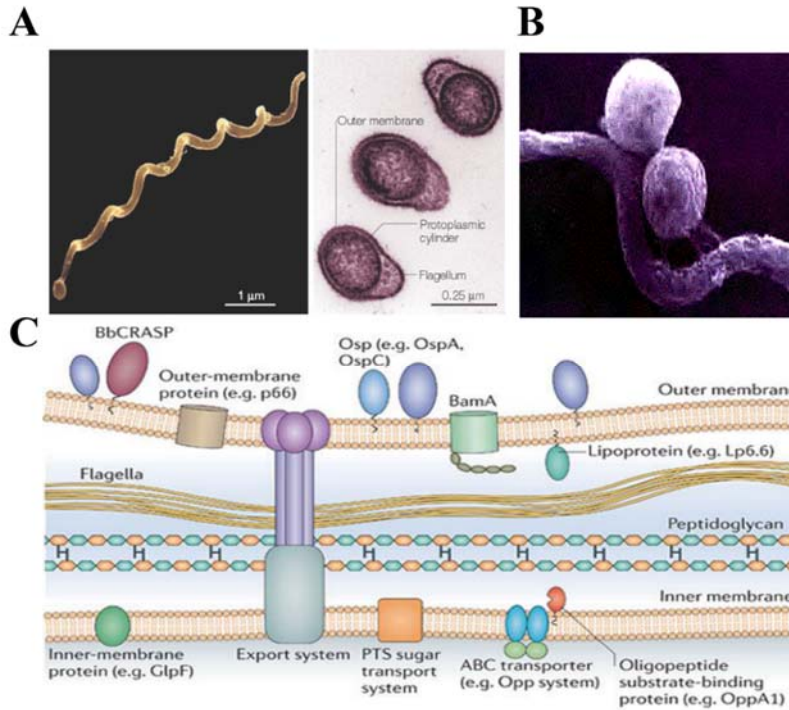
Figure 3. Morphology and cellular architecture of *B. burgdorferi*. A) Scanning (left) and transmission (right) electron micrographs of *B. burgdorferi* showing helical shape of spirochetes which is primarily imparted by their endoflagella. **B)** Scanning electron micrograph shows two membrane cysts or outer membrane vesicles observed in *B. burgdorferi* (electron micrographs panels are reproduced from (57, 58)). **C)** Schematic of cellular architecture and molecules present in periplasmic space and outer and inner membrane of *B. burgdorferi.* This figure is reproduced from (14).

    B. burgdorferi strains have highly unusual segmented genomes composed of a linear chromosome of approximately 910 kb and numerous linear and circular plasmids (in the 5-56 kb size range) totaling approximately 610 kb (59, 60). Genomic analysis of *B. burgdorferi* strains have shown that the chromosome carries the majority of housekeeping genes that encode metabolic enzymes while plasmids largely carry genes

that encode surface lipoproteins. With the only exception of cp26 that appear to encode

functions critical for *B. burgdorferi* survival, the rest of the circular and linear plasmids

are not required for *in vitro* growth of spirochetes (61, 62). Plasmid cp26 carries genes

that encode several nucleotide metabolic enzymes, peptide, purine, chitobiose, and

glucose transporters, and a telomere resolvase that is required for replication of the linear

chromosome and plasmids (62, 63). Plasmid cp26 also encode the *ospC* gene that is

important for mouse infectivity (49, 64, 65).

Regulation of outer membrane proteins for mammalian infection

As mentioned above, *B. burgdorferi* is maintained in nature by a complex life

cycle involving ticks and small mammals. To support this lifestyle, *B. burgdorferi* adapts

to these two markedly distinct host environments by coordinately regulating the

expression of numerous genes. Dr. Frank Yang's lab and other groups have demonstrated

the Rrp2-RpoN-RpoS canonical pathway (also called the σ^{54}-σ^S sigma factor cascade,

Figure 4) plays a central role in modulating gene expression during different phases of

the enzootic cycle (66-68). In this pathway, the two-component response regulator Rrp2

directly activates the alternative sigma factor RpoN (σ^{54} or σ^N), which in turn is required

for transcription of the *rpoS* (66, 67). The alternative sigma factor RpoS (σ^S) then acts as

global regulator and can activate transcription of approximately 145 genes that appear to

be important for transmission or are involved during different stages of mammalian

infection. Many of these genes encode surface lipoproteins such as OspC, DbpBA,

BBK32, and BBA64 that are important for virulence within the mammalian host (69).

Conversely, this pathway represses important tick phase-specific genes such as *ospA*

(67). Evidence has accumulated that *rpoS* expression is upregulated by several

environmental cues when nymphal ticks start feeding on mammals (70). These environmental cues lead to the activation of RpoS that subsequently leads to upregulation of *ospC* and other genes required for host adaptation. Consistent with this notion, *rpoS* or *ospC* mutants are incapable of establishing infection in mammals. Similar phenotype is observed for *B. burgdoferi* strains lacking Rrp2 or RpoN since neither of these mutants can establish infection in the mammalian host (69, 71, 72). Recently another transcriptional regulator termed BosR was shown to bind the *rpoS* promoter region at three different sites and induce the expression *ospC* and *dbpAB* in an RpoN-RpoS dependent manner (73, 74). In fact, inactivation of *bosR* in *B. burgdorferi* also resulted in a noninfectious phenotype in mice (73, 75). These findings further support that the RpoN-RpoS pathway is essential for *B. burgdorferi* to establish mammalian infection.
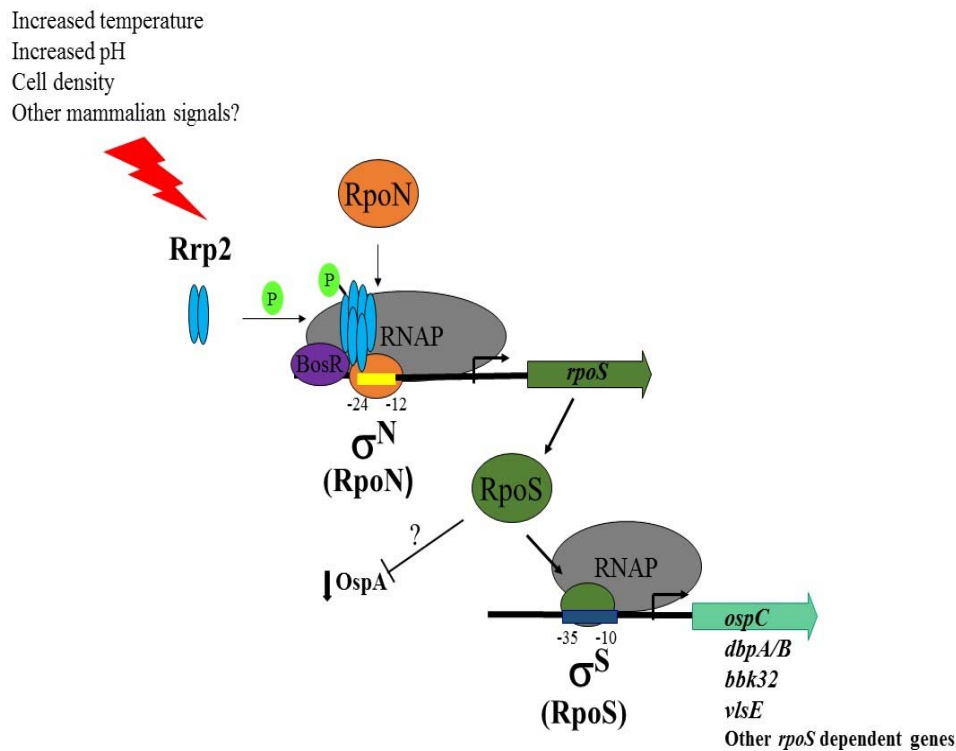
Figure 4. The Rrp2-RpoN-RpoS pathway plays a central role in the regulation of *B. burgdorferi* outer membrane proteins during mammalian infection. It has been proposed that activation of the response regulator Rrp2 occurs by several environmental signals after nymphal ticks start feeding on mammals. An increase in temperature (from 25°C to 37°C) and pH (from 6.8 to 7.4) are some environmental cues that appear to activate this pathway as spirochetes transtions from ticks to mammals. These signals lead to phosphorylation of Rrp2 to initiate transcription of *rpoS* through the alternative sigma factor RpoN (σ^N), which also interacts with RNA polymerase (RNAP). RpoS (σ^S) in turn induces the expression of genes such as *ospC* that are important for spirochetes to infect mammals while repressing the expression of genes such as *ospA* that are important for tick colonization. BosR also plays a role in the initiation of transcription of *rpoS* and has been proposed to form a trimeric complex with phosphorylated Rrp2 and RpoN that sits on the *rpoS* promoter region, but the exact interaction of these proteins has not been elucidated.

B. burgdorferi traits during infection in mammals.

Unlike most classical Gram-negative bacterial pathogens, *B. burgdorferi* does not produce LPS or toxins or have specialized secretion and translocation systems (14). Instead, the *B. burgdorferi* genome encode a large number of surface lipoproteins that allow spirochetes to adapt, adhere, invade, and persist in mammalian tissues. These surface proteins can also trigger innate and adaptive inflammatory reactions at different stages of mammalian infection (76). After spirochetes are deposited into the host skin by a tick bite, they replicate locally in the dermis and then disseminates to tissues by

different means (77, 78). *B. burgdorferi* utilizes its endoflagella to migrate locally

through connective tissue or hematogenously to distant organs from the initial site of

infection (76-78). Intravital microscopy studies have characterized motility and

dissemination patterns of single live fluorescent spirochetes within the mouse's skin,

vasculature, and organs (50, 79). Spirochetes can easily be observed in living mouse skin

for up to one month after subcutaneous inoculation. Spirochetes are predominantly found

in the perivascular region of the mouse dermis where they bind to and translocate through

ECM constituents such as type I collagen to access small vessels for hematogenous

dissemination (76, 79). Once in the circulation, spirochetes frequently adhere to the

vascular endothelium and migrate up (against the blood flow) and down the blood vessel

surface to extravasate into tissues (50). In addition, Drs. Nicole Bamgaurth and Stephen

Barthold and coworkers have recently proposed that *B. burgdorferi* can actively

disseminate through the lymphatic system as live spirochetes are frequently re-isolated

and detected in draining lymph nodes proximal to the inoculation site prior to the

detection of spirochetes in other tissues (80, 81). Furthermore, *B. burgdorferi* strains

lacking one of the major endoflagellar filaments such as FlaB (e.g. *flaB* mutant) are

nonmotile and cannot survive at the skin site of inoculation of mice (82), a finding that

clearly illustrates that the endoflangella is essential for spirochetes to disseminate and

establish infection in mammals.

To successfully adhere and colonize tissues in mammals, *B. burgdorgferi* deploys

a variety of surface proteins that mediate attachment with host cells and components of

the ECM (83). These *B. burgdorferi* adhesins bind to a variety of ligands in tissues,

including fibronectin, glycosaminoglycans, proteoglycan decorin, collagen, laminin, and

integrins (83, 84). To date, there are 5 fibronectin binding proteins (BBK32, RevA/B, BB0347, and CRASP-1), 3 glycosaminoglycan binding proteins (BBK32, DbpAB, and Bgp), 1 decorin binding protein (DbpAB), 1 collagen binding protein (CRASP-1), 2 laminin binding proteins (CRASP-1 and CRASP-2), and 4 integrin binding proteins (BBK32, P66, BBB07, BB0172), all identified in *B. burgdorferi* using mostly *in vitro* systems and in some cases *in vivo* (79, 84). Among these adhesins, P66 has been shown to be essential for infection of immunocompetent mice (ID_{50} was greater than 10^8 spirochetes). The *p66* mutant was rapidly cleared within the first 48 h in these mice and could not even establish infection in TLR2$^{-/-}$ and q$^{-/-}$ mice (85). The *dbpAB* mutant showed a significant defect in infectivity in immunocompetent mice during the early phase of infection that was dependent on acquired immunity (84, 86, 87). The *bbk32* mutant showed mild attenuation of infectivity in mice and a significant decrease in vascular adhesion *in vivo* (79). In contrast, the Bgp mutant remained infectious in immunodeficient mice (88). Although these adhesins exhibit overlapping and redundant interactions with more than one component of the ECM, they likely have distinct roles in homing of *B. burgdorferi* to different tissue compartments throughout the course of mammalian infection. Thus, adhesion of *B. burgdorferi* to host cells and ECM components is an important first step in the establishment of infection.

Previous studies have proposed that *B. burgdorferi* utilizes host proteases such as plasmin to break down components of the ECM as a mechanism to promote invasiveness of spirochetes in tissues. *B. burgdorferi* has the ability to bind to host plasminogen using several known outer membrane proteins, such as OspC, OspA, ErpA, ErpC, ErpP, CRASP-1, CRASP-2, and BBA70 proteins (84, 89). This surface-bound plasminogen can

be converted into the serine protease plasmin by host-derived plasminogen activators to enhance the ability of spirochetes to penetrate endothelial cells monolayers (90, 91). However, the contribution and functional relevance of this surface-bound plasmin during spirochetal infection is not well understood. In studies using plasminogen deficient mice, plasmin appeared to be important in enhancing spirochetemia during dissemination of *B. burgdorferi* but did not play a role in establishing infection in distant tissues (92). Thus, binding of plasminogen may be important during the early stage of infection in mice when spirochetes migrate from the dermis into the vasculature for hematogenous dissemination.

Role of OspC during Lyme borreliosis

OspC is a 22 kDa immunodominant lipoprotein that is primarily alpha helical in structure with five parallel α-helices connected by intervening loops (93, 94). OspC is highly expressed during early infection and can elicit protective antibody responses against *B. burgdorferi* infection in the mammalian host. OspC is also highly polymorphic in sequence among *B. burgdorferi* strains with approximately 28 different *ospC* genotypes (95). Because of this OspC diversity among strains, the antibody response elicited during early infection appears to be OspC-type specific (95). In addition, *B. burgdorferi* strains producing certain OspC-types are associated with invasive infections in patients and experimentally infected animals (96, 97).

To date, the precise function of OspC still remains elusive. Several lines of evidence suggest that OspC is a major virulence factor that is required for the establishment of mammalian infection (65, 98). OspC-deficient spirochetes are rapidly cleared from mammalian hosts (64, 99). Also, the structural similarity of OspC to the

ligand-binding domain of the aspartate receptor from Salmonella enterica serotype Typhimurium suggests that OspC could bind to distinct ligands during mammalian infection (93). Our studies in part I of this dissertation evaluated the role of OspC in the protection of spirochetes against innate host factors *in vivo* and *in vitro*. Studies on the role of OspC during mammalian infection are discussed in more detail in part I of this dissertation.

Immune evasion strategies

B. burgdorferi has evolved strategies to escape immune clearance and persist within infected hosts for several months or years. The two main strategies utilized for immune evasion are antigenic variation and complement resistance. Other observations of spirochetal persistence in the host include the following: homing of spirochetes in protective niches such as collagen bundles; changes in *B. burgdorferi* gene expression in response to the stage and site of infection; and formation of outer membrane vesicles or cysts as a strategy of spirochetal survival during antibiotic therapy (76, 100-102). For the purpose of this literature review, I have focused on the immune evasion strategies that are well understood.

Evasion of humoral immunity

Accumulated evidence has shown that B cell activation and antibody responses play an important role in the control of *B. burgdorferi* burden and disease resolution during infection in immunocompetent mice (35, 43, 45, 80). However, these wild-type mice remain persistently infected for months after the initial challenge because humoral immunity against *B. burgdorferi* appears to lack a robust functional adaptive memory response (35, 80, 103). In fact, mice are commonly re-infected by tick-transmitted *B. burgdorferi* in nature (52, 104). One possible explanation why *B. burgdorferi* escape the

humoral response and persist in the mammalian host is due to variations on the antigenic surface of spirochetes. The plasmid lp28-1 of *B. burgdorferi* contains a *vlsE* locus that codes for a surface lipoprotein named VlsE (102). The *vlsE* gene is flanked by 15 silent cassettes upstream that undergo random recombination with the *vlsE* central cassette, leading to gene conversion events and variations in the antigenic properties of VlsE (76, 102). It is well-accepted that the *vlsE* locus undergoes extensive recombination events over the course of mammalian infection that can be detected in *B. burgdorferi* reisolates as early as 4 days post-infection in mice. The *vlsE* locus is required for *B. burgdorferi* to establish infection and reinfection in immunocompetent mice (105, 106). In contrast, *vlsE* mutants can infect and persist in SCID mice (105-107) but cannot establish infection in passively immunized SCID mice with *Borrelia* specific immune sera (106). Together, these findings have shown that *vlsE* permits the evasion of host humoral responses during *B. burgdorferi* infection.

An alternate explanation why *B. burgdorferi* evade humoral immunity may rely on the ability of this pathogen to alter an effective memory B cell response during infection (80). Recent studies have proposed that the lack of functional T cell-dependent B cell responses is due to the presence of short-lived and low-affinity antibodies during active *B. burgdorferi* infection in mice (80, 103). These T cell dependent antibodies begin to decline after 6 weeks of infection when spirochetes or antigens are still detected in multiple mouse tissues (43, 103). Thus, these findings suggest that *B. burgdorferi* modulate the quality of T cell dependent humoral responses during active infection, allowing some spirochetes to persist and escape immune clearance.

Resistance to complement

The complement system, an arm of the innate immune system, is a complex cascade of plasma proteins and membrane associated proteins involved in the early detection of invading pathogens. Complement activation occurs through three different pathways: the classical, lectin, and alternative (108). All three pathways converge at the level of C3 convertases, which in turn are responsible for generating the main effector functions of the complement system such as the secretion of peptide mediators of inflammation (C3a/C5a), formation of membrane attack complex (e.g. C5b-9) for pathogen lysis, and opsonization of pathogens (e.g. C3b) (108). Previous studies have proposed that *B. burgdorferi* resist complement mediated killing through the recruitment of host complement regulators, interaction with tick salivary proteins, and evasion of the lytic alternative pathway (109). *In vitro* studies also showed that *B. burgdorferi* is able to grow in the presence of human sera, a feature that was correlated with the expression of complement regulator acquiring surface proteins (CRASPs) in spirochetes (76). To date, there are 5 CRASPs (CRASP-1 to 5) proteins identified in *B. burgdorferi* (84). These proteins bind to the complement regulator Factor H and its related proteins, which enables spirochetes to reduce activation of the complement alternative pathway which in turn prevents the deposition of C3b and formation of membrane attack complex on the cell surface (109). Another mechanism by which *B. burgdorferi* evades complement mediated killing is by binding to tick salivary proteins. *B. burgdorferi* OspC binds a tick salivary protein named Salp15 to protect spirochetes from complement mediated killing via the alternative pathway (110, 111). Recently, another group showed that *B. burgdorferi* co-opts another tick salivary protein named TSLP1 to protect spirochetes

from complement mediated killing via the lectin pathway (109). The third proposed mechanism that *B. burgdorferi* uses to evade complement is inherent to changes in its outer membrane composition that sterically inhibits the lytic activity of the membrane attack complex (109). *In vivo* studies using mice deficient in C5 provided further evidence that clearance of *B. burgdorferi* does not require activation of the alternative pathway (112). In contrast, studies using mice deficient in C3 (113, 114) suggest that C3b-mediated phagocytosis plays a role in controlling spirochetal burden in these mice.

Innate cellular response against *B. burgdorferi*

Innate cellular responses play a central role in the recognition and clearance of *B. burgdorferi* in infected tissues from humans and animal models (35, 114). Histopathological EM lesions from infected patients have demonstrated that cellular infiltration in the skin samples is predominantly composed of macrophages/monocytes, DCs and T cells, few neutrophils, and rare plasma cells (115). Neutrophils and macrophages are also commonly detected in the skin within the first 3 days after *B. burgdorferi* challenge in the rabbit model of Lyme borreliosis (116). Although mice do not develop EM lesions, many studies have also demonstrated that macrophages/monocytes and neutrophils commonly infiltrate joints and hearts during early and disseminated stages of *B. burgdorferi* infection (35). During the first 2-3 weeks (acute phase) of infection, macrophages/monocytes are the dominant cell infiltrate driving the inflammatory response in the heart, and neutrophils are the predominant cell infiltrate associated with joint inflammation in wild-type mice (35, 114). These observations provided the first evidence that different mechanisms may be involved in the pathogenesis and pathology of Lyme borreliosis in these two organs (114).

Spirochetes are found within all regions of the heart and joints, but as the phagocyte responses evolve, spirochetes are restricted to specific sites where they can persist in the heart (e.g. aortic wall and base of the heart) and joints (e.g. tendons and ligaments) (33, 35, 77). At the acute stage, spirochetes are also commonly detected in subcutaneous tissue which is slightly infiltrated with neutrophils and macrophages (35). Thus, phagocytes are an essential component in the early host defense against *B. burgdorferi in vivo*.

Recognition of *B. burgdorferi* by macrophages and neutrophils

The recognition of *B. burgdorferi* is a complex process involving several PRRs that initiate an innate immune response against invading spirochetes (114). The outer membrane of *B. burgdorferi* is decorated by numerous surface lipoproteins anchored to the membrane lipid bilayer via tripalmitoyl-*S*-glyceryl-cysteine (Pam$_3$Cys) modifications (117). This is an important ligand for the recognition of *B. burgdorferi* by Toll-like receptor (TLR) 2/1 heterodimers on the phagocyte surface (118, 119). TLR2 then signals through the MyD88-dependent pathway leading to the activation of NF-κB that subsequently results in the production of cytokines (e.g. TNF-α, IL-1β, IL-6, IL-10, and IFN-γ), chemokines (e.g. IL-8 and CCL2), and adhesion molecules (e.g. ICAMs) (114, 119, 120). Although the interaction of spirochetal lipoproteins with the TLR2/1 receptor has been primarily focused on monocytes and macrophages, these lipoproteins also serve as TLR2 ligands for human neutrophils as this TLR receptor is commonly present on the surface of these cells (121). In addition, CD14 is a glycosylphosphatidylinositol (GPI)-anchored membrane protein expressed on phagocytes (122) that serves as a co-receptor for TLR2 to facilitate the activation of the innate immune response against *B.*

burgdorferi. The loss of either TLR2 or CD14 in mice leads to a defective innate immune response against *B. burgdorferi* as infected TLR2$^{-/-}$ and CD14$^{-/-}$ mice displayed a severe defect in the control of spirochetes in tissues when compared to controls (41, 122). In contrast, both TLR2$^{-/-}$ and CD14$^{-/-}$ mice showed an increased severity of arthritis (41, 122) indicating that other regulatory pathways induced by lipoproteins contribute to the inflammatory responses in infected tissues.

In addition, several other TLR members and Nucleotide Oligomerization Domain-like receptors (NLR) have been linked to the recognition of *B. burgdorferi*. TLR5, a cell surface receptor for bacterial flagellin, has been shown to play a role in the recognition of *B. burgdorferi* products and induction of cytokines and chemokines in murine macrophages and human monocytes (123, 124). TLR2 may also cooperates with other endosomal TLRs (e.g.TLR7/8/9) in the induction of cytokines and/or type I interferons (e.g. IFN-α /-β) in human monocytes and PBMCs (124-126). Several lines of evidence suggest that these endosomal TLRs can sense *B. burgdorferi* products such as RNA and DNA after phagocytosis (125-127), which leads to the activation of NF-κB as well as IRF7 and IRF3 MyD88-independent pathways.

Intracellular NLR receptors such as Nod2 and NLRP3 inflammasome have been reported to participate in the recognition of *B. burgdorferi*, but the mechanism for how these receptors are activated is not well understood. Studies using Nod1 or Nod2 deficient PBMCs suggest that Nod2 played a major role in the recognition of spirochetes, as the production of cytokines was markedly lower in *B. burgdorferi*-stimulated cells from individuals with non-functional Nod2 when compared to healthy controls. However, Nod2$^{-/-}$ mice displayed much higher inflammation in the heart and joints during infection

than controls indicating that Nod2 is involved in down-regulating inflammation in Lyme borreliosis (128, 129). NLRP3 multi-protein complex belong to the NLRP family of inflammasomes that are activated by a unique set of microbial and endogenous ligands that triggers the assembly of this complex. This activated complex then induces maturation of inflammatory cytokines IL-1β and IL-18 through the action of caspase-1 (130). To date, there is limited information on which *B. burgdorferi* ligands activate the inflammasome; however, activation of NLRP3 complex is involved in the production of IL-1β in *B. burgdorferi*-stimulated murine macrophages (131). This finding was illustrated by the marked reduction of IL-1β levels in stimulated cells from mice deficient in NLRP3, the adaptor molecule ASC, or caspase-1 when compared to control mice (131). Caspase-1 dependent maturation of pro-IL-1β (inactive) appeared to regulate this reduced production of IL-1β in these cells (131). Despite the presence of proinflammatory cytokines that are the result of Nod2 and NLRP3 activation, the role of these NLR receptors in host defense and disease during Lyme borreliosis has not been fully characterized.

Phagocytosis of *B. burgdorferi*

Macrophages, monocytes, and neutrophils can also efficiently recognize and phagocytose *B. burgdorferi* spirochetes in large numbers (132, 133). Early studies into the kinetics of phagocytosis showed that spirochetes are internalized in human and murine macrophages as early as 5 min after incubation and are progressively detected within the cell's lysosomal compartments after 60 - 180 min incubation (132-135). Phagocytosis of spirochetes occurs through at least three mechanisms such as coiling phagocytosis, opsonic-mediated phagocytosis (132, 136), and conventional phagocytosis

(137, 138) (**Figure 5**). Phagocytic uptake of *Borrelia* by macrophages via coiling phagocytosis is characterized by the formation of actin-rich filopodial protrusions that capture and enwrap spirochetes, which ultimately are converted into coiling pseudopods inside the cell (139). The molecular mechanism of actin polymerization and rearrangement in macrophages during coiling phagocytosis of *Borrelia* is complex and involves several actin nucleation (e.g. mDia1 Arp2/3 complex, WASP, and FMNL1-formin) and regulatory factors (e.g. Daam1 CDC42, Rac1, and Rho GTPases) (139, 140). Following internalization of spirochetes, they are degraded within the phagolysosomes (133, 139). In addition, MyD88-dependent PI3K signaling appeared to play a role in the formation of this filopodium for phagocytosis of *Borrelia* by murine macrophages (141). Furthermore, inhibition of PI3K kinase in murine macrophages showed that phagocytosis was markedly reduced in MyD88 deficient cells to a similar level as controls (141), suggesting that the TLR2/MyD88/PI3K signaling pathway may be involved in the regulation of coiling phagocytosis of spirochetes.

Opsonic phagocytosis is a process mediated by the deposition of IgG antibodies on the surface of *B. burgdorferi* that target them for recognition and internalization by Fc receptors on phagocytes (132, 142). Macrophages have shown to be able to ingest spirochetes avidly with or without antibody-mediated opsonization (132, 143). In contrast, opzonization of spirochetes appeared to be required for monocytes and neutrophils to efficiently internalize them (142, 143). The Fc receptor has been proposed to play a role in the ingestion of spirochetes during the early stage of Lyme disease as immune complexes containing spirochetal antigens were commonly detected in serum samples in patients with EM lesions (142, 144). Studies using mice deficient in the Fc

common gamma chain (FcR$_\gamma^{-/-}$ mice) displayed higher bacterial burden in urinary

bladders and arthritis severity than infected control mice at early time points of infection

(145). This defective clearance of spirochetes during early infection suggests the

possibility of the involvement of at least two defects in antimicrobial defenses, as FcR$_\gamma^{-/-}$

mice are defective in macrophage-mediated opsonic phagocytosis and antibody-

dependent NK cell-mediated cytotoxicity (146).

In conventional phagocytosis, *Borrelia* ligands are directly recognized by

phagocytic receptors which are the main drivers in the engulfment of spirochetes by

macrophages (125). Several phagocytic receptors have been reported to mediate this

process that is discussed in the Results section below.
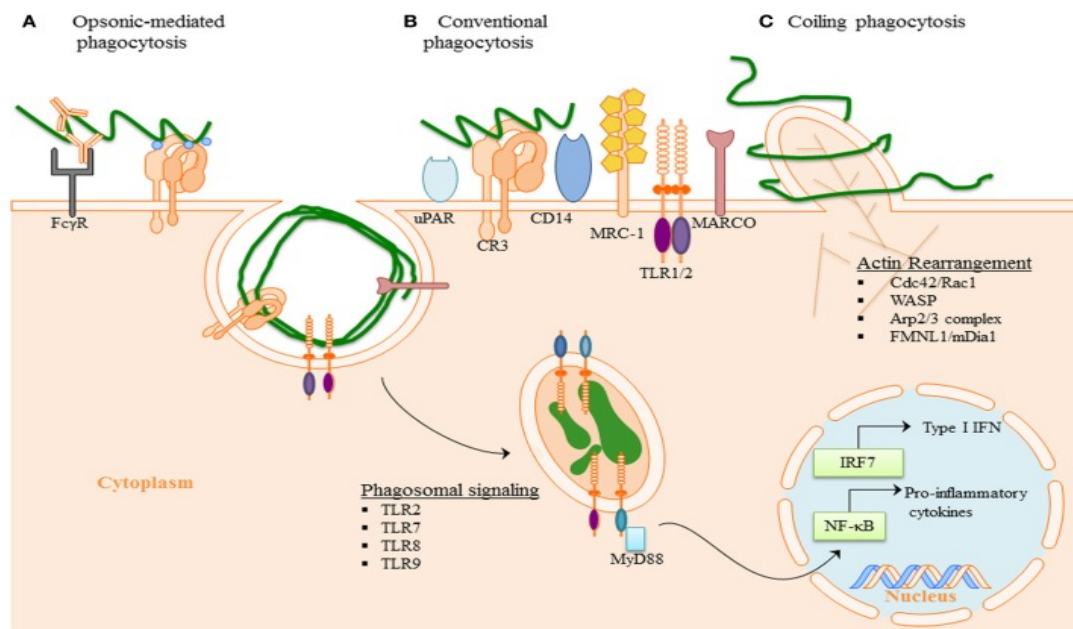
Figure 5. Proposed mechanisms of phagocytosis of *B. burgdorferi*. A) Opsonic

phagocytosis primarily involves the interaction of Fc receptors with opsonic antibodies

bound to the surface of spirochetes leading to internalization of this organism**.**

Additionally, complement receptor 3 (CR3 or CD11b/CD18) can also participate in the

uptake of spirochetes in the presence or absence of complement-derived opsonins, such as C3b and C3bi. **B)** Conventional phagocytosis involves the interaction of different phagocytic receptors (e.g. CR3 and scavenger receptors) that specifically recognize ligands on the surface of spirochetes, leading to the formation of pseudopod cups that move around the organisms. TLR2/1 heterodimers, CD14 receptors and other PRRs also contribute in the recognition of spirochetes and appear to have a positive role on conventional phagocytosis. **C)** Coiling phagocytosis involved the formation of unilateral F-actin filopodial protrusions which enwraps the spirochete and pulls it inside the phagocyte. TLR signaling can also occur from the phagosome after spirochetes are degraded in this compartment (schematic drawing of phagocytosis is reproduced from (125)). Following recognition of spirochetes by TLRs, phagocytes signal via MyD88-dependent or -independent pathways to generate inflammatory mediators (e.g. cytokines and type I IFN).

Antimicrobial killing mechanisms of phagocytes.

In order to survive in the mammalian host, *B. burgdorferi* must be able to overcome a variety of oxidative and non-oxidative stressors produced by professional phagocytes. Neutrophils can kill spirochetes either in the intracellular compartments or extracellularly by both oxidative and non-oxidative killing mechanisms (135, 143, 147-149). Neutrophils have been shown to ingest opsonized spirochetes more effectively than nonopsonized organisms (148), which eventually are killed within the phagolysosome. However, it is thought that the majority of spirochete killing by neutrophils occurs outside the cell (143). *In vitro* studies have shown that *B. burgdorferi* and the surface

lipoprotein OspA activate neutrophils to produce reactive oxygen species and nitrate species (150, 151). In fact, *B. burgdorferi* is susceptible to killing by both oxidative and nitrosative stresses, likely because its genome encodes a small number of antioxidant enzymes that defend against these stresses (152, 153). Neutrophils also produce granules filled with proteases and proinflammatory proteins that can kill spirochetes either in the phagolysosome or in the extracellular milieu. Among antibacterial granules produced by neutrophils, *B. burgdorferi* have been shown to be highly susceptible to elastase, LL-37, BPI protein, and human neutrophil peptide-1 (148, 154). Ongoing stimulation of neutrophils can also lead to the release of neutrophil extracellular traps, which are composed of DNA, antimicrobial histones, and granular proteases, that can capture and kill *B. burgdorferi* (149).

Macrophages are also critical in the clearance of *B. burgdorferi* during infection as they readily kill spirochetes by the action of proteases and oxidative stress (134, 143). Furthermore, opsonization of spirochetes has been shown to enhance killing of spirochetes mediated by both reactive oxygen and nitrogen species inside the cell (155). Although extracellular killing of spirochetes by macrophages can also occur, most of the killing of spirochetes by macrophages takes place in the phagolysosome vacuole (134, 155). Despite the susceptibility of *B. burgdorferi* to oxidative and nitrosative stress *in vitro*, no differences in spirochetal burden are observed in mice lacking either the subunits of the NADPH oxidase complex (Gp91phox$^{-/-}$ and Ncf1$^{-/-}$) (156) or the inducible nitric oxide synthase (iNOS$^{-/-}$) (157) when compared to wild-type mice. Thus, these findings raise the possibility that lacking the NADPH oxidase complex or inducible nitric oxide synthase could compensate for one another to control spirochetal burden *in vivo* or

29

have a compensatory role in other antimicrobial mechanisms during spirochetal infection.

Another possibility is that *B. burgdorferi* may exploit specific tissue milieus (114) and/or

host metabolites such as pyruvate (153) to resist oxidative stress.

Dendritic cells

Dendritic cells are a group of highly specialized antigen presenting cells whose

primary tasks are to recognize, ingest, process, and present antigens to T cells in

lymphoid tissues. Unlike neutrophils and macrophages, their major function is not to

ingest and kill bacteria but to alert and activate other effector cells of the innate and

adaptive immune systems (158). Traditionally, DCs are classified based on their

phenotypic and functional characteristics into four major groups such as epidermal

Langerhans cells (LCs), conventional DCs, monocytoid DCs, and plasmacytoid DCs

(158). Histologic and electron microscopy studies have demonstrated that DCs are

commonly present in the dermis and spirochetes can be observed within vacuoles in LCs

in the epidermis of EM lesions of patients infected with Lyme borreliosis (24, 159).

Dermal DCs from EM lesions were further characterized as plasmacytoid and

monocytoid DCs (115) and have been shown to have a higher ability to engulf

spirochetes than LCs *in vitro* (160). *B. burgdorferi* has been shown to induce the surface

expression of TLR1 and TLR2 in dermal DCs from EM lesions, suggesting that TLR2/1

heterodimer are important in the recognition of spirochetes and development of an

inflammatory response in the skin (115). However other TLRs may be involved in the

recognition of spirochetes by DCs since they can express all TLRs with the exception of

TLR9 (115, 161). DCs and LCs incubated with spirochetes *in vitro* showed that they were

also able to process and present spirochetal antigens via MHC class II molecules to T

helper cells (160). *B. burgdorferi*-pulsed DCs incubated with T and B cells mixtures *in vitro* can also induce the production of antibodies against *Borrelia* antigens (e.g. OspA) (160, 162). Another mechanism for how DCs can present *Borrelia* lipid antigens on the cell surface to interact with T cells or NKT cells is via the group I of CD1 molecules (163). Furthermore, *in vivo* studies showed that CD1d$^{-/-}$ mice had defective spirochetal clearance in tissues (164). Thus, together these data indicate that DCs contribute to the initial innate immune response in the skin during Lyme borreliosis.

Natural Killer cells

NK cells are large granular lymphocytes of the innate immune system that have the ability to kill abnormal cells and pathogens as well as to modulate inflammatory responses by secreting cytokines and engaging interactions with different immune cells, including DCs, macrophages, T cells, and endothelial cells (165). In Lyme disease, the role of NK cells during *B. burgdorferi* infection is not fully characterized. IFN-γ producing NK cells have been shown to be increased in the synovial fluid of infected patients with either antibiotic-responsive or antibiotic-refractory Lyme arthritis (166), suggesting that these cells could contribute to both spirochetal killing in patients without arthritis and in joint inflammation in patients with arthritis. NK cell cytotoxic activities against tumor cells *in vitro* have been shown to be markedly reduced in peripheral blood lymphocyte fractions from untreated patients with EM lesions and from patients in the chronic active stage of Lyme disease (167). This reduction in NK cell activity appeared to be mediated by the presence of viable spirochetes via an unknown mechanism (167). In contrast, antibody depletion studies with murine models of Lyme disease have shown that NK cells were not necessary for the development of arthritis (168, 169) and were not

31

involved in the control of bacterial burden in joints or the ability to prevent dissemination of spirochetes to tissues during infection (169). In addition, murine NK cells produce IFN-γ when co-incubated with *B. burgdorferi*-primed or OspA/B-primed macrophages (170). This observation suggests that NK cells could play a role in the activation of phagocytes at particular points of *B. burgdorferi* infection in mice.

Summary of introduction

B. burgdorferi is a tick-transmitted pathogen that has shown a great ability to survive and adapt to different host environments and to cause invasive and persistent infections in humans and other mammals. Once inoculated in the dermal tissue, this extracellular pathogen rapidly replicates at the site of inoculation and disseminates to multiple organs, causing disease (14). The outer membrane of *B. burgdorferi* is highly abundant with surface lipoproteins which play roles at distinct stages of mammalian infection (76). OspC expression has been shown to play an important role in the initial stage of colonization of tissues in the murine model of Lyme borreliosis. Other surface lipoproteins mediate attachment to different ECM components and host cells, resistance to complemement, and variation of antigens, which allow the spirochete to invade tissues and evade host defenses during disseminated infection (76, 84). At the same time, these surface lipoproteins stimulate the activation of tissue-specific resident and innate and adaptive effector cells at the site of infection. This leads to the production of inflammatory mediators and recruitment of leukocytes that are associated with the acute inflammatory lesions in humans and experimental animal models (18, 35). Studies using mouse models deficient in different components of the innate and adaptive immune systems have demonstrated that both arms of the immune system are required for

activation of host defenses against *B. burgdorferi* infection (114). Although *B. burgdorferi* burden is effectively controlled by innate and adaptive immunities in the mouse model of Lyme borreliosis, these animals can remain persistently infected for months to over one year as non-cultivable spirochetes are detected in collagen bundles in various tissues with minimal histopathological evidence of inflammation (35). Persistence of *B. burgdorferi* infection using different experimental animal models of Lyme disease is an area of active investigation.

CHAPTER II: RESEARCH GOALS

The role of *B. burgdorferi* OspC in protection against phagocytes

The *B. burgdorferi* genome encodes a large number of surface lipoproteins, many of which are expressed during mammalian infection (14, 67). One of these lipoproteins is the major outer surface lipoprotein C whose production is induced within infected nymphal ticks during feeding (49, 171). OspC remains produced during the early phase of infection and is highly immunogenic in mice (172, 173). As one of the strategies to evade host humoral responses, spirochetes downregulate OspC production in response to anti-OspC antibodies within 2-3 weeks after infection in mice (174, 175). OspC has shown to be required for *B. burgdorferi* to establish infection in mammals (49, 176). Infectivity studies demonstrate that the *ospC* mutant cannot establish infection in immunocompetent and SCID mice (lacking B and T cells) when inoculated at a dose of $10^3 – 10^5$ spirochetes per mouse (49, 65, 98, 177). The *ospC* mutant is cleared within the first 48 h of infection in the murine host (64), suggesting a protective role of surface lipoproteins against innate defenses. OspC also has been proposed to play roles in promoting survival and/or dissemination of spirochetes within the mammalian host. For example, OspC binds to a tick salivary protein, Salp15, which can protect spirochetes from complement- and antibody- mediated killing (111, 178). OspC has shown to bind host plasminogen (89, 179), and this phenotype correlates with invasiveness of spirochetes within mice (180). In addition, constitutive expression of heterologous lipoproteins in the *ospC* mutant has shown to restore infection in SCID mice, suggesting that OspC may have a non-specific structural role for *B. burgdorferi* (176, 177). On the other hand, another study suggested that the residues within the putative ligand-binding

domain are important for OspC function (179). Despite all research efforts, the precise biological function of OspC during infection remains unclear.

Innate immunity represents the first line of defense against *B. burgdorferi* infection in mammals (125, 143). Professional phagocytes, such as monocytes/macrophages and neutrophils, are among the first innate cells that spirochetes encounter during early infection in mammals (148, 181, 182). These phagocytes are essential in controlling the spirochetal burden and directing the development of adaptive immune responses during infection in the murine host (31, 32, 39). Phagocyte recognition of spirochetes is initiated by multiple TLR receptors, including TLR2/1 heterodimers, which signal through the adaptor molecule Myeloid differentiation primary response 88 (MyD88) (125). In murine models, deficiency of MyD88 results in markedly elevated *B. burgdorferi* burdens in tissues when compared to infected wild-type mice (38, 39). However, the *ospC* mutant remained non-infectious in MyD88$^{-/-}$ mice (183). Despite the understanding of the immune mediators that modulate host defense and inflammation in the murine model of Lyme borreliosis, the role of professional phagocytes and other innate cells in the clearance of the *ospC* mutant has not been examined.

In our studies, we investigated the role OspC for protection of spirochetes against innate host factors using a genetic, antibody-mediated, and pharmacological approach. We showed that the *ospC* mutant was not capable to establish infection in NODSCID-*IL2rγ^{null}* and anti-Ly6G-treated SCID mice, suggesting that NK cells, lytic complement, and neutrophils were not critical in the clearance of the *ospC* mutant *in vivo*. However, our results showed that F4/80^{+} phagocytes at the skin-site of inoculation are important in the clearance of the *ospC* mutant in clodronate-treated SCID mice. We further showed that

35

OspC played a role for *B. burgdorferi* in macrophage phagocytosis by reducing the uptake of GFP-expressing wild-type spirochetes in these phagocytes. Together our findings suggest that OspC protects *B. burgdorferi* strains from F4/80$^+$ phagocytes by promoting spirochete's evasion of these innate cells during early infection in mammals.

The role of elongation factor EF-Tu during Lyme borreliosis

B. burgdorferi expresses a large number of outer surface lipoproteins that are the major interface in interacting with host environments. Accumulated evidence has demonstrated that these surface proteins play a central role for the successful maintenance of *B. burgdorferi* within the enzootic life cycle involving *Ixodes* ticks and mammals (14, 184, 185). *B. burgdorferi* must adapt to these two markedly different host environments by coordinately altering its gene expression and antigen profile (67, 186, 187). A well-characterized example is the reciprocal regulation of the outer surface lipoproteins OspA and OspC (67, 188) when *B. burgdorferi* transitions between ticks and mammals. Spirochetes also use many of these surface lipoproteins during infection to bind a variety of ECM components, proteases and complement regulators such as plasminogen and factor H, and host cell types (83, 84). Some of these surface proteins also trigger an immune response and have been selected as serodiagnostic markers and potential vaccine candidates (189-191).

While much work on surface proteins have focused on lipoproteins, proteome analysis has recently described that known cytosolic proteins of *B. burgdorferi* are associated with membrane fractions in variable amounts (192, 193). One such protein is enolase, an enzyme that catalyzes the conversion of 2-phosphoglycerate into phosphoenolpyruvate for glycolysis in *B. burgdorferi* (60), that has also been shown to

associate with the cell surface and be present in outer membrane vesicles of spirochetes (193-195). Although the mechanism of how enolase is transported to the surface remains unclear, several reports have shown that enolase binds to plasminogen/plasmin *in vitro*, suggesting a role in assisting spirochetes to disseminate during mammalian infection. *B. burgdorferi* enolase also triggered an antibody response that reduced tick acquisition of spirochetes from mice (195). Another cytoplasmic protein that can be found on the surface of bacteria is the elongation factor Tu (EF-Tu). Surface EF-Tu from pathogenic bacteria has shown to perform functions involved in adhesion, invasion, and modulation of the host immune system (196, 197). For example, surface EF-Tu serves as fibronectin binding protein for *Mycoplasma pneumoniae*, which may facilitates the interaction of this pathogen with extracellular matrix (198). Surface EF-Tu from *Leptospira interrogans*, *Streptococcus pneumoniae*, and *Pseudomonas aureginosa* binds to the complement regulators factor H and plasminogen and may have roles in immune evasion and tissue invasion (199-201). Surface EF-Tu also plays a role in *Franciscella tularensis* adhesion and invasion of monocyte-like cells via interaction with nucleolin (202). Furthermore, proteome analysis have demonstrated that EF-Tu is membrane-associated in other pathogenic bacteria and could serve as an immunodominant protein (203-205). Thus, these observations complement recent reports describing EF-Tu as a novel moonlighting protein that exhibit multiple biological functions involved in bacterial benefit or virulence (196, 197).

The *B. burgdorferi* genome carries one copy of *eftu* gene (*bb0476*) which encodes for EF-Tu, a GTP binding protein (206) that is involved essentially in protein synthesis (60). Since surface EF-Tu has shown to play roles in virulence in other organisms, we

reasoned that EF-Tu localizes on the cell surface to play roles in *B. burgdorferi* infection in mammals. In this pilot study, we demonstrated that EF-Tu was highly immunogenic during mammalian infection since it was recognized by antibodies from infected mice and Lyme disease patients. However, we found that immunization of mice with recombinant EF-Tu (rEF-Tu) in Freund's adjuvant did not show protection against challenge with *B. burgdorferi*. Our finding demonstrated that EF-Tu resides primarily in protoplasmic cylinder inner membrane enriched fractions and associated with outer membrane vesicles in small quantities. Nevertheless, our results suggest that protoplasmic EF-Tu is an immunoreactive protein that could be examined as a serodiagnostic marker during early stages of *B. burgdorferi* infection.

CHAPTER III: MATERIALS AND METHODS

Bacterial strains and culture conditions

B. burgdorferi strain B31-A3 and the isogenic *ospC*K1 mutant (referred to as *ospC*) and the *ospC* complemented strains were kindly provided by Dr. P. Rosa and Dr. K. Tilly (Rocky Mountain Laboratories, National Institute of Allergy and Infectious Diseases, National Institutes of Health) (65). AH130 is an infectious low-passage strain derived from wild-type strain 297 (207). The *ospC* mutant (referred to as *ospC*) generated in the background of *B. burgdorferi* strain 297 was previously described (208). Low-passage, virulent *B. burgdorferi* strain 5A4NP1 (kindly provided by H. Kawabata and S. Norris, University of Texas Health Science Center at Houston) was derived from wild-type strain B31 by inserting a kanamycin resistance marker in the restriction modification gene *bbe02* on plasmid lp25.(209). Spirochetes were grown using standard Barbour-Stoenner-Kelly II (BSK-II) medium containing the relevant antibiotic. Cultures were maintained at 37 °C, pH 7.5 °C in a 5% CO_2 incubator and were passaged no more than three times from the original stocks. To measure growth rate of GFP-expressing spirochetes, cells were grown in BSK-II medium at 37 °C, pH 7.5 or pH 6.8. The cell density of cultures was monitored by counting spirochetes under the dark-field microscope (Olympus America Inc, Center Valley, PA).

Generation of GFP-expressing *B. burgdorferi* strains

Wild-type *B. burgdorferi* strain B31-A3 or AH130 and the isogenic *ospC* mutants were transformed with shuttle vector pTM61 (generously provided Dr. G. Chaconas, University of Calgary), that harbors a gene encoding GFP under the control of a constitutive *flaB* promoter from *B. burgdorferi* (50). Electrotransformation of *B.*

burgdorferi strains was performed as previously described (210). Selection for transformants was performed from cultures plated in a 96-well tissue culture plates (200 μl/well) containing liquid BSK-II medium and relevant antibiotic markers (50 μg ml^{-1} gentamicin and 200 μg ml^{-1} kanamycin or 50 μg ml^{-1} streptomycin). Positive wells containing transformants were identified by a color change of the medium, and the presence of fluorescent spirochetes was confirmed with an Axio Imager.A2 fluorescence microscope (Carl Zeiss, Jena, Germany).

The complemented *ospC* mutant carrying GFP was performed by transforming the *ospC* mutant with pTM61-derived shuttle vector carrying both a GFP gene and a wild-type *ospC* gene (pSEC002, primers to generate this construct listed in **Table 2**). Transformants were visualized by fluorescent microscopy and subjected to immunoblotting to verify the restoration of OspC (*ospC-gfp/ flgB*p-*ospC* referred as *ospC*-co).

Recombinant protein

The *B. burgdorferi* gene *bb0476* encoding EF-Tu from strain B31 was amplified by PCR using the primer pair Sa-bb0476-5 (forward) and Sa-bb0476-3 (reverse) (**Table 2**). The resulting amplicon was cloned into pET100/D-TOPO (Invitrogen, Carlsbard, CA) to generate plasmid pSCEFTUCT2, which was then entirely sequenced on both strands to rule out the possible introduction of undesired mutations during PCR and cloning procedures. EF-Tu-6×His fusion protein was expressed in *Escherichia coli* Rosetta (DE3) (Novagen, Madison, WI). Briefly, exponentially grown cells (A$_{600}$, 0.5) were induced for 5 h at 37°C with 0.1 mM (final concentration) of isopropyl-β-d-thiogalactopyranoside (IPTG). Cells were pelleted and resuspended in a buffer containing 400 mM NaCl, 40

mM NaH_2PO_4 (pH 7.2), 500 mM DTT, and 100 mM protease inhibitor PMSF (Sigma-Aldrich, St. Louis, MO). Cells were then lysed by brief sonication and debris was cleared by centrifugation. The resulting supernatant was loaded onto nickel-charged resin (Ni NTA, Qiagen, Valencia, CA) for affinity purification. After washing, protein was eluted with 500 mM imidazole and then concentrated with 40% ammonium sulfate. Protein was collected by centrifugation, dissolved in buffer solution (50 mM potassium phosphate, 10% glycerol, 0.1 mM EDTA buffer), and dialyzed against the same buffer overnight at 4°C. The dialysate was centrifuged at $5,000 \times g$ for 15 min, and the supernatant was filtered in 10,000 kDa molecular mass cutoff membranes (Fisher Scientific, Pittsburgh, PA) prior to use. Protein purity was assessed by SDS-PAGE. Protein concentration was measured using a Bradford protein assay kit (Bio-Rad, Hercules, CA).

Construction of a shuttle vector for constitutive expression of EF-Tu

To constitutively express the wild-type *eftu*, the DNA fragment of *eftu* was amplified by PCR from *B. burgdorferi* B31-A3 using primers PRYY7 and PRYY8 with restriction enzyme sites NdeI and PstI and a HA epitope tag sequence, respectively. The PCR products were digested with NdeI and PstI and inserted into the pBSV2-derived shuttle vector pJD55 under the control of a constitutive *Borrelia* promoter, P*flaB*. The resulting shuttle vector, pYY003, was verified by sequencing and then transformed into B31-A3 as described previously (184). The transformants (B31-A3/P*fla*B-*eftu*-HA) were selected in a 96-well tissue culture plates (200 μl/well) containing liquid BSK-II medium and relevant antibiotic markers (200 μg ml^{-1} kanamycin). The level of expression of EF-Tu in *B. burgdorferi* transformants was also verified by immunoblotting.

Protein electrophoresis and immunoblotting

SDS-PAGE and immunoblotting were performed as previously described (211). Monoclonal antibodies directed against OspC (182-105-D2), OspA (14D2-27), and the loading control FlaB (8H3-33) were described previously (212), and a dilution of 1:2000, 1:1,000, and 1:500 dilutions, respectively were used in our studies. A polyclonal mouse antibody against EF-Tu (1:15,000 dilution) was used to detect recombinant EF-Tu and EF-Tu in B31 whole-cell lysates using nitrocellulose membranes (Bio-Rad). HA.11 monoclonal antibody (1:1,000; clone 16B12; Covance, Princeton NJ) was used to detect HA-tagged EF-Tu in whole-cell lysates. OspA, FlaB, and/or EF-Tu antibodies were detected with horseradish peroxidase (HRP)-conjugated goat anti-mouse IgG secondary antibody (1:1,000; Santa Cruz Biotechnology, Santa Cruz, CA). Detection of peroxidase activity was determined in membranes using both 4-chloro-1-napthol and H_2O_2 (Fisher Scientific) solution or an enhanced chemiluminescent method (Pierce ECL Western Blotting Substrate, Thermo Scientific, Rockford, IL).

Sera from four C3H/HeN mice infected with 5A4NP1 (10^6 spirochetes / mouse) were pooled and used to assess the appearance of antibody response against recombinant EF-Tu protein. Sera was diluted 1:600 in 1 x PBS - 0.05% Tween-20 (PBS-Tween) and incubated at RT for 2 h with nitrocellulose membrane strips containing approximately 500 ng of recombinant EF-Tu protein per strip.

Human sera obtained from the CDC Lyme patient serum panels were used in immunoblotting assays to determine antibody reactivity to recombinant EF-Tu (500 ng/per strip). We used sera from 10 Lyme disease patients that tested positive by ELISA

and Western Blot to Lyme disease. Additionally, sera from 3 healthy donors, collected

from areas of the U.S. where Lyme disease is not endemic, were used as controls in these

immunoblotting assays. All human sera were diluted 1:100 in PBS-Tween for

immunoblotting (213), as described above.

Immunofluorescence assay

To determine whether EF-Tu is surface exposed, B31-A3 and B31-A3/P*fla*B-*eftu*-

HA spirochetes from mid-logarithmic phase cultures were probed in solution as

previously described (214, 215). Briefly, unfixed live spirochetes were incubated at room

temperature for 1 h in blocking solution (2% BSA in 1 x PBS with 5mM $MgCL_2$)

containing the primary antibodies of interest. A polyclonal antibody against EF-Tu and a

monoclonal antibody directed against HA.11 were used at a final dilution of 1:40 and

1:1000, respectively. Monoclonal antibodies directed against OspA and FlaB were used

at a final dilution of 1:40. After the primary incubation, spirochetes were washed twice

and gently resuspended in blocking solution, and then 20 μl of cell mixtures were added

on silylated microscope slides and air dried (CEL Associates, Pearland, TX). Slides were

then incubated with a 1:1,000 dilution of fluorescein isothiocyanate - conjugated goat anti

-mouse IgG (Jackson ImmunoResearch Inc, West Grove, PA) for 1 h at 37°C in a dark,

humid chamber. Slides were gently washed with blocking soltution and then mounted

with antifade light mounting medium (Molecular Probes, Eugene, OR). As an additional

control for these unfixed IFA experiments, spirochetes were incubated for 1h with

BacTrace fluorescein isothiocyanate-conjugated goat anti-*B. burgdorferi* antibody

(Kirkegaard and Perry Laboratories, Gaithersburg, MD) at a 1:100 dilution in blocking

solution. The presence of fluorescent spirochetes was confirmed with an Axio Imager.A2 fluorescence microscope (Carl Zeiss).

To detect the presence of EF-Tu, FlaB, and OspA in spirochetes, we also used an alternate IFA method in which spirochetes were placed onto silylated slides, air dried, and fixed and permeabilized by immersion in acetone solution (71, 214). This fixed IFA method was also used to detect the presence of fixed spirochetes in smears of fed tick larvae (71). Slides were then incubated at 37°C for 1 h with blocking solution (PBS-Tween 20 with 5% goat serum) in a humid chamber. Fixed spirochetes were incubated at room temperature for 1 h in blocking solution containing the primary antibodies of interest and then followed by washes and incubation with a secondary antibody, as described for the unfixed IFA method above.

Proteinase K accessibility assay

Proteinase K (PK) accessibility assays were performed as described (216, 217). Briefly, *B. burgdorferi* B31-A3 or B31-A3/P*fla*B-*eftu*-HA (1×10^8/ml) were gently washed three times in PBS (pH 7.4) and collected by centrifugation at 4,000 × g for 30 min. Washed spirochetes were then gently resuspended in 2.5 ml of PBS and split into five equal 500 μl volume samples. Four samples were treated with proteinase K (25, 50, 100 or 200 ug of PK) (Sigma-Aldrich) for 1 h at room temperature (RT) while one sample was incubated with 1 × PBS as a control. After incubation, samples were treated with 10 μl of PMSF (Sigma-Aldrich) to inactivate PK activity. Samples were subsequently pelleted by centrifugation at 10,000 × g for 10 min and resuspended in PBS for SDS-PAGE and immunoblotting.

TX-114 phase partitioning

To determine whether EF-Tu has the amphiphilic properties expected of an integral membrane protein, *B. burgdorferi* B31-A3 cells (10^9 organisms) were harvested and phase-partitioned as described previously (218). The resulting protein pellets were resuspended in PBS and subjected to SDS-PAGE and immunoblot analysis using the polyclonal antibody directed against EF-Tu or the monoclonal antibody against OspA, which is a well-characterized amphiphilic lipoprotein.

Isolation of outer membrane vesicles

Isolation of the OMVs of *B. burgdorferi* was performed as described (219, 220). Briefly $5 \times 10^{10} – 10^{11}$ *B. burgdorferi* cells were washed twice in 1 x PBS (pH 7.4) containing 0.1% BSA, resuspended and incubated on a rocker at room temperature for 2 h in ice-cold 25 mM citrate buffer (pH 3.2) containing 0.1% BSA. The resulting outer membrane vesicle and protoplasmic cylinder (PC) inner membrane enriched fractions were separated and purified on a sucrose density gradient as detailed (219). This PC fraction contains a number of axial filaments and periplasmic and inner membrane elements (219). The OMVs were monitored for purity by immunoblotting using antibodies against OspA and FlaB.

Cell lines

J2-retroviral infected alveolar macrophage cell line (AMJ2-C11) was purchased from ATCC, and grown in DMEM complete culture medium, as described previously (221). THP-1 human monocytic cell line was kindly provided by Dr. Janice Blum (Indiana University School of Medicine) and cultured in RPMI 1640 medium

supplemented 10% FBS, 2mM L-glutamine and 1% penicillin/streptomycin solution. Cells were passaged every 3-4 days in fresh RPMI medium. THP-1 cells were differentiated into macrophage-like cells by culturing with 100 nM of PMA in RPMI medium for 3 days as previously described (222). PMA-treated THP-1 cells were rested in fresh RPMI for a further 4 days before they were used for phagocytosis assays. PMA treated THP-1 cells were detached from the flask with nonenzymatic cell dissociation solution (Sigma-Aldrich). HL60 human promyelocitic cell line was kindly provided Dr. Hal Broxmeyer (Indiana University School of Medicine) and differentiated into neutrophil-like cells (PMN-HL60) by culturing with 1.25% (vol/vol) DMSO in DMEM medium for 6 days as previously described (223).

Isolation and immortalization of inflammatory peritoneal macrophages

Elicited murine macrophages from C57BL/6 mice were collected by peritoneal lavage with PBS 4 days after the injection of 4% thioglycollate, as described previously (224). Cells were resuspended in DMEM conditioned medium containing 10% FBS, 10 mM HEPES, 10 ng M-CSF, and 1% penicillin/streptomycin/amphotericin B solution (HyClone; Thermo Scientific) and incubated in a 6-well plate (Costar, Corning, NY) for 12 h at 37°C with a 5% CO_2. Nonadherent cells were removed by washing the monolayers with warm serum-free medium. Adherent peritoneal macrophage monolayers were infected with the supernatants of J2 cell line producing oncogenic retrovirus and mixed with DMEM conditioned medium and 1 μg/ml polybrene (Santa Cruz Biotechnology). After 24 h, cells were infected with a second treatment of J2 virus under the same conditions to improve transfection efficiency. Immortalized peritoneal

macrophages (PMs) were obtained about 4 weeks later and isolated using a previously described method (221).

Mouse strains and inoculation with *B. burgdorferi* strains.

NOD-*scid IL2rγ^{null}* mice (designated NODSCIDg) were acquired from either Jackson Laboratories (Bar Harbor, ME) or the *In vivo* Therapeutics Core at the Indiana University Simon Cancer Center (Indianapolis, IN). C57BL/6 (B6) *bTie2*-Cre mice were acquired from Jackson Laboratories, and B6 *eTie2*-Cre and B6 Stat3 floxed mice (Stat3$^{F/F}$) were a gift from Dr. Xin Yuan Fu (Indiana University School of Medicine). Mice with conditional deletion of Stat3 in endothelial cells (Stat3$^{E-/-}$) or myeloid cells (Stat3$^{B-/-}$) were generated by mating Stat3$^{F/F}$ with either *eTie2*-Cre or *bTie2*-Cre as previously described (225, 226). Of note, Stat3$^{B-/-}$ do not survive beyond 6 weeks of age, whereas Stat3$^{E-/-}$ and Stat3$^{F/F}$ are viable and develop normally (225, 226). C.B-17 *scid* and C3H/HeN mice were acquired from either Harlan Laboratories (Indianapolis, IN) or Taconic Laboratories (Germantown, NY). Some C.B-17 *scid* mice (hereafter designated SCID) were also from a breeding colony maintained at the Laboratory Animal Research Center (LARC) in Indiana University School of Medicine. Plac8$^{-/-}$ mice were acquired from Jackson Laboratories. Mice were housed under specific pathogen-free conditions at LARC. All mouse strains used in these studies are listed in Table 3.

For mouse infection, groups of 4- to 6-week-old C3H/HeN, SCID, and NODSCIDg were inoculated intradermally (i.d.) at the base of the tail, intraperitoneally (i.p.) or intravenously (i.v.) with a dose of either 10^3 or 10^5 spirochetes per mouse as indicated in each experiment. Groups of 4 week-old B6 Stat3$^{B-/-}$ and Stat3$^{F/F}$ mice and 8 week old B6 Stat3$^{E-/-}$ and Stat3$^{F/F}$ mice were i.d. inoculated with 10^5 or 10^6 spirochetes

per mouse as indicated in the appendix section. Mice were euthanized at specified time points ranging from 2 days to 6 weeks post-inoculation. All experiments were performed with the approval of the Indiana University Institutional Animal Care and Use Committee.

Infectivity was assessed weekly by culturing ear-punch biopsies in BSK-II medium supplemented with relevant antibiotic markers used to select each strain as well as the *Borrelia* antibiotic cocktail (50 μg ml^{-1} rifampicin, 20 μg ml^{-1} phosphomycin and 2.5 μg ml^{-1} amphotericin B). Cultures were evaluated for the presence of spirochetes by dark-field microscopy for up to 4 weeks before being designated as negative. A single growth-positive culture occurred within 1–3 weeks post-harvest and was used as the criterion to determine positive mouse infection in OspC or Stat3 studies.

Active immunization and infection studies

Groups of C3H/HeN mice were immunized with 50 μg recombinant EF-Tu in PBS (1:1) with adjuvant (complete Freund's adjuvant; Sigma-Aldrich). Mice received 2 boosts of 50 μg recombinant EF-Tu in PBS (1:1) with incomplete Freund's adjuvant (Sigma-Aldrich) at 14-day intervals. One week after the final boost, mice were inoculated with *B. burgdorferi* strain 5A4NP1 with a dose of 10^4 spirochetes per mouse. Mice were euthanized at either two weeks or five weeks post-inoculation. Infectivity was assessed by culturing ear pinna, joints, and heart tissues in BSK-II medium supplemented with the relevant antibiotic marker (kanamycin or 50 μg ml^{-1}) as well as the *Borrelia* antibiotic cocktail. A single growth-positive culture occurred within 1 week post-harvest and was used as the criterion to determine positive mouse infection.

For tick studies, pathogen-free *Ixodes scapularis* larvae were obtained from the Tick-Rearing Center at Oklahoma State University (Stillwater, OK). The tick-mouse experiments were conducted in the Vector-borne Diseases Laboratory at Indiana University School of Medicine. At three weeks post-inoculation, unfed larvae were placed on immunized mice (~ 50 larvae per mouse). At 72-96 h, these larvae had fully engorged and naturally dropped off the mice. A subset of fed larvae were subjected to IFA and qPCR analysis to determine *B. burgdorferi* acquisition and loads. The remaining fed larvae were maintained in a humidified chamber and allowed to molt to the nymphal stage (about 5 weeks). Two months after molting, unfed nymphs were then allowed to feed on immunized mice (~3 nymphs per mouse) and collected within 48 h after repletion. Two weeks after tick feeding, mouse tissues were collected and tested for infection by culture as described above.

Fluorometric phagocytosis assay

Murine PMs and PMA-treated THP-1 cells were seeded at a density of 3×10^5 cells/well in replicates of 5 in 96-well tissue culture plates with opaque sides and optically clear bottoms (Costar). On the following day, a subset of wells were preincubated for 30 min with the phagocytosis inhibitor cytochalasin D (5 µg/ml; EMD Chemicals, Gibbstown, NJ) before phagocytosis assays. PMs or PMA-treated THP-1 cells were challenged with GFP-expressing spirochetes at a multiplicity of infection (MOI) of 100:1 and co-incubated at 37°C with 5% CO_2 for 2 h. In scavenger receptor blocking experiments, a subset of wells were pretreated for 30 min with cytochalasin D (5 µg/ml) as a control of noninternalized spirochetes or 2.4G2 hybridoma supernatants containing antibodies that specifically block mouse Fcγ receptor (227). Then the

experimental samples were preincubated with scavenger receptor blockers for 30 min

before phagocytosis assay. Selected compounds for scavenger receptor experiments

included fucoidan (100-500 µg/ml; Sigma-Aldrich); poly I or the negative control

compound poly C (400 µg/ml; Sigma-Aldrich); monoclonal anti-mouse MARCO (12

µg/ml, clone ED31, AbD Serotec, Raleigh, NC) or anti-mouse IgG_1 (12 µg/ml, clone R3-

34, BD Pharmingen, San Diego, CA); monoclonal anti-mouse CD36 (50 µg/ml, clone

ME542, Santa Cruz Biotechnology) or anti-mouse IgA (50 µg/ml, clone M18-254, BD

Pharmingen) for phagocytosis assays. PMs were then challenged with GFP-expressing

spirochetes at MOI of 100 and incubated at 37°C with 5% CO_2 for 2 h. After infection,

cells were washed 3 times with PBS before adding 0.2% of trypan blue (Sigma-Aldrich)

to quench fluorescence of extracellular bacteria. Fluorescence was determined using a

microplate fluorometer, SPECTRAMax GEMINI EM at settings of 485 excitation/535

emission (Molecular Devices, Sunnyvale, CA). The phagocytic index (PI) represents the

fluorescence of intracellular spirochetes phagocytosed by macrophages and is expressed

in relative fluorescence units (RFUi) as previously described (228). The PI was

calculated by subtracting the fluorescence of extracellular spirochetes from cytochalasin

D treated wells from the total fluorescence of the experimental samples.

Flow cytometry and microscopy

GFP-expressing spirochetes were harvested for phagocytosis assay as described

above. Murine PMs, PMA-treated THP-1 cells or PMN-HL60 cells were challenged with

GFP-expressing spirochetes at an MOI of 100:1 for 2 h. Unstained cells (without GFP-

expressing spirochetes) were used as negative controls. Cells were washed twice in

FACS buffer (1x PBS, 2 mM EDTA and 0.5% FCS) and then fixed in FACS buffer

containing 1% paraformaldehyde. Samples were analyzed using a FACSCalibur flow

cytometer (BD Biosciences, San Jose, CA). To estimate the percentage of GFP-positive

macrophages, cells were gated by forward and side scatter properties, and GFP-positive

cells were identified in the FL1 channel. Cell debris interpreted as dead cells were

excluded from analysis. Data were analyzed with Cellquest (BD Biosciences) software

and histograms were edited in FlowJo software (Tree Star, Ashland, OR).

For immunofluorescence microscopy using murine PMs, cells were seeded at a

density of 3×10^5 cells/well in triplicates in 12-well tissue culture plates (Costar). PMs

were challenged with GFP-expressing spirochetes at an MOI of 100:1 and co-incubated

at 37°C with 5% CO_2 for 2 h. Samples were then washed three times with 1 x PBS and

incubated with 0.2% trypan blue before microscopy analysis. Fluorescent signal

corresponding to GFP positive cells was then imaged using an EVOS fl digital

fluorescence microscope (Advanced Microscopy Group, Bothell, WA) using GFP filter

(magnification, x10). As a control for these experiments, a subset of infected cells were

not quenched with trypan blue and another subset cells were treated with cytochalasin D

(5 µg/ml) to assess background fluorescence. Image J software was used for image

analysis and quantifications of the number of GFP positive cells.

In vivo phagocyte depletions

Clodronate encapsulated in liposomes (clodronate liposomes) were purchased

from www.clodronateliposomes.com (Vrije University, Amsterdam, The Netherlands).

To deplete F4/80$^+$ phagocytes in the skin, 50 µl of clodronate liposomes or PBS-

containing liposomes (PBS liposomes, control) were i.d. injected into SCID mice 48 and

24 h before challenge with *B. burgdorferi* strains at the same treatment site. SCID mice

were then i.d. and i.p. (150 µl) injected with either clodronate- or PBS- liposomes after

24 h post-challenge. In order to reduce recruitment of monocytes to the skin, SCID mice

were i.p. injected with either clodronate- or PBS- liposomes 48 h or 96 h post-challenge

(229).

For neutrophil depletion studies, we used the anti-Ly6G antibody method (clone

1A8, Bio-X-Cell, West Lebanon, NH) that effectively induces neutropenia in mice (230,

231). Briefly, groups of SCID and C3H/HeN mice were treated with intraperitoneal

injections of 250 µg/dose of anti-Ly6G 24 h and 2 h before *ospC* challenge and 24 h post-

challenge. As a comparison control group, SCID and C3H/HeN mice were injected with

three doses of 250 µg/dose of isotype antibody rat IgG_{2a} (clone R35-95, BD Biosciences)

or control rat IgG (Sigma-Aldrich).

Quantitative PCR and real-time RT-PCR

For quantification of *B. burgdorferi* DNA in mice and ticks, total DNA was

isolated from joint tissue and fed larvae (9-18 ticks per group) using DNeasy blood &

tissue kit as described in the manufacturer's protocols (Qiagen). qPCR of genomic DNA

was performed using the RT^2 SYBR Green ROX qPCR Mastermix (Qiagen). The

oligonucleotide primer pairs used to detect *flaB*, mouse *nidogen* (a gene coding for a 150

kDa glycoprotein), mouse β-*actin*, and tick *actin* were *flaB*-XF F/R, *nidogen* F/R,

qhxM*actin* F3/R3, and qT*actin*-F/R, respectively (**Table 2**) (210, 232, 233). Reactions

were carried out on an ABI Prism 7000 real-time PCR machine (Applied Biosystems,

Pleasanton, CA). Calculations of DNA copy number of *flaB* were normalized with the

copy numbers of either the mouse *nidogen* or *actin* genes or the tick actin gene, as

indicated in Results.

For real-time RT-PCR experiments, total RNA from murine peritoneal macrophages was extracted using TRIzol reagent (Invitrogen) according to the manufacturer's instructions. Complementary DNA was synthesized using a reverse transcription system (iScript, Bio-rad), and RT-PCR was performed with primers for *tnfa*, *il1b*, *il10*, and β-*actin* (**Table 2**) on the CFX96 Real-Time PCR Detection System (Bio-Rad Laboratories) as previously described (234). Expression levels of transcripts studied were normalized to the β-*actin* level, and the relative changes in gene expression were calculated using the comparative threshold cycle (C_t) and calculated relative to control uninfected cells ($\Delta\Delta C_t$ method).

The genotype of the offspring from crossing Stat3$^{F/F}$ × *eTie2*-Cre or Stat3$^{F/F}$ × *bTie2*-Cre was determined by conventional PCR as previously described (225). To determine the genotype of mice deficient in Stat3 in endothelial cells, we used CreF/CreB primers specific for Cre recombinase that yield a PCR product of 300 bp and I-17F/E-17B primers that yield a PCR product of 490 bp for the Stat3 wild-type allele and 520 bp for the floxed allele. To determine the genotype of mice deficient in Stat3 in myeloid cells, we used CreF/CreB primers for Cre recombinase and 12867-F/13071-R or oIMR9042-R primers that yield a PCR products of 361 bp for the Stat3 wild-type allele and 377 bp for the floxed allele (**Table 2**).

Leukocyte counts, Histology and Immunohistochemistry (IHC)

Peripheral blood from mice was collected by cardiac puncture after carbon dioxide narcosis. Leukocyte numbers were immediately determined using the hematology analyzer Hemavet 950FS (Drew Scientific, Oxford, CT).

For histology, skin sections (site of inoculation) were collected with 8-mm punch biopsy (Acuderm, Fort Lauderdale, FL) and fixed in 4% paraformaldehyde. Rear limbs were fixed in 10% neutral buffered formalin and decalcified with 10% EDTA solution. Tissues were embedded in paraffin, sectioned at 5 μm, and stained with H&E. Sections were viewed on a Leica DM3000 microscope (Leica Microsystems Inc., Buffalo Grove, IL).

Immunohistochemical staining for F4/80$^+$ cells was performed at the IHC core facility at Indiana University School of Medicine. Briefly, antigen retrieval was carried out in Dako PT module using low pH retrieval buffer (Dako, Carpintenia, CA). Sections were incubated with rat anti-mouse F4/80 antibody at a 1:100 dilution (AbD Serotec), and subsequently incubated with biotinylated donkey anti-rat antibody at 1:100 dilution (Jackson ImmunoResearch, West Grove, PA). Detection was accomplished using the LSAB2 method (Dako). Of note, the F4/80 monoclonal antibody has been widely used to detect mature tissue macrophages in mice (235, 236). Thus, murine macrophages from a spleen section were used as positive control.

To perform quantitative analysis of F4/80$^+$ stained sections, slides were scanned with an Aperio whole-slide digital imaging system (ScanScope CS, Aperio Technologies, Inc., Vista, CA). Skin sections were analyzed using the ImageScope Positive Pixel Count algorithm. The default parameters of the Positive Pixel Count (hue of 0.1 and width of 0.5) were used to detect F4/80$^+$ cells in sections. Data were collected by counting the number of strong positive staining per high power field, then averaging the results of 3 randomly selected regions (fixed region size = width of 300 pixels and height 300 pixels) per skin section.

Similar skin sections (site of inoculation) were evaluated by Warthin-Starry stain and indirect IHC for the presence of *B. burgdorferi* using a previously described methods (237, 238). Sections were incubated for 12 h at 4 °C with 1:1000 dilution of a polyclonal immune serum from *B. burgdorferi*-immunized rabbits (generously provided by Stephen Barthold, University of California-Davis).

Statistics

Data are presented as the mean ± SEM and were analyzed with the Prism 5.0 statistical program (GraphPad Software, San Diego, CA). Comparisons among groups were performed with one-way ANOVA followed with post hoc test as indicated in figure legends. Comparisons among two experimental groups were analyzed by Student's *t*-test. A *p* value ≤ 0.05 was considered significant.

Table 2. Primers used in these studies.

Primer	Sequence (5' → 3')
ospC B31-3 F	GGAGGTTTCCATGAAAAAGAATACATTAAGTGCA
ospC B31-3 R	ATGCTGCAGTTAAGGTTTTTTTGGACTTTCTGC
*flgB*p F	TGAGGTACCATGTTTAAGGTTT
*flgB*p R	TTCTTTTTCATGGAAACCTCCCTCAT
pSEC002-F1	GAGACCACATGGTCCTTCTTGAG
pSEC002-R1	GCGATTAAGTTGGGTAACGCC
Sa-bb0476-5	CACCATGAAATTTAGGAGGTTAGTCATGGC
Sa-bb0476-3	CTATTCCAATATCTCAAGAATTCTTCCTG
PRYY7	GCAGCCATATGGCAAAAGAAGTTTTTCAA
PRYY8	CGTCTGCAGTTAAGCGTAATCTGGAACATCGTATGGGTATTCC AATATCTCAAGAATTCTTCCT
qT*actin*-F	CGGGACCTGACCGACTACCTGATG
qT*actin*-R	CTCCTTGATGTCGCGGACAATTTC
qhxM*actin*-F3	AGAGGGAAATCGTGCGTGAC
qhxM*actin*-R3	CAATAGTGATGACCTGGCCGT
flaB-XF F	GCTCCTTCCTGTTGAACACCC
flaB-XF R	CTTTTCTCTGGTGAGGGAGCTC
nidogen F	CCAGCCACAGAATCACATCC
nidogen R	GGACATACTCTGCTGCCATC
tnfa-F	ACTTGGTGGTTTGCTACGA
tnfa-R	GATGAGAAGTTCCCAAATGGC
il1b-F	CTCTTGTTGATGTGCTGCTG
il1b-R	GACCTGTTCTTTGAAGTTGACG
il10-F	ATGGCCTTGTAGACACCTTG
il10-R	GTCATCGATTTCTCCCCTGTG
mouse-BAC-F	CTGCCTGACGGCCAAGTC
mouse-BAC-R	CAAGAAGGAAGGCTGGAAAAGAG
CreF	CGATGCAACGAGTGATGAGG
CreB	CGCATAACCAGTGAAACAGC
I-17F	ATTGGAACCTGGGACCAAGTGG
E-17B	ACATGTACTTACAGGGTGTGTGC
12867-F	AGTTCTCGTCCACCACCAAG
13071-R	CCTTGTGTGGTCTGAGAACGT
oIMR9042-R	CTTCGTATAGCATACATTATA

Table 3. Mouse strains used in these studies.

Mouse strain	Immune system phenotype
C3H/HeN	Normal immune system
NOD-*scid IL2rγ*^{null}	Lacks mature B and T cells, functional NK cells and C5 complement
C.B-17 *scid*	Lacks mature B and T cells
C57BL/6 *bTie2*-Cre	Myeloid-specific *Tie2* gene promoter drives the expression of Cre
C57BL/6 *eTie2*-Cre	Endothelial-specific *Tie2* gene promoter drives the expression of Cre
C57BL/6 Stat3 floxed	The *stat3* gene is flanked by loxP sites
C57BL/6 Stat3$^{B-/-}$	Deletion of *stat3* gene from myeloid cells
C57BL/6 Stat3$^{E-/-}$	Deletion of *stat3* gene from endothelial cells
C57BL/6 Plac8$^{-/-}$	Targeted mutation of *plac8* gene from epithelial cells, macrophages, and granulocytes

CHAPTER IV: RESULTS

Part I- Outer Surface Protein OspC protects *Borrelia burgdorferi* from phagocytosis by macrophages

The *ospC* mutant cannot establish infection in NODSCIDg mice deficient in lytic complement and NK, B and T cells

Previous studies have shown that the *ospC* mutant cannot establish infection in C3H/HeN and SCID mice that lack functional T and B cells (49, 64, 65, 177), suggesting that innate immunity is involved in clearance of *ospC* mutant spirochetes in mice. To investigate which innate factors are involved in clearance of the *ospC* mutant *in vivo*, we examined the infectivity of the *ospC* mutant in another mouse strain, NODSCIDg, which are deficient in T and B cells, as well as lacking C5 complement and functional NK cells (239). Loss of complement-factor C5 prevents the activation of C5b and thereby inhibiting the formation of the C5b-9 membrane attack complex (239, 240). Groups of NODSCIDg mice were i.d. injected with either wild-type B31-A3 or the *ospC* mutant. We used an inoculum of 10^3 spirochetes per mouse, as previously reported (49, 64, 65, 99). NODSCIDg mice were also inoculated intravenously, to assess whether the injection site plays a role in the infectivity of the *ospC* mutant. As controls, groups of SCID and C3H/HeN mice were also challenged with wild-type or the *ospC* mutant. Whereas wild-type B31-A3 spirochetes were readily detectable in all tested tissues from NODSCIDg, SCID and C3H/HeN mice after 3 weeks post-challenge, no *ospC* mutant spirochetes were detected in tissues from mice inoculated with 10^3 spirochetes per mouse (**Table 4**). This result is similar to previous studies with immunocompetent and SCID mice (49, 65, 177). The *ospC* mutant was not infectious in NODSCIDg mice even after 6 weeks post-

inoculation (data not shown), regardless of the route of inoculation. These results suggest that, in addition to lymphocytes, innate components such as lytic complement and NK cells are not the major factors that eliminate the *ospC* mutant *in vivo*.

Table 4. **Infectivity of wild-type *B. burgdorferi* (B31-A3) and the isogenic *ospC* mutant in NODSCIDg, SCID, and C3H/HeN mice.**

	Route of Inoculation*	Dose	*B. burgdorferi* strain	3 weeks PI^
NODSCIDg	i.d.	10^3	B31-A3	3/3
NODSCIDg	i.d.	10^3	*ospC*	0/3
NODSCIDg	i.v.	10^3	B31-A3	3/3
NODSCIDg	i.v.	10^3	*ospC*	0/3
SCID	i.d.	10^3	B31-A3	3/3
SCID	i.d.	10^3	*ospC*	0/6
C3H/HeN	i.d.	10^3	B31-A3	3/3
C3H/HeN	i.d.	10^3	*ospC*	0/6

* Spirochetes were inoculated either intradermally (i.d.) or intravenously (i.v.) in BSK as vehicle.
^ All mice were euthanized at 3 weeks post-inoculation (PI). Isolation of spirochetes was attempted from skin-site of inoculation, ear pinna, tibio-tarsal joint, heart base and spleen. Culture results expressed as number of mice infected/number of mice tested. Infectivity experiments were conducted 3 separate times.

Establishment of dose and vehicle for inoculation to study the *ospC* mutant *in vivo*

Since NODSCIDg have defective functions in different innate cells, we chose an immunodeficient model with an intact innate immune system such as SCID mice to assess the role of innate cells in clearance of the *ospC* mutant. To establish a system to study the *ospC* mutant in SCID mice, the infectious dose and the vehicle to deliver spirochetes were evaluated in a series of infectivity experiments. Spirochetes used in the infectivity studies above were inoculated in mice using BSK-II growth medium, which is a commonly used vehicle to test infectivity of *B. burgdorferi* strains and mutants in mice.

Since BSK-II is a complex medium with 6% rabbit serum and 5% BSA (241) that may alter the host immune response at the skin-site of spirochetal inoculation, we next tested whether the *ospC* mutant can establish infection using a minimal medium vehicle such as PBS buffer. We also compared two routes of inoculations, intradermal or intraperitoneal.

Groups of SCID mice were injected with an inoculum of 10^5 of either B31-A3 or *ospC* mutant spirochetes per mouse. We increased the inoculum size to 10^5 spirochetes since PBS or saline could affect viability of spirochetes based on our preliminary infectivity experiments (data not shown). Similar to infectivity experiments above, the *ospC* mutant was not detected by culture in any harvested tissues from SCID mice when injecting 10^5 spirochetes per mouse, regardless of vehicles used (PBS buffer or BSK-II medium) or route of inoculation (i.d. or i.p.) (**Table 5**). Thus, the infectivity results using 10^5 spirochetes with PBS as a vehicle provide a well-defined minimum medium with which to explore the interaction of OspC-lacking spirochetes with innate host factors *in vivo*.

Table 5. Infectivity of wild-type *B. burgdorferi* (B31-A3) and the *ospC* mutant in SCID mice using different vehicles and routes of inoculation.

Bb strain	Dose	Route of Inoculation*	Vehicle	3 weeks PI^
B31-A3	10^5	i.d.	PBS	3/3
	10^5	i.p.	PBS	3/3
	10^5	i.d.	BSK	3/3
ospC	10^5	i.d.	PBS	0/3
	10^5	i.p.	PBS	0/3
	10^5	i.d.	BSK	0/3

* Spirochetes were inoculated either intradermally (i.d.) or intraperitoneally (i.p.) in either PBS or BSK as vehicles.
^ All mice were euthanized at 3 weeks PI. Isolation of spirochetes was attempted from skin-site of inoculation, ear pinna, tibio-tarsal joint, heart base and spleen. Culture results

expressed as number of mice infected/number of mice tested. Infectivity experiments were conducted in 2 separate trials.

Phagocytes contribute to the clearance of the *ospC* mutant at the skin inoculation site

The data above, along with previous studies by others, suggest that B cell, T cell, lytic complement and NK cells were not the major host factors that eliminate the *ospC* mutant *in vivo*. We next investigated whether professional phagocytes may play an important role in the clearance of the *ospC* mutant. For this purpose, we chose SCID mice since they have a functional innate immune system (240, 242). Groups of SCID mice were treated with clodronate liposome to induce depletion of phagocytes in the skin-site of inoculation of *B. burgdorferi* strains. Immunostaining of skin sections harvested 7 days post-challenge confirmed a significant reduction in F4/80 positive phagocytes in SCID mice treated with clodronate and challenged with either wild-type or *ospC*-deficient spirochetes (**Figure 6**). These immunostaining results are in agreement with previous studies showing that subcutaneous injections of clodronate liposomes selectively depleted the number of resident macrophages in mouse models of skin disorders (229, 236).
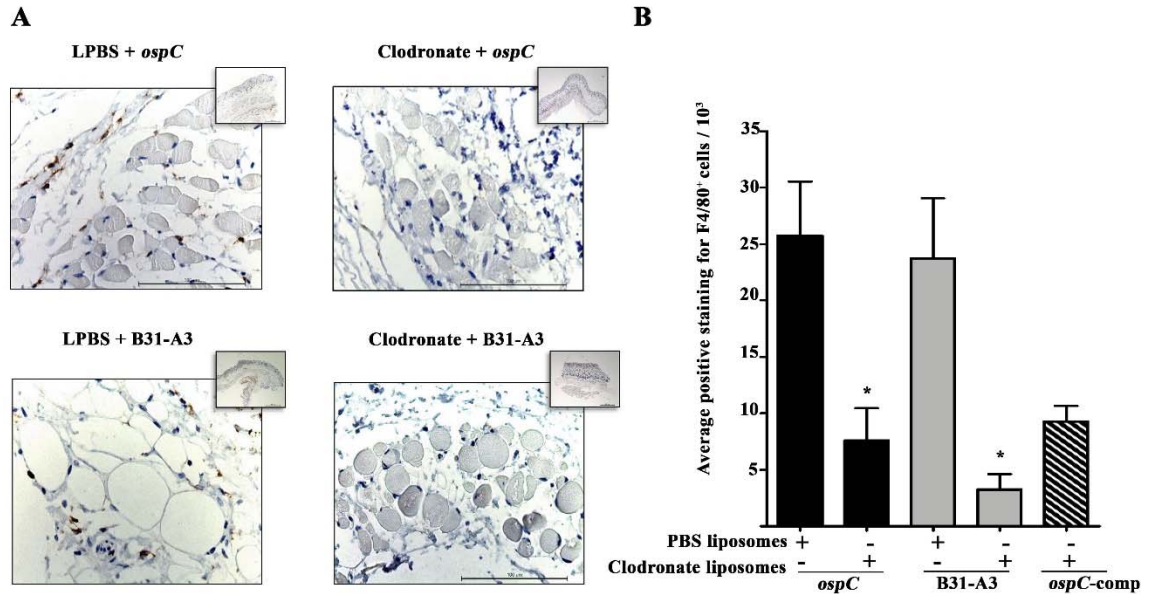
Figure 6. Clodronate liposome administration reduced the number of F4/80$^+$ phagocytes at the site of inoculation. A) Representative images of immunohistochemical staining for detection of F4/80$^+$ cells (brown) in skin sections (magnification, ×40) from SCID mice treated with either clodronate or PBS liposomes (LPBS) 7 days after infection. **B)** Quantification of F4/80$^+$ cell of the images in (**A**) using Aperio image analysis algorithms (y-axis represents the number of positive staining within the analyzed region / 10^3). Data represent the mean ± SEM for three separate fixed regions per mouse skin section (n = 3 mouse skin section per group). Student's t test was used to determine significance (*, $P < 0.05$).

To determine the effect of phagocyte depletion on the infectivity of the *ospC* mutant, we examined the presence of spirochetes in various tissues 7 days post-challenge. As shown in **Figure 7**, the *ospC* mutant spirochetes were able to establish infection in the majority of mice (90%; 9/10) treated with clodronate. The *ospC* mutant was re-isolated

from skin-site of inoculation, heart blood and/or joints. Furthermore, *ospC* spirochetes were detected by special staining of spirochetes at the skin-site of inoculation in clodronate-treated SCID mice even at day 7 post-challenge (**Figure 7**). As expected, the *ospC* mutant could not infect the SCID mice treated with PBS liposomes (**Figure 7A-B)**. In clodronate-treated mice, the *ospC* mutant disseminates to tissues distant from the inoculation site, and the dissemination correlated with high neutrophil counts in blood similar to what is observed in SCID mice infected with wild-type spirochetes (**Figure 7A & 8**). Collectively, these results show that phagocytes contribute to the clearance of the *ospC* mutant at the skin inoculation site in SCID mice.

Spirochetal burden in joint tissues was quantified by real-time qPCR analyses at day 7 post-infection. When infected with wild-type spirochetes, clodronate-treated mice developed the highest spirochetal burden in joints (**Figure 7C**). When infected with the *ospC* mutant, joints from PBS liposome-treated SCID mice did not have detectable *B. burgdorferi* DNA (**Figure 7C**), which was consistent with the culture-negative results from tissues, including joints from this group of animals (**Figure 7C**). This result provides evidence that the *ospC* mutant was not able to colonize the joint in PBS liposome-treated mice, whereas the wild-type strain was readily detectable in joints at 7 days post-infection in PBS liposome-treated animals. Although the *ospC* mutant spirochetes were readily detectable in joints of clodronate-treated animals, the bacterial load was at least ten-fold lower than the bacterial load in joints from clodronate-treated mice that were infected with wild-type spirochetes (**Figure 7C**). These data suggest that phagocytes contribute to the clearance the *ospC* mutant in SCID mice, but removal of these cells in SCID mice is not sufficient to restore *ospC* spirochetal burden in joints to

wild-type levels.
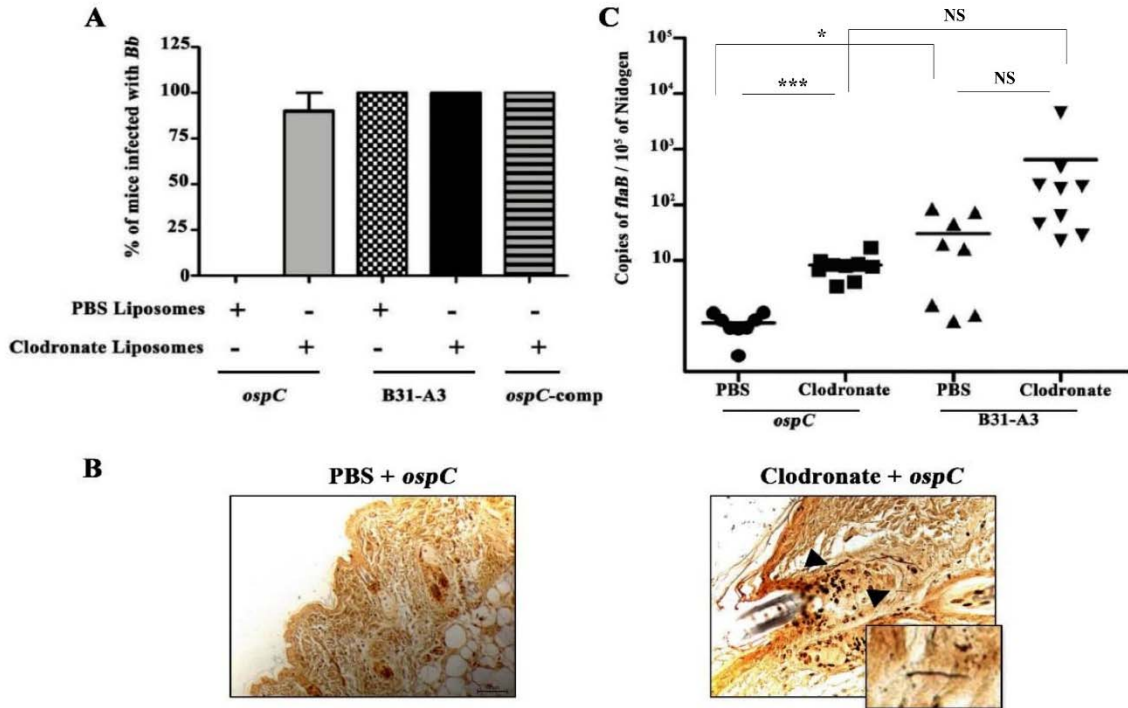
Figure 7. The *ospC* mutant disseminates and colonizes F4/80[+] phagocyte-depleted SCID mice. A) Infectivity of wild-type, the *ospC* mutant, or the complemented mutant strain (*ospC*- comp) in mice either treated with clodronate or PBS liposomes (control). The number of mice used in each group for wild-type, *ospC* mutant, and the complemented strains was 9, 10, and 7, respectively. Infectivity for each bacterial strain was determined from cultivation of spirochetes from the skin-site of inoculation, heart blood, tibio-tarsal, and ear pinna at day 7 post-challenge. **B)** A representative Warthin-Starry stain that demonstrated the presence of *ospC* mutant spirochetes at the skin site of inoculation (right bottom inset, magnification, x40) from clodronate liposome-treated SCID mice (culture positive, N = 5). Spirochetes were observed in dermis (black arrows) and fasciae underneath skeletal muscle**.** No *ospC* mutant spirochetes were detected at the skin site of inoculation (left bottom inset) of PBS liposome-treated SCID mice at day 7

post-challenge (culture negative, N = 5). **C)** Quantitation of spirochetal burden in tibio-tarsal joints of clodronate-treated mice. The isolated DNA was subjected to qPCR analyses for *B. burgdorferi flaB* gene and mouse *nidogen* housekeeping gene. Data are representative of two separate experiments, and each black line indicates the mean ± SEM for nine to ten mice in each group. Comparisons of PBS- and clodronate-treated animals were performed using unpaired Student's *t* test with Welch's correction (*, $P \leq$ 0.05, ***, $P \leq 0.0005$, NS = not significant).

To determine whether systemic dissemination *B. burgdorferi* had an effect on leukocytes, we compared leukocyte numbers from peripheral blood collected at day 7 post-challenge from PBS- and clodronate- liposome treated animals. Neutrophils were significantly elevated in PBS- or clodronate-liposome treated groups of mice with disseminated *B. burgdorferi* infection. Conversely, neutrophils were normal in uninfected SCID mice that were treated with PBS- liposomes and challenged with *ospC* spirochetes (**Figure 8**), as this group of mice had cleared the *ospC* mutant from the skin-site of inoculation. The leukocytes in blood from this group of animals were at normal levels comparable to naïve mice (**Figure 8**). Together, these findings suggest that spirochetal dissemination triggered the recruitment of neutrophils in SCID mice, regardless of clodronate treatment.
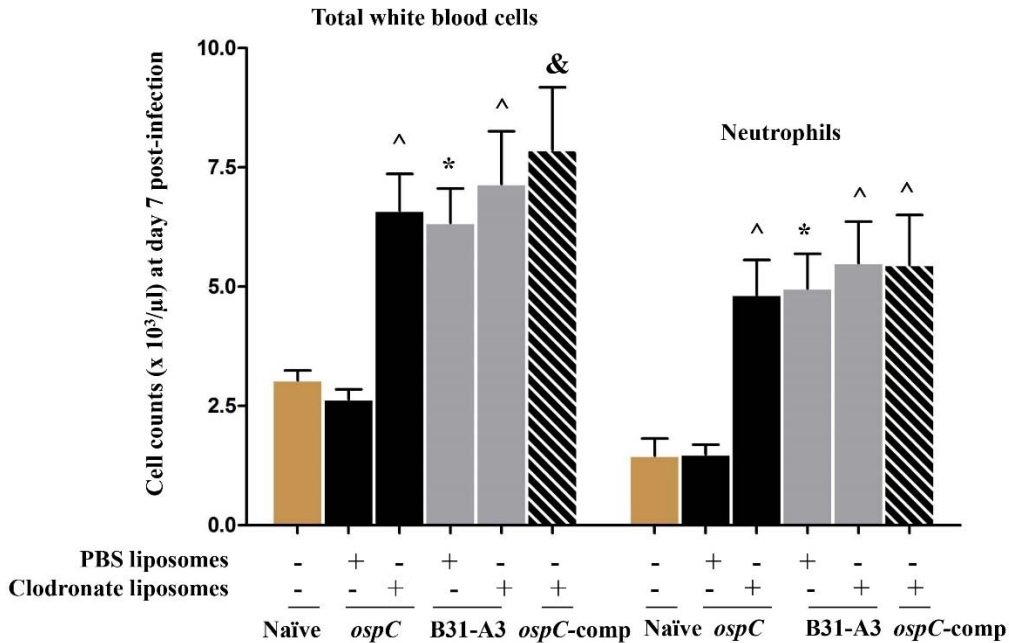
Figure 8. Neutrophils are increased in the circulation when *B. burgdorferi* strains have established infection in SCID mice treated with clodronate or PBS liposomes. Peripheral blood was collected at day 7 post-challenge in EDTA-coated tubes and was analyzed with a HEMAVET 950 multispecies hematology cell counter. Normal reference values of total white blood cells and neutrophils in mice are ≤ 10.7 and ≤ 2.5 (x $10^3/\mu l$), respectively. Data are representative of two separate experiments and each bar represents mean ± SEM for seven to ten mice per treatment group. Total white blood cell and neutrophil counts from 3 naïve age-matched SCID mice are shown as a comparison group (brown bars). Comparisons of experimental treated-groups were performed with one-way ANOVA followed by Bonferroni's post hoc test (*, $P < 0.05$; ^, $P < 0.01$; &, $P < 0.001$).

Treatment of mice with neutrophil-depleting antibody does not restore infectivity of the *ospC* mutant

Since neutrophils are commonly recruited to the sites of spirochetal infection in mice (143, 181), we then assessed whether removal of neutrophils in mice would allow the *ospC* mutant to survive and disseminate *in vivo*. To test this, groups of SCID and C3H/Hen mice were treated with anti-Ly6G monoclonal antibody that specifically depletes neutrophils in mice (230). We found that the *ospC* mutant was not able to survive at the skin-site of inoculation and disseminate to tissues in anti-Ly6G treated SCID mice 48 h and 7 days post-challenge (**Table 6**). Furthermore, the *ospC* mutant could not establish infection in anti-Ly6G-treated C3H/HeN mice that exhibited a profound neutropenia (85% depletion, **Figure 9**) during the first 48 h post-challenge. Together, these results indicate that removal of neutrophils during early events of spirochetal infection is not sufficient to restore the *ospC* mutant infectious phenotype.

Table 6. The *ospC* mutant cannot establish infection in SCID and C3H mice treated with anti-Ly6G monoclonal antibody.

Mouse strain	Treatment	Dose	Bb strain	48 hr PI^	1 week PI^
SCID	Anti-Ly6G	10^5	*ospC*	0/3	0/3
SCID	Control IgG	10^5	*ospC*	0/3	0/3
C3H/HeN	Anti-Ly6G	10^5	*ospC*	0/3	ND[+]
C3H/HeN	Control IgG	10^5	*ospC*	0/3	ND

^ All mice were euthanized at either 48 h or 1 week PI. Isolation of spirochetes was attempted from skin-site of inoculation, ear pinna, tibio-tarsal joint, and heart blood. Culture results expressed as number of tissues infected/number of tissues tested from mice after 48 h and 1 week post-inoculation with *ospC* spirochetes.
+ Not determined (ND).
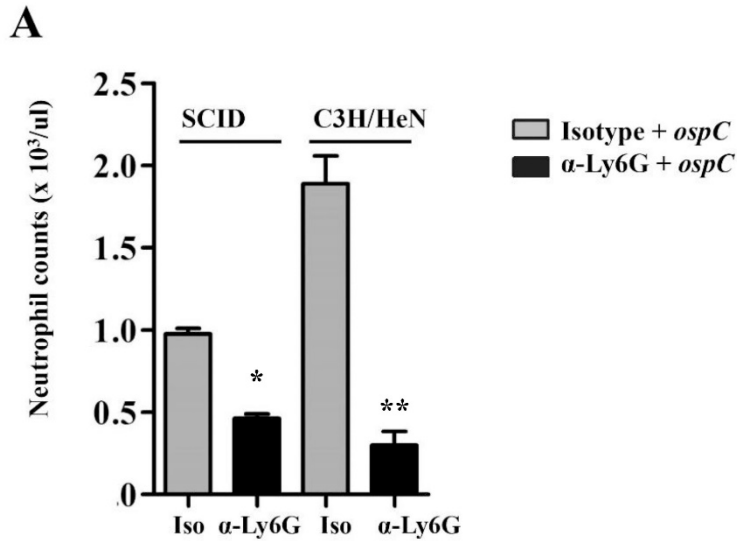
Figure 9. **Treatment with anti-Ly6G reduces neutrophils in circulation of SCID and C3H/HeN mice after 48 h post-challenge with the *ospC* mutant. A)** Peripheral blood from mice treated with either anti-Ly6G antibody or isotype (Iso) control was analyzed with a HEMAVET 950 multispecies hematology cell counter within 24 h after the last antibody treatment. Data represent the mean ± SEM for three mice per treatment group. Comparisons of anti-Ly6G- and isotype-treated groups were performed using unpaired Student's *t* test with Welch's correction (**, $P \leq 0.001$, * $P < 0.01$).

Abrogation of OspC increases phagocytosis by macrophages

The above observation that phagocytes contributed to the clearance of the *ospC* mutant *in vivo* prompted us to assess the interaction of these cells with spirochetes. To assess this interaction, we first generated GFP-expressing wild-type, *ospC* mutant, *ospC* complemented spirochetes. Our immunoblotting results showed that both GFP-expressing wild-type and complemented strains (B31 and 297) were not defective in

OspC expression when cells were harvested for these experiments (**Figure 10A-B**). In addition *in vitro* growth analysis showed that the GFP-expressing *ospC* mutant spirochetes exhibited a similar growth pattern as the GFP-expressing wild-type (B31) spirochetes when cultivated under conditions analogous to those present in the mammalian host (e.g. 37°C, pH 7.5) and feeding ticks (e.g. 37°C, pH 6.8) (**Figure 11A-B**).
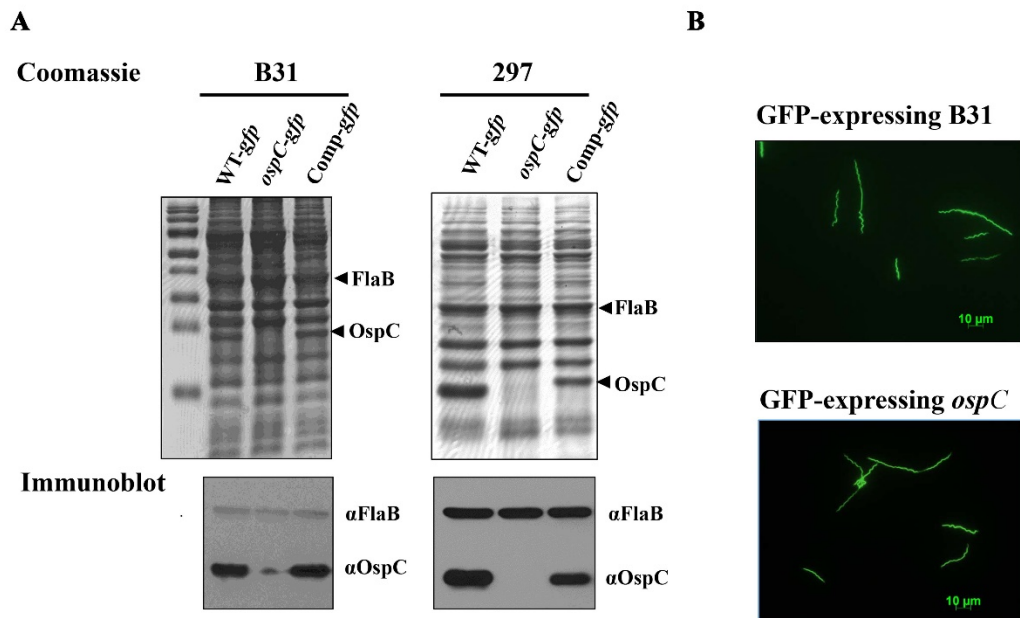
Figure 10. Generation of wild-type, *ospC* mutant and complemented mutant strains expressing GFP. **A)** Immunoblot showing the OspC production in GFP-expressing strains of *B. burgdorferi*. Top: Coomassie blue-stained gel. Bottom: Immunoblot probed with antibodies recognizing FlaB (control) and OspC. **B)** Immunofluorescence micrograph showing GFP-expressing wild-type (B31-A3, top panel) and the *ospC* mutant (bottom panel) *B. burgdorferi* strains (Scale bar: 10 μm.)

A

Bb-GFP grown in BSK II, 37 °C / pH 7.5

B

Bb-GFP grown in BSK II, 37 °C / pH 6.8
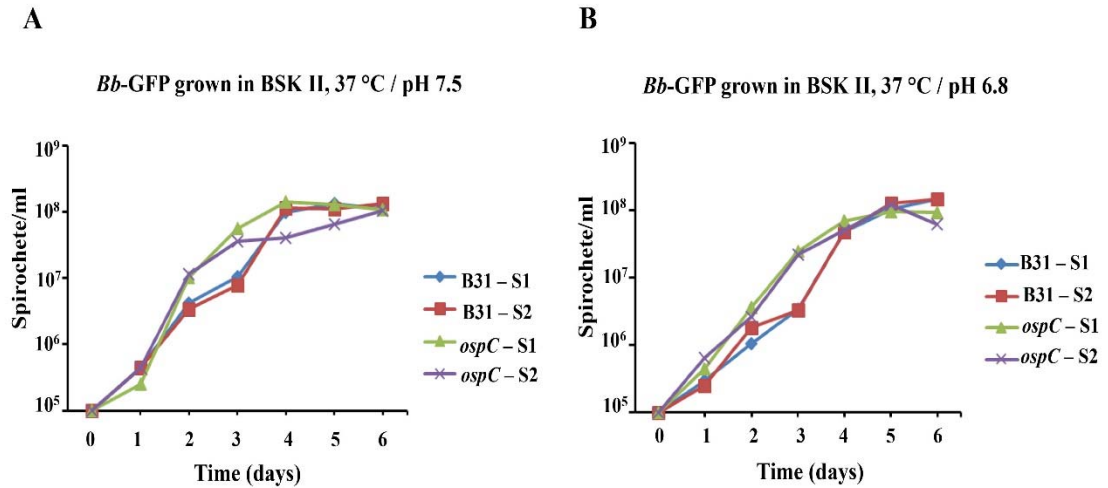
Figure 11. **The GFP-expressing *ospC* mutant exhibited a growth pattern similar to that exhibited by the B31 wild-type strain when cultivated in standard BSK-II medium. A-B)** Growth curves were measured while cells were growing in BSK-II medium at 37°C and pH 7.5 or pH 6.8. The initial cell density was 3×10^5 spirochetes/ml for each strain. Spirochetes were enumerated daily under dark-field microscopy. Data presented here is from one experiment with two independent cultures (S1 = sample 1 and S2 = sample 2). Each data point is expressed as the mean from six independent fields.

Given that phagocytosis is an innate mechanism that phagocytes employ to eliminate spirochetes (118), we then investigated the uptake of these GFP-expressing *B. burgdorferi* strains by phagocytes using a fluorometric-based method. We selected macrophages for these experiments because these cells are highly phagocytic and express the F4/80 marker at high levels on the cell surface. To evaluate the internalization of spirochetes in our fluorometric-based phagocytosis assays, murine or human macrophages were preincubated for 30 min with 5 µg/ml cytochalasin D prior to the addition of spirochetes. We found that cytochalasin D effectively blocked internalization

70

of spirochetes in PMs (**Figure 12**). This result is consistent with phagocytosis assays using *B. burgdorferi* and human monocytes or murine BMDM, as cytochalasin D has been used to inhibit the internalization of spirochetes in these cells (124, 147). Thus, we used cytochalasin D in our assays to estimate the background fluorescence from extracellular spirochetes adhered to macrophages, which in turn was subtracted to the total relative fluorescence of the experimental sample to obtain a corrected unit that was used as a surrogate marker of spirochetal ingestion by macrophages. Our fluorometric based phagocytosis assay showed the *ospC* mutant had approximately 75% higher phagocytosis by murine PMs than the wild-type and the *ospC*-complement strains (**Figure 13A left**). Based on our preliminary data using MOIs of 10:1 and 100:1, we found that an MOI of 100:1 had the greatest effect on phagocytosis of the *ospC* mutant and selected this MOI for the rest of our phagocytosis assays. We also found that phagocytosis was enhanced when using a different *ospC* mutant that was generated in *B. burgdorferi* strain 297 (202) (**Figure 13A right**). Flow cytometry also confirmed that the *ospC* mutant had approximately 70% higher uptake by murine PMs than the parental wild-type spirochete (**Figure 13B**). Additionally, we used immunofluorescent microscopy to count the number of GFP positive PMs during phagocytosis and found that the number of GFP positive events for PMs challenged with the *ospC* mutant was enhanced when compared to the wild-type 297 strain (**Figure 14A-B**). Together, these results suggest that OspC could have an anti-phagocytic function on murine macrophages as phagocytosis of OspC-expressing spirochetes was markedly reduced when compared to spirochetes lacking OspC.
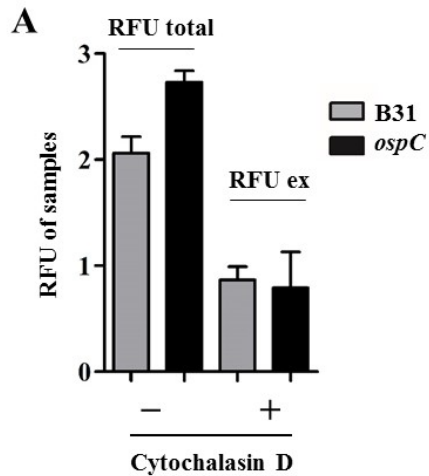
Figure 12. **Cytochalasin D prevents the uptake of *B. burgdorferi* strains. A)**. Murine PMs were preincubated for 30 min with or without 5 μg/ml cytochalasin D prior to the addition of GFP-expressing spirochetes (B31 strains). The numbers of spirochetes remaining after 2 h of incubation were determined using a microplate fluorometer as detailed in materials and methods. The relative fluorescence units of internalized (RFUi) spirochetes is determined by subtracting the fluorescence of unquenched, extracellular spirochetes (RFU ex from cytochalasin D treated cells) from the total fluorescence of the experimental well (RFU total from experimental samples). Values represent mean ± SEM from at least five experimental replicates used in a representative experiment.
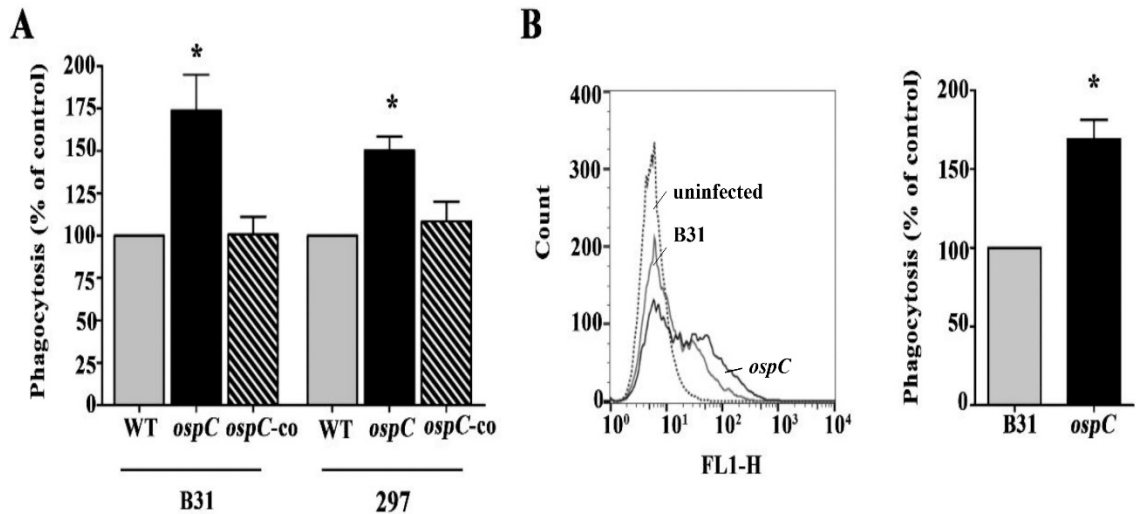
Figure 13. **Abrogation of OspC enhances phagocytosis of *B. burgdorferi* by murine macrophages. A)** Quantitation of phagocytosis of GFP-expressing wild-type spirochetes (B31 and 297-strains) by murine PMs determined using a microplate fluorometer. PMs were incubated with GFP-expressing spirochetes at an MOI of 100:1 for 2 h. The phagocytic index (PI) represented the fluorescence of intracellular bacteria phagocytosed by macrophages. Data are representative of 3 or 4 separate experiments with at least 4-5 replicates per experiment. Values represent mean ± SEM. Comparisons among experimental groups were performed with one-way ANOVA followed by Dunnett's post hoc test (*, $P < 0.05$; **, $P < 0.005$). **B)** Representative histograms of phagocytosis of B31-A3-*gfp* (grey solid line) and *ospC-gfp* (black solid line) spirochetes analyzed by flow cytometry. PMs were incubated with GFP-expressing spirochetes at an MOI of 100:1 for 2 h, followed by washing and fixation prior to flow cytometric analysis. The black dotted line represents control uninfected cells. Percentage of phagocytosis is shown on the right. Data represent the percentage of GFP-expressing spirochetes phagocytosed by PMs

obtained from three separate experiments (Student'*t* test *, *P* < 0.05). Values are expressed as mean ± SEM.
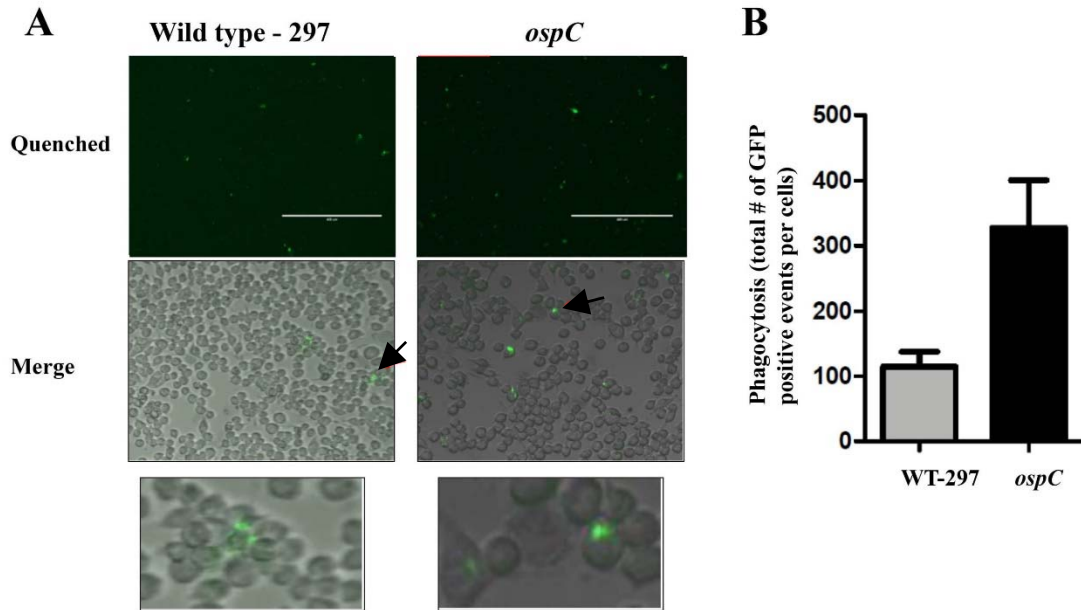
Figure 14. Enhanced uptake of GFP-expressing *ospC* mutant spirochetes by murine macrophages. A) Fluorescence and bright field micrographs of PMs incubated with GFP-expressing wild-type (WT-297) or *ospC* mutant strains for 2 h at an MOI of 100:1**.** At the end of a 2 h incubation time, cells were washed twice with 1 x PBS and incubated with trypan blue for 5 min to quench extracellular fluorescence. Cells were imaged using an EVOS fl digital fluorescence microscope. Black arrows indicate GFP-positive PMs (merge images from middle panel, magnification x10) that were zoomed in bottom panels. **B)** Quantitation of phagocytosis is defined as the total number of GFP positive events counted from fluorescent micrographs using ImageJ as described in material and methods. Data are representative of 3 fields per experiment from two separate experiments. Values are expressed as mean ± SEM.

We next examined whether OspC expression in spirochetes had an effect on phagocytosis by THP-1 macrophage-like cells. Similar to murine macrophages, the *ospC* mutant had significantly higher phagocytosis by THP-1 macrophage-like cells than the wild-type and the complement spirochetes (**Figure 15A-B**). In addition to macrophages, we further examined the role of OspC in phagocytosis of GFP-expressing spirochetes using neutrophil-like HL60 cells (PMN-HL60), since neutrophils are another type of professional phagocyte that can avidly phagocytose *B. burgdorferi* (133, 151). We found that uptake of the *ospC* mutant by PMN-HL60 cells was similar to the parental wild-type strain (**Figure 16A-B**), suggesting that OspC does not play a role in phagocytosis of *B. burgdorferi* by neutrophils. Taken together, our data suggest that OspC could have an anti-phagocytic property that reduces phagocytosis of *B.burgdorferi* strains by murine and human macrophages.
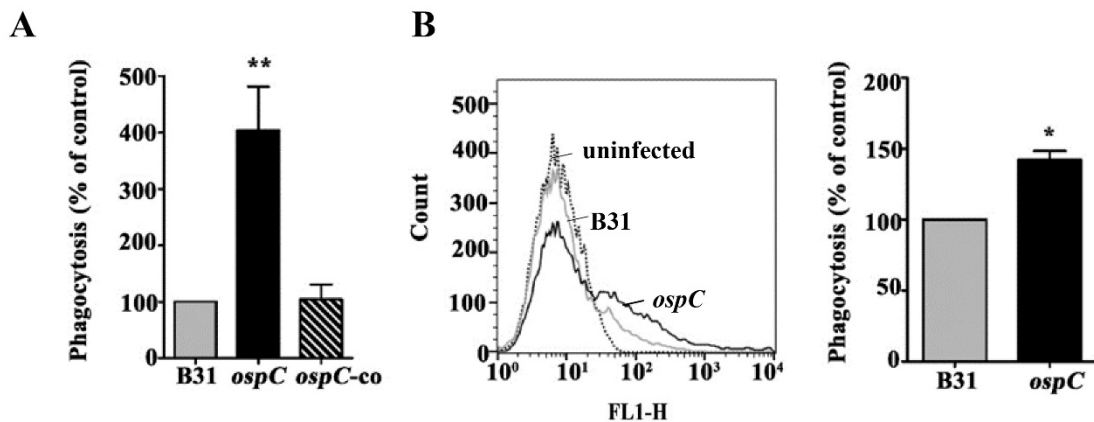
Figure 15. Abrogation of OspC enhances phagocytosis of *B. burgdorferi* by human macrophage-like cells. A) Quantitation of phagocytosis of GFP-expressing spirochetes (B31) by THP-1 macrophage-like cells (PMA-treated THP1 cells) determined using a

microplate fluorometer. THP-1 macrophage-like cells were incubated with GFP-expressing spirochetes at an MOI of 100:1 for 2 h. The phagocytic index (PI) represented the fluorescence of intracellular bacteria phagocytosed by THP-1 macrophage-like cells. Data are representative of 3 or 4 separate experiment with at least 4-5 replicates per experiment. Values represent mean ± SEM. Comparisons among experimental groups were performed with one-way ANOVA followed by Dunnett's post hoc test (*, $P < 0.05$; **, $P < 0.005$). **B)** Representative histograms of phagocytosis of B31-A3-*gfp* (grey solid line) and *ospC-gfp* (black solid line) spirochetes analyzed by flow cytometry. THP-1 macrophage-like cells were incubated with GFP-expressing spirochetes at an MOI of 100:1 for 2 h, followed by washing and fixation prior to flow cytometric analysis. The black dotted line represents control uninfected cells. Percentage of phagocytosis is shown on the right. Data represent the percentage of GFP-expressing spirochetes phagocytosed by THP-1 macrophage-like cells obtained from three separate experiments (Student'*t* test *, $P < 0.05$). Values are expressed as mean ± SEM.
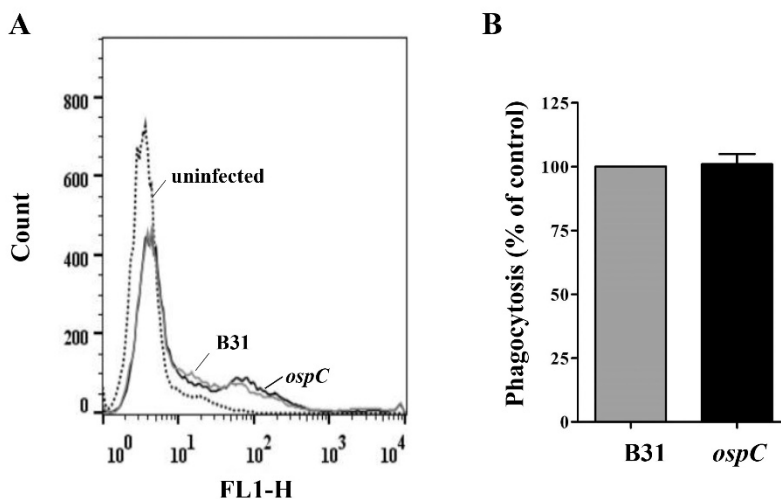
Figure 16. Uptake of *B. burgdorferi* by PMN HL60 cells is independent of OspC. **A)**
Representative histograms of phagocytosis of B31-A3-*gfp* (grey solid line) and *osp*C-*gfp*
(black solid line) spirochetes analyzed by flow cytometry. The black dotted line
represents control uninfected cells. **B)** GFP-expressing spirochetes were incubated with
PMN-HL60 cells at an MOI of 100 for 2 h, followed by washing and fixation prior to
flow cytometric analysis. Data represent the percentage of GFP-expressing spirochetes
phagocytosed by 1.25% DMSO-treated HL60 cells obtained from three separate
experiments. Values are expressed as mean ± SEM.

**Scavenger receptor A and B mediates phagocytosis of *B. burgdorferi* independently
of OspC**

To date, conventional phagocytosis of *B. burgdorferi* has been shown to be
mediated by different phagocytic receptors, including complement receptor-3 (137, 138),
Fc receptors (132, 136), and the scavenger receptor Macrophage Receptor with
Collagenous Structure (MARCO) (243). In addition, other members of the scavenger
receptor family as well as the mannose receptor have been proposed to bind or participate
in this process (125, 243, 244); however, their roles as phagocytic receptors are not fully
understood. Because *B. burgdorferi* induces the expression of the class-A scavenger
receptor family (CASR), including the scavenger receptor A I/II (SR-AI/II) and MARCO,
when internalized by murine bone marrow-derived macrophages (243), we then
examined whether this scavenger receptor family played a role in this enhanced
phagocytosis of the *ospC* mutant (**Figure 17A**). To test this, murine PMs were
preincubated with non-selective inhibitory ligands of CASR such as poly I and fucoidan

(245) before phagocytosis of spirochetes. Uptake of wild-type and *ospC* mutant spirochetes was substantially reduced in PMs treated with poly I and fucoidan at 400 µg/ml and 500 µg/ml, respectively (**Figure 17B-C**). Treatment of PMs with fucoidan at 100 µg/ml significantly reduced phagocytosis of the *ospC* mutant when compared to PMs incubated with the *ospC* mutant alone. However, OspC did not have an effect on phagocytosis of spirochetes in treated PMs as phagocytosis of the *ospC* mutant was higher than the wild-type strain even after CASR treatment (**Figure 17D**). Representative RFU of internalized spirochetes (RFUi) values from a single experiment are shown in figure 17D.
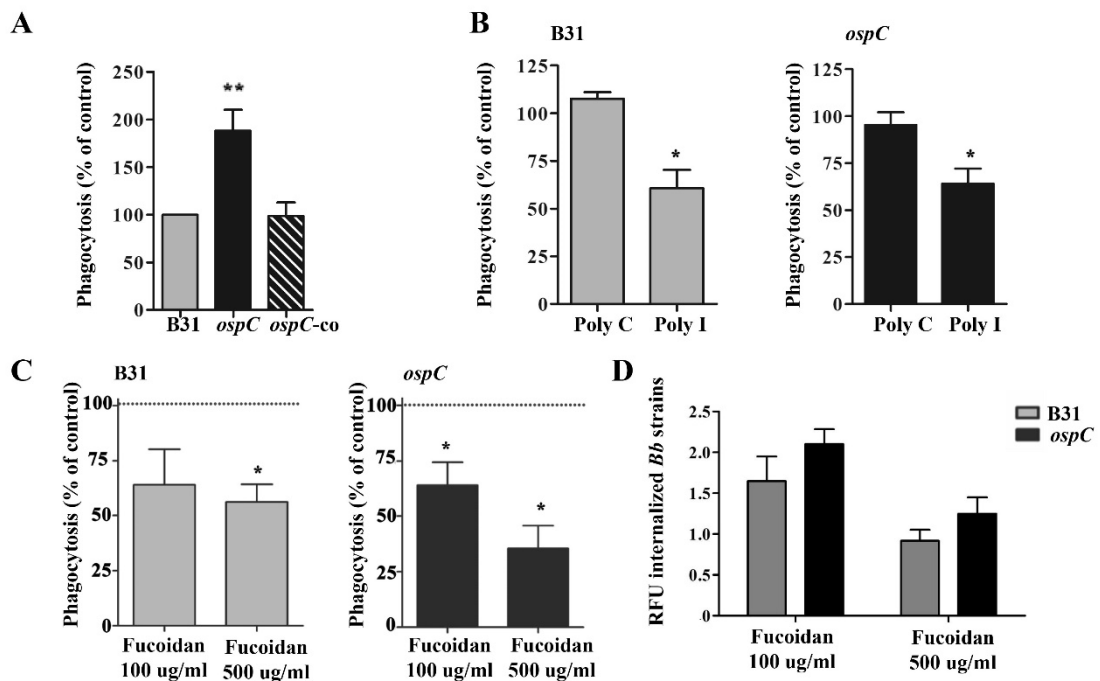
Figure 17. Class-A scavenger receptor blockers reduces phagocytosis of GFP-expressing *B. burgdorferi* strains independently of OspC. Fluorescence was determined using a microplate fluorometer after 2 h as detailed in materials and methods.

The phagocytic index (PI) represented the fluorescence of intracellular bacteria phagocytosed by murine peritoneal macrophages (PMs). **A)** Phagocytosis of GFP-expressing spirochetes (B31-strains) by PMs at an MOI of 100:1. **B-C)** Murine PMs were pretreated with nonselective CASR blockers poly I (at 400 ug/ml) and fucoidan (at 100 μg/ml or 500 μg/ml), and the phagocytosis of GFP-expressing spirochetes at an MOI of 100:1 was quantified by fluorometry. Comparison of % of phagocytosis of treated PMs relative to untreated controls (black dotted line). **D)** Representative RFUi values of phagocytosed spirochetes by CASR treatment. Data are representative of 3 or 4 separate experiment with at least 4-5 replicates per experiment. Values represent mean ± SEM. Comparisons among experimental groups were performed with one-way ANOVA followed by Dunnett's post hoc test (*, $P < 0.05$; **, $P < 0.005$).

To demonstrate that CASR was indeed involved in phagocytosis of spirochetes, we next preincubated PMs with a monoclonal antibody (ED31, 12 μg/ml) against MARCO, a class A scavenger receptor, before measuring phagocytosis. MARCO receptor was selected to block CASR-mediated phagocytosis since uptake of *B. burgdorferi* has shown to be reduced by MARCO deficient macrophages (243). Prior to these experiments, as Fc receptors have been shown to mediate phagocytosis of nonopsonized and opsonized spirochetes (137, 138), we preincubated PMs with 2.4G2 antibodies to block nonspecific Fc receptor-mediated interactions that might occur during phagocytosis either directly with spirochetes or indirectly with antibodies bound to spirochetes. Representative data from our phagocytosis assays showed that blocking Fcγ receptor did not alter phagocytosis of spirochetes as RFUs of internalized spirochetes

(RFUi) from 2.4G2-treated PMs were similar to the values shown by untreated PMs

(**Figure 18**). In our anti-MARCO blocking experiments, we found that blocking MARCO

significantly reduced MARCO-mediated phagocytosis of wild-type and *ospC* mutant

spirochetes (**Figure 19A**), and this effect was independent of the expression of OspC in

spirochetes **Figure 19C**). RFUi values from a representative experiment are shown in

figure 19C. Together, our CASR blocking experiments support the notion that members

of the class A family of scavenger receptors participate in phagocytosis of *B. burgdorferi*

in mouse macrophages.
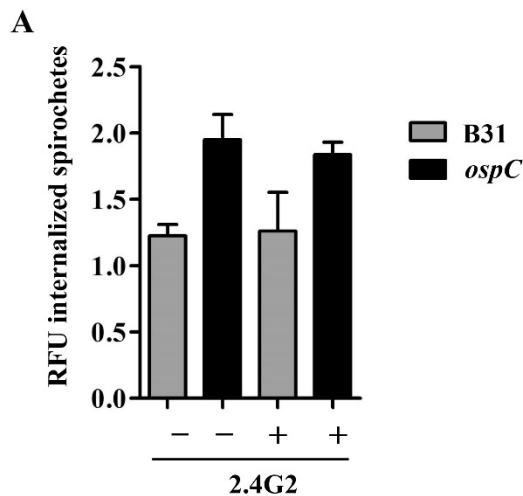
**Figure 18. Pretreatment of murine PMs with Fc receptor blocking antibodies does
not alter phagocytosis of non-opsonized GFP-expressing spirochetes. A)**
Representative RFUi values of phagocytosed spirochetes by 2.4G2 treatment. Murine

PMs were preincubated for 30 min with or without 2.4G2 supernatants containing

antibodies to specifically block mouse Fcγ receptor prior to the addition of GFP-

expressing spirochetes (B31 strains). The numbers of spirochetes remaining after

phagocytosis for 2 h were determined using a microplate fluorometer and RFUi was

calculated as detailed in materials and methods. Data are representative of 3 separate

experiments with at least 4 replicates per experiment.
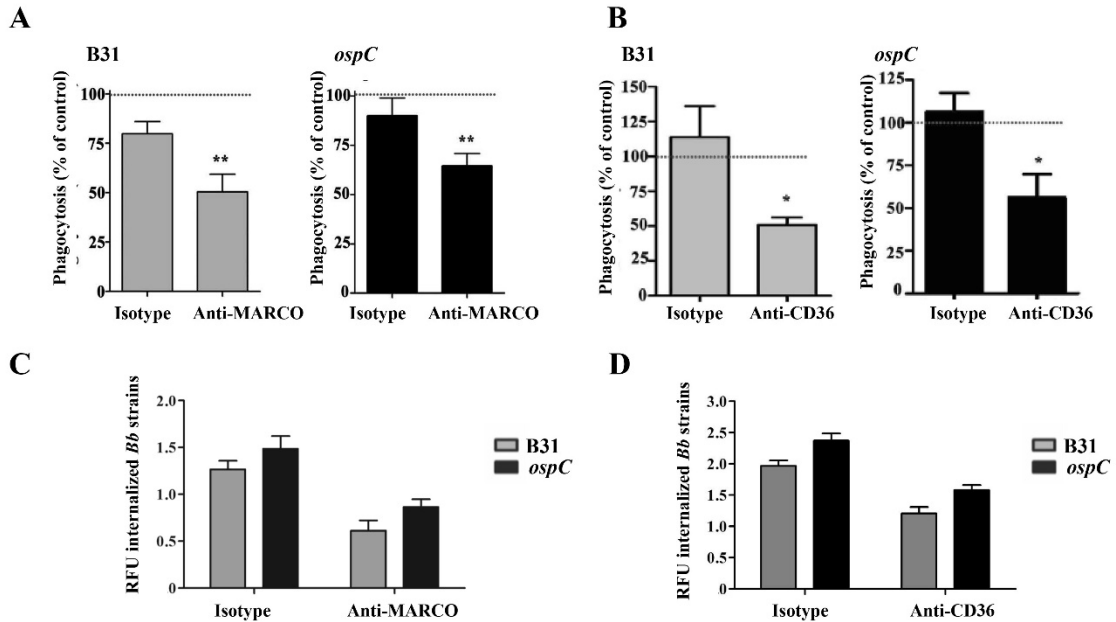
**Figure 19. MARCO and CD36 mediates phagocytosis of GFP-expressing *B.
burgdorferi* strains independently of OspC.** The phagocytic index (PI) represented the

fluorescence of intracellular bacteria phagocytosed by murine peritoneal macrophages

(PMs) at an MOI of 100:1. PMs were pretreated with 2.4.G.2 antibodies that block Fcγ

receptor as detailed in materials and methods. **A)** PMs were treated with rat anti-mouse

directed against MARCO or an isotype control at 12 µg/ml, and the phagocytosis (MOI

100 for 2 h) of GFP-expressing spirochetes was quantified by fluorometry. **B)** PMs were

treated with rat anti-mouse directed against CD36 or an isotype control at 50 µg/ml, and

the phagocytosis (MOI 100:1 for 2 h) of GFP-expressing spirochetes was quantified by

fluorometry. Comparison of % of phagocytosis of treated PMs relative to untreated

controls (black dotted line). **C-D)** Representative normalized RFUi values of phagocytosed spirochetes by antibody treatments. Data are representative of 3 or 4 separate experiments with at least 4 replicates per experiment. Values represent mean ± SEM. Comparisons among experimental groups were performed with one-way ANOVA followed by Dunnett's post hoc test (*, $P < 0.05$; **, $P < 0.005$).

The data above suggest that OspC production did not play a major role in scavenger receptor A-mediated phagocytosis. Therefore, we focused our efforts in studying another phagocytic receptor that recognizes lipoproteins and internalizes bacterial pathogens. One such phagocytic receptor is CD36, a class B scavenger receptor that mediates adhesion and internalization of Gram-positive and -negative bacteria and TLR2 ligands (246, 247). Furthermore, several studies have indicated that CD36 also cooperates with TLR2 dependent signaling responses associated with bacterial recognition (246). Thus, we examined whether CD36 was involved in this different uptake between wild-type and the *ospC* mutant by macrophages. Fcγ-treated PMs were preincubated with anti-CD36 before measuring phagocytosis of *B. burgdorferi* strains as described above. We found that treatment of PMs with anti-CD36 antibodies significantly reduced the uptake of both the wild-type and the *ospC* mutant strain (**Figure 19B**). OspC also did not appear to play a role in CD36-mediated phagocytosis by PMs as phagocytosis of the *ospC* mutant was higher than the wild-type strain even after CD36 treatment (**Figure 19D**). RFUi values from a representative experiment are shown in figure 19D.

Expression of cytokines by murine peritoneal macrophages infected with wild-type or the *ospC* mutant

Seminal studies demonstrated that *B. burgdorferi* lipoproteins are recognized by TLR-2/1 heterodimers on the surface of phagocytes inducing activation of NF-kB and the subsequent production of cytokines (118, 119). Recent studies have also proposed that the release of spirochetal byproducts within the phagosomal compartment of monocytes/macrophages are recognized by intracellular TLRs leading to the production of cytokines (120, 248). Thus, we next examined whether the production of OspC in spirochetes was associated with an alteration in cytokine expression by murine PMs. To test this, murine PMs were infected with the wild-type strain or the *ospC* mutant at an MOI of 100:1 for 2, 6, and 24 h. RNA was extracted from infected PMs to quantify the mRNA levels of TNF-α, IL-1β, and IL-10 as these cytokines are expressed during infections of monocytes/macrophages with *B. burgdorferi* (120, 170). Our findings showed that the mRNA levels of these cytokines was not affected by OspC expression in spirochetes, as there were no significant differences in the mRNA level produced by PMs infected with the wild-type and the *ospC* mutant at any of the time points post-challenge (**Figure 20**). Transcripts of these cytokines from a representative experiment are shown in figure 20. We observed that the highest level of TNF-α occurred after 2 h post-infection in PMs challenged with the *ospC* mutant while the expression of this cytokine was lowered at 6 h post-infection. Conversely, we noted that the highest level of TNF-α occurred 6 h post-infection in PMs challenged with the wild-type strain while the expression of this cytokine was lowered at 2 h post-infection. Cytokine expression in infected PMs were nearly at the basal level similar to unstimulated PMs at 24 h.
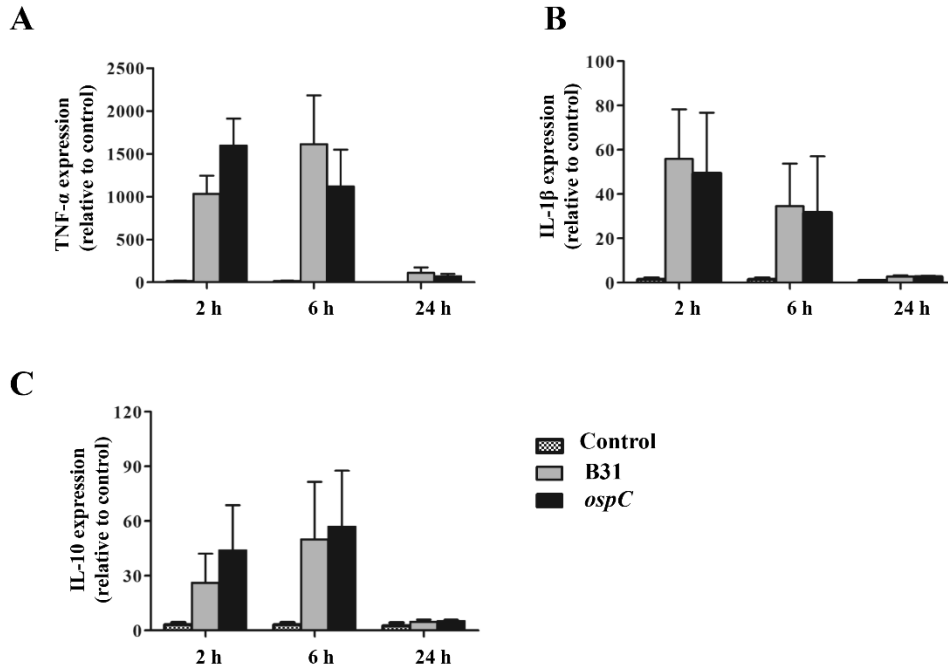
Figure 20. **Expression of TNF-α, IL-1β, and IL-10 after infection of murine peritoneal macrophages by wild-type (B31-A3) and *ospC* mutant spirochetes**. mRNA levels of TNF-α, IL-1β, and IL-10 were determined from control uninfected cells and *B. burgdorferi*-infected PMs (MOI of 100:1) by RT-PCR after 2, 6 and 24 h of incubation. The data were normalized to the housekeeping gene β-*actin* and are expressed as the fold difference compared to unstimulated cells. Data are representative of 3 separate experiments. Values represent mean ± SEM. Comparisons of B31-infected and *ospC*-infected PMs were performed using paired Student's *t* test.

The *ospC* mutant can establish infection when inoculated in mice with a high dose

Our *in vivo* data above showed that the *ospC* mutant cannot establish infection using a standard (10^3 spirochetes/mouse) and an intermediate inoculum (10^5 spirochetes/mouse). We also attempted to infect immunocompetent and immunodeficient

mouse strains with a high inoculum (10^6 spirochetes/mouse) of the *ospC* mutant. Groups

of C3H/HeN NODSCIDg, and SCID mice were injected with either wild-type B31-A3 or

the *ospC* mutant with an inoculum of 10^6 spirochetes per mouse using BSK-II medium as

vehicle. As comparison for SCID mice, groups of SCID mice were also challenged with

wild-type or the *ospC* mutant using PBS buffer as vehicle. Unexpectedly, we observed

that when inoculated in the skin with a high dose, the *ospC* mutant was able to establish

infection (**Table 7)** in different mouse strain backgrounds. *ospC* mutant reisolates were

analyzed by immunoblotting to confirm that these spirochetes were indeed not expressing

OspC (**Figure 21A**). Infected immunodeficient mice developed joint swelling and

showed evidence of arthritis in tibio-tarsal joints (**Figure 21B**). These findings suggest

that high doses of inoculation can overcome the survival defect of the *ospC* mutant at the

skin site of inoculation in mice.

Table 7. **Infectivity of wild-type *B. burgdorferi* (B31-A3) and the isogenic *ospC***

mutant in NODSCIDg, SCID, and C3H/HeN mice when inoculated with a high dose.

	Route of Inoculation*	Dose	Bb strain	Vehicle	3 weeks PI^
NODSCIDg	i.d.	10^6	B31-A3	BSK	3/3
NODSCIDg	i.d.	10^6	*ospC*	BSK	3/3
SCID	i.d.	10^6	B31-A3	BSK	3/3
SCID	i.d.	10^6	*ospC*	BSK	6/9
Balb/c *scid*	i.d.	10^6	ospC	BSK	1/6
C3H/HeN	i.d.	10^6	B31-A3	BSK	3/3
C3H/HeN	i.d.	10^6	*ospC*	BSK	3/6
SCID	i.d.	10^6	B31-A3	PBS	3/3
SCID	i.d.	10^6	*ospC*	PBS	3/3
SCID	i.p.	10^6	B31-A3	PBS	3/3
SCID	i.p.	10^6	*ospC*	PBS	2/3

* Spirochetes were inoculated intradermally (i.d.) in BSK or PBS and intraperitoneally in
PBS as vehicles.
^ All mice were euthanized at either 3 weeks post-inoculation (PI). Isolation of
spirochetes were attempted from skin-site of inoculation, ear pinna, tibio-tarsal joint,

heart base and spleen. Culture results expressed as number of mice infected/number of mice tested. Infectivity experiments were conducted in 3 separate trials.
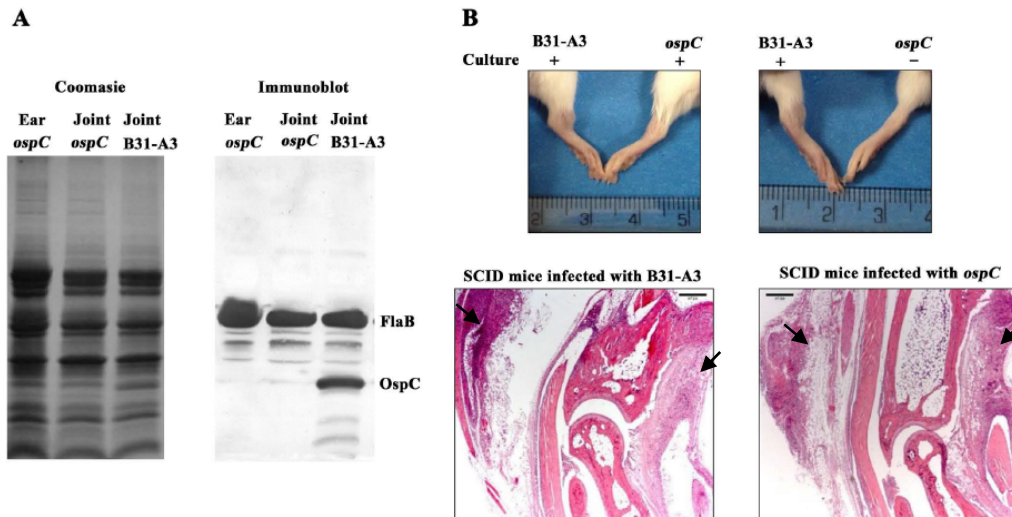
Figure 21. The *ospC* mutant can infect SCID mice and cause arthritis when inoculated at a high dose. Tibio-tarsal joints from SCID mice were collected 4 weeks post-challenge with either wild-type or the *ospC* mutant spirochetes (10^6 spirochetes/mouse) and subjected to cultivation for re-isolation of spirochetes or for histological analyses. **A)** Immunoblot analysis confirming that the spirochetes re-isolated from mice infected with the *ospC* mutant remained lacking OspC. Re-isolated spirochetes were cultivated in the standard BSK-II medium at 37°C and harvested at the stationary growth phase, and subjected to immunoblotting analysis using a mixture of monoclonal antibodies against FlaB (control) and OspC. **B)** Macroscopic observation of ankle thicknesses in SCID mice infected with *ospC* 4 weeks post-intradermal inoculation with 10^6 spirochetes (top panel). Representative images of H&E-stained histological sections from tibio-tarsal joints of SCID mice 4 weeks post-challenge (bottom panel,

magnification, ×2.5). Tibio-tarsal joints exhibited severe periarticular inflammation involving ligaments and tendon sheaths (black arrows) with cellular infiltrates primarily composed by macrophages with few neutrophils.

Part II- *B. burgdorferi* EF-Tu is an immunogenic antigen during Lyme borreliosis

***B. burgdorferi* EF-Tu is recognized by mouse and human sera during infection**

EF-Tu has been shown to be an immunogenic protein during active infection and after exposure for a number human and animal bacterial pathogens (205, 249-251). To determine whether *B. burgdorferi* EF-Tu is immunogenic during infection in mice, sera from infected mice with Lyme borreliosis were tested for reactivity to purified rEF-Tu (**Figure 22A**). We found that antibodies to rEF-Tu were detectable in sera of infected mice as early as 2 weeks after needle inoculation of mice with in vitro-cultivated *B. burgdorferi.* Seroreactivity to rEF-Tu was detectable even at 6 weeks or 11 weeks (data not shown) post-infection (**Figure 22B**), suggesting that *B. burgdorferi* anti-EF-Tu antibodies are maintain after 2 months of infection in mice. This result prompted us to evaluate if sera from Lyme disease patients could be reactive to rEF-Tu. We found that 70% of samples tested (7 positives out 10 patients tested) were reactive to rEF-Tu (**Figure 22C**). Seroreactivity to rEF-Tu was detected in samples from seropositive patients with different clinical manifestations associated with Lyme disease, including *erythema migrans,* arthritis and/or neurologic symptoms. Four samples exhibited strong reactivity to rEF-TU and were also seropositive by ELISA and Western blot with IgM and IgG antibodies against *B. burgorferi* antigens. Two samples that exhibited strong reactivity to rEF-Tu were also seropositive by ELISA and Western blot for IgM

87

antibodies against *B. burgorferi* antigens. One sample was also reactive to rEF-TU and tested positive by ELISA and Western blot for IgG when blotted against *B. burgorferi* antigens. Together, these results indicate that *B. burgdorferi* rEF-Tu can be recognized by antibodies during natural and artificial Lyme infection in mammals.

A

B

C
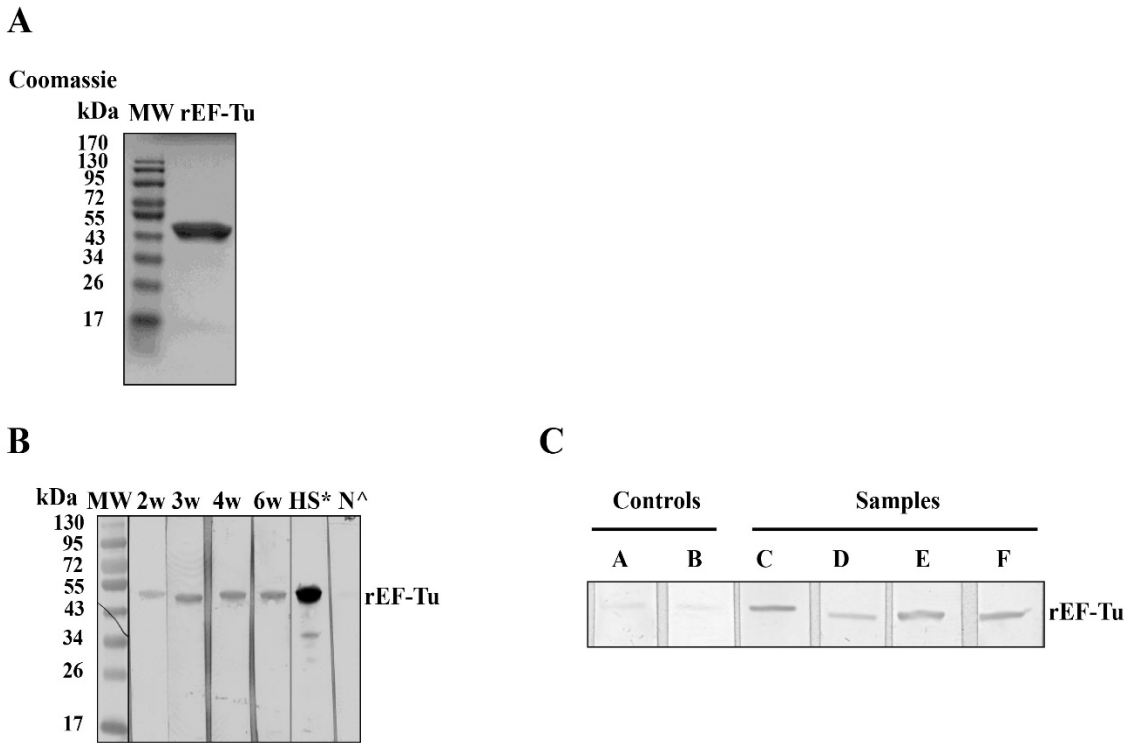
Figure 22. Serologic reactivity of sera from infected mice and selected Lyme disease patients to recombinant EF-Tu. **A)** SDS-PAGE results from purified recombinant EF-Tu protein (~15 ug loaded). Predicted size for *B. burgdorferi* EF-Tu is 43kDa. **B)** Appearance of antibodies against rEF-Tu during the course of infection in C3H/HeN mice after needle inoculation of mice with *B. burgdorferi* strain 5A4NP1. Recombinant EF-Tu (~ 500 ng/strip) was subjected to SDS-PAGE. Nitrocellulose strips were immunoblotted with 1:600 dilutions of murine infectious sera collected at various intervals post-challenge. The lane at the right (N^) is a strip probed with sera from naïve

mice. The lane labeled HS* is a strip probed with mouse antiserum against rEF-Tu (αEF-Tu, 1:10000 dilution). **C)** Serologic reactivity of sera from Lyme disease patients to rEF-Tu. Nitrocellulose strips (~ 500 ng rEF-Tu/strip) were immunoblotted with 1:100 dilutions of human sera. Panels A-B are strips probed with sera from healthy controls from areas that are non-endemic to Lyme disease. Panels C to F are representative results from strips probed with sera from 4 different Lyme disease patients. Data are representative of two separate experiments.

Active immunization of mice with rEF-Tu is not protective against artificial and tick-borne *B. burgdorferi* infection

The observation above showing that immune sera from infected mice contain antibodies against rEF-Tu led us to assess whether immunization of mice with rEF-Tu could elicit protective immunity against *B. burgdorferi* infection. Groups of four to six mice were actively immunized with rEF-Tu or Freund's adjuvant alone (control), antibody titers were verified, and then mice were intrademally challenged with wild-type *B. burgdorferi* strain 5A4NP1. Cultures from ear-punch biopsies showed that all mice, regardless of their vaccination status, were culture positive after 2 weeks post-challenge (**Table 8**). Spirochetes were also cultured from tibio-tarsal joints and hearts in mice from both treatment groups at either 2 or 5 weeks post-challenge. In addition, we used real-time qPCR to quantify *flaB* DNA in joint tissues after 2 weeks of needle inoculation of spirochetes. Our qPCR results showed no significant differences in the bacterial load of mice treated with rEF-Tu in comparison to control mice (**Figure 23A**). We next challenged a second group of immunized mice and controls using infected unfed nymphs

to determine the role of EF-Tu antibodies during natural infection. Similar to needle-inoculated infected mice, we found that spirochetes were cultured from every single tissue from both treatment groups after 2 weeks of tick feeding (**Table 8**). These data indicate that immunization of mice with rEF-Tu does not play a role in the control of *B. burgdorferi* infection.

Table 8. Active immunization of mice with rEF-TU did not elicit a protective response after *B. burgdorferi* challenge.

Method of inoculation	Group	Culture result^
Needle	Adjuvant	4/4
	Adjuvant + rEF-Tu	6/6
Nymphal ticks	Adjuvant	2/2
	Adjuvant + rEF-Tu	2/2

^ Mice were euthanized at either 2 or 5 weeks post-challenge. Isolation of spirochetes were attempted from ear pinna, tibio-tarsal joint, and heart base.

To determine whether immunization of mice with rEF-Tu could influence acquisition of spirochetes by ticks, naïve larvae were fed on a group of immunized or control mice that were infected with *B. burgdorferi* as described above. The spirochete load from fully engorged larvae was then assessed by qPCR after 72-96 h of feeding. We found no significant differences in spirochete loads in fed larvae from immunized and control groups at day 34 post-infection (**Figure 23B**). In addition, we also did not observe, by IFA, noticeable differences in the number of spirochetes in tick-smears collected from both treatment groups (data not shown). Together, these results indicate that EF-Tu antibodies did not interfere with *B. burgdorferi* acquisition by ticks.
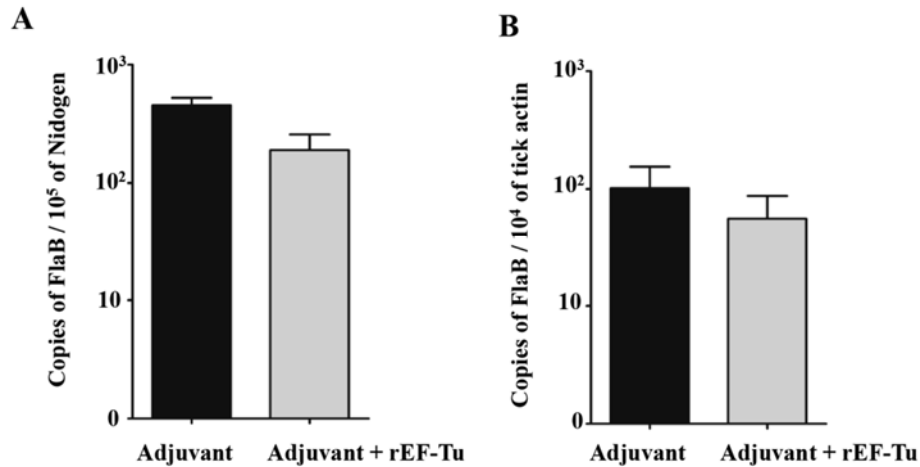
Figure 23. Active immunization of mice with rEF-Tu does not affect spirochetal loads in tibio-tarsal joints and interfere with acquisition of spirochetes by tick larvae. **A)** qPCR results showing copies of *B. burgdorferi flaB* relative to the copies of mouse *nidogen*. Samples contained joint DNA from groups of mice treated with either adjuvant alone or adjuvant + rEFTU at day 14 post-infection. **B)** qPCR analyses of spirochete load in fed larvae. qPCR for the *B. burgdorferi flaB* gene was performed with DNA extracted from fed larvae (9-18 ticks for each group). The number of copies of the *flaB* gene compared to the number of copies of the tick *actin* gene. Samples contained tick DNA from mice treated with either adjuvant alone or adjuvant + rEF-Tu at day 34 post-infection. Data are representative of two separate experiments. Differences between mice immunized with rEF-Tu and controls was analyzed using a Student *t* test ($P \leq 0.05$).

B. burgdorferi EF-Tu is not surface exposed

Since rEF-Tu binds to antibodies present in sera from infected individuals, this led us to hypothesize that a fraction of EF-Tu is surface exposed in the outer membrane of *B. burgdorferi*. Recent studies have also revealed novel functions of EF-Tu since it is

associated with the cell surface in several pathogenic and commensal bacteria (196, 197, 200). To investigate whether EF-Tu is a membrane-associated protein in *B. burgdorferi*, we first examined, by IFA, the ability of intact and permeabilized *B. burgdorferi* to bind antibodies directed against EF-Tu. Monoclonal antibodies directed against the periplasmic FlaB protein and the surface-exposed OspA lipoprotein of *B. burgdorferi* were used as controls. Our IFA results showed that antibodies directed against EF-Tu recognize this protein in permeabilized spirochetes (**Figure 24A, top panel**). Both FlaB and OspA were also readily detected in fixed, permeabilized spirochetes. However, we found that unfixed, non-permeabilized spirochetes were unable to bind anti- EF-Tu antibodies (**Figure 24A, bottom panel**). FlaB was also inaccessible, while OspA were readily detected in intact spirochetes (**Figure 24A, bottom panel**). We then reasoned that EF-Tu could be expressed at different levels in *in vitro*-cultivated *B. burgdorferi,* and this would explain the inaccessibility of anti-EF-Tu antibodies since EF-Tu was not abundantly expressed on the surface of viable wild-type spirochetes at the time point of this assay. Thus, we generated a *B. burgdorferi* strain (B31-A3/P*fla*B-*eftu*-HA) that constitutively expresses EF-Tu (**Figure 25**). Our IFA experiments provided evidence that endogenous EF-Tu and HA-tagged EF-Tu were inaccessible to anti-EF-Tu and anti-HA antibodies in intact B31-A3/P*fla*B-*eftu*-HA spirochetes (data not shown). Taken together, these results suggest that EF-Tu is not expressed on the outer membrane of *B. burgdorferi*.

Previous studies have indicated that outer surface proteins, such as OspA, can hinder access of antibodies to epitopes of other integral membrane proteins of *B. burgdorferi* (252, 253). To address this possibility, we then examined whether EF-Tu was

susceptible to in *situ* proteolysis using proteinase K. This protease can degrade surface-exposed proteins in *B. burgdorferi,* whereas subsurface proteins are protected from proteolysis. Our results showed that the bulk of OspA in intact B31-A3/P*fla*B-*eftu*-HA spirochetes was degraded by high concentrations (100-200 ug/ml, **Figure 24B***)* of proteinase K while neither FlaB nor EF-Tu (**Figure 24B**) in intact spirochetes was affected by high concentrations of proteinase K. This protease was also unable to digest EF-Tu from intact wild-type B31-A3 spirochetes (**Figure 24B**). These results further demonstrate that EF-Tu is not a surface exposed protein in *B. burgdorferi*.
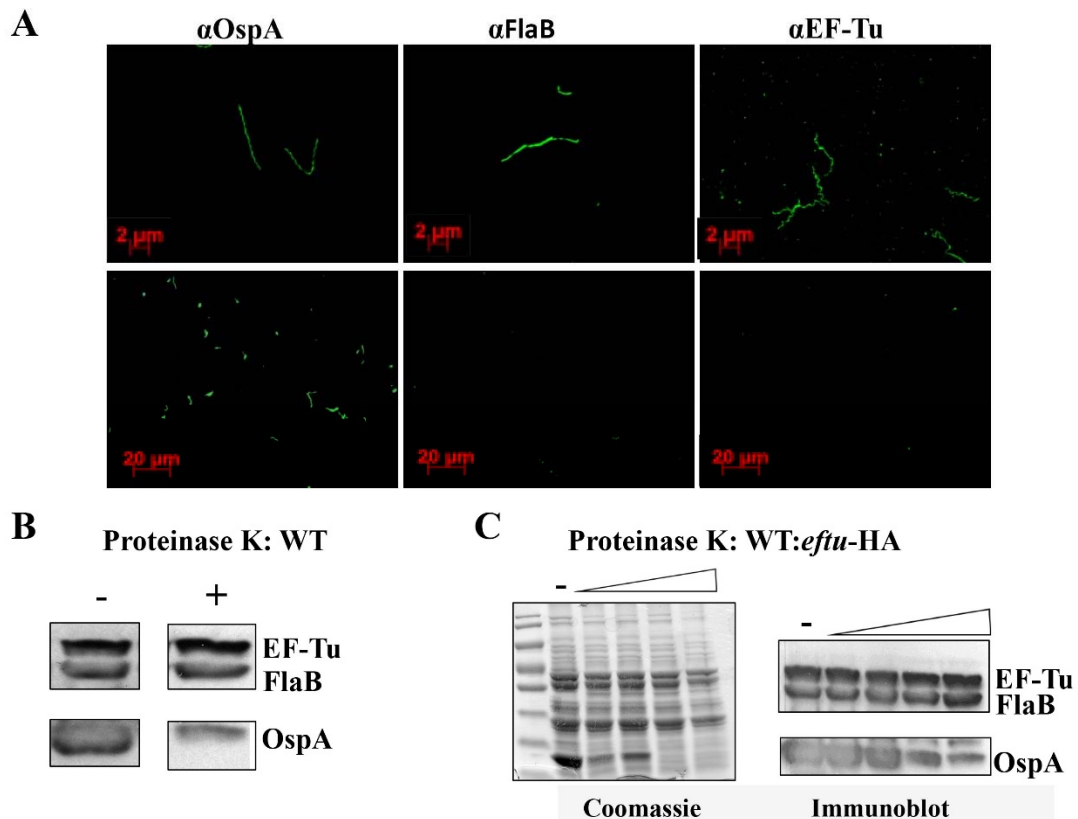
Figure 24. EF-Tu does not localize in the outer membrane of *B. burgdorferi*. A) Indirect immunofluorescence of fixed and unfixed *B. burgdorferi* strain B31-A3. Spirochetes were fixed (top panel) in acetone as described in material and methods. Fixed

93

and unfixed spirochetes (bottom panel) were probed with monoclonal antibodies directed against OspA or FlaB and mouse polyclonal directed against EF-Tu. Fluorescein isothiocyanate (FITC) - conjugated goat anti-mouse IgG was used to detect bound antibodies (Bar, 2-20 μm). **B)** Cell lysates from wild-type *B. burgdorferi* strain B31-A3 (WT) was incubated with either PBS alone (lane −) or PBS containing 200 μg/ml proteinase K (lane +). The treated cells were then subjected to immunoblot analysis using a combination of antibodies against OspA, FlaB, and EF-Tu. **C)** SDS-PAGE (left panel) and immunoblot analysis (right panel) of the effect of proteinase K on EF-Tu proteins from B31-A3/P*fla*B-*eftu*-HA that constitutively expresses EF-Tu. Intact cells were incubated for 1 h with 25, 50, 100 or 200 μg/ml of proteinase K. After being washed, the cells were subjected to SDS-PAGE stained with Coomassie blue, and immunoblots of the cell lysates were probed using a mixture of antibodies against OspA, FlaB, and EF-Tu. OspA, a surface-localized lipoprotein, served as a positive control, and FlaB served as a negative control. Data are representative of four separate experiments.
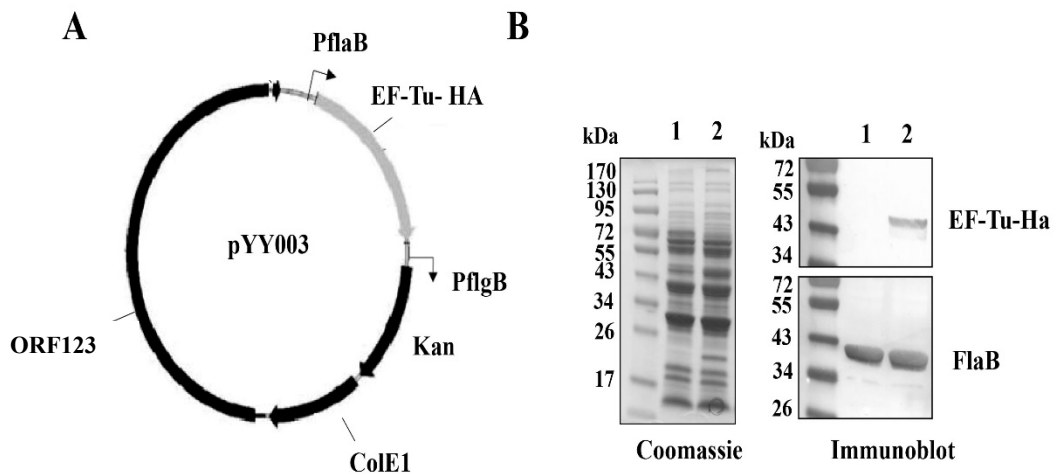
Figure 25. Transformation of *B. burgdorferi* strain B31-A3 to constitutively express HA-tagged EF-Tu (B31-A3/P*fla*B-*eftu*-HA). **A)** Construction of pYY003 shuttle vector. EF-Tu-HA and Kanamycin (Kan) are under the control of a constitutive *Borrelia* promoters P*fla*B and P*flg*B, respectively (ColE1 = *E. coli* origin of replication and ORF123 = plasmid replication genes from cp9 of *B. burgdorferi*). **B)** Confirmation of HA-tagged EF-Tu production by immunoblotting. Wild-type B31-A3 strain (lane 1) and B31-A3/P*fla*B-*eftu*-HA clone (lane 2) were grown to mid-log phase in BSK-II medium, harvested by centrifugation and subjected to SDS-PAGE stained with Coomassie blue (left) and immunoblotting (right). Samples were probed with a mixture of FlaB and HA.11 monoclonal antibodies.

EF-Tu localizes in cytoplasm and is a protoplasmic cylinder-associated protein in *B. burgdorferi*

To further examine the cellular localization of EF-Tu, we next performed Triton X-114 (TX-114) phase partitioning studies with *B. burgdorferi* cells to separate fractions based on their amphiphilic properties. As shown in Figure 26A, EF-Tu partitioned exclusively into the soluble aqueous (non-membrane-enriched) fractions, suggesting that they are cytoplasmic proteins. As expected, OspA, a known outer surface lipoprotein, was found in the detergent (membrane-enriched) fractions (**Figure 26A**).

Because *B. burgdorferi* is able to form OMVs that contain immunogenic surface and cytoplasmic proteins (193, 219, 254), we then assessed whether EF-Tu could be part of the protein cargo that is released in OMVs from spirochetes. To test this, intact spirochetes were separated into two major fractions, outer membrane vesicles and PC

inner membrane associated proteins, which were then subjected to immunoblot analyses

with anti-EF-Tu and anti-OspA antibodies. We found that EF-Tu protein was primarily

associated with the PC inner membrane enriched fractions; however, small quantities of

EF-Tu were detected in OMVs fractions (**Figure 26B**). As expected, OspA was

predominantly detected in the OMVs fractions (**Figure 26B**). Collectively, our data

shows that EF-Tu localizes primarily in the cytoplasm, associates with PC structures, and

is detected in small quantities in OMVs.
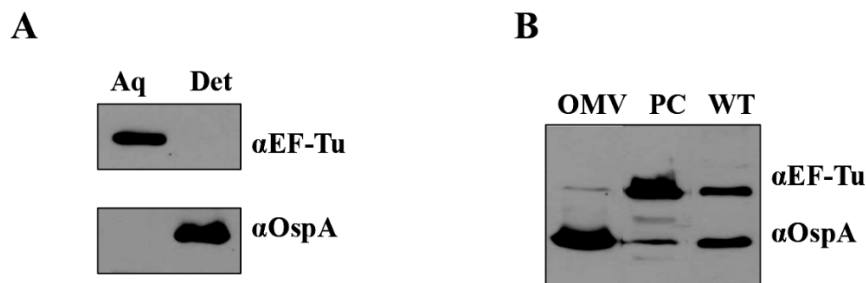
**Figure 26. A fraction of *B. burgdorferi* EF-Tu is associated with protoplasmic

cylinder fractions**. **A)** EF-Tu is in the soluble fraction. Immunoblot analysis of whole-

cell phase partitioning. The detergent-enriched (Det) and aqueous-enriched (Aq) phases

were immunoblotted with antibodies against EF-Tu or OspA, which is known to localize

in the detergent phase. **B)** EF-Tu is associated with protoplasmic cylinder fractions. *B.

burgdorferi* PC and OMVs were separated by sucrose density gradient centrifugation and

equal amounts of protein from two subcellular fractions were separated by SDS-PAGE,

and immunoblotted with antibodies directed against EF-Tu or OspA. These antibodies

were also immunoblotted against wild-type (WT, right lane) *B. burgdorferi* whole-cell

lysates.

CHAPTER V: DISCUSSION

Part-I Role of *B. burgdorferi* OspC during Lyme borreliosis

Since the discovery of *Borrelia burgdorferi* in 1975 as the sole etiological agent of Lyme disease, the number of Lyme disease cases have exponentially increased to the point that this tick-borne illness has become a significant public health problem in endemic areas of United States. During these past three decades, considerable research efforts have enhanced the understanding on the phylogenetic diversity, molecular biology, pathogenesis, and host interactions of *B. burgdorferi*. The development of genomic tools and genetic manipulation of *B. burgdorferi* have contributed to the understanding of genes involved during infection within the tick and mammalian host. However, most of the genes encoded by *B. burgdorferi* plasmids (~535 putative genes) and about a third of the genes encoded by its chromosome (~30%) are unique and most of them have unknown biological functions (60, 61). One characteristic feature of the *B. burgdorferi* genome is that it encodes numerous surface lipoproteins that are essential for the maintenance of this pathogen in the enzootic life cycle (14). The surface lipoprotein OspC is a major virulence factor that is induced when ticks start feeding on the mammalian host (171) and is required for *B. burgdorferi* to establish mammalian infection (49, 64, 65). However the precise function of OspC during the early stage of infection remains unclear.

Previous studies have indicated that OspC could exhibit numerous properties that could promote dissemination and survival during early infection in the mammalian host. OspC could serve as an adhesin to bind host plasminogen (89, 180, 255), suggesting that OspC-expressing spirochetes utilize the plasminogen/plasmin system to facilitate tissue

invasiveness within the host. Additionally, OspC may bind to other mammalian derived factors using a putative small ligand-binding domain (known as LBD1) that was demonstrated to play a critical role in survival of spirochetes during the initial stage of infection (179). In a demonstration of the versatility of this protein, OspC also binds to tick salivary proteins, such as Salp15, which is a major immunosuppressive protein in tick saliva that seems to protect *B. bugdorferi* from host defenses (111, 256-258). Evidently, the ability of OspC to bind multiple ligands contributes to the difficulty in defining the role of OspC during infection.

In addition, previous studies have proposed that OspC directly protects spirochetes against innate immunity during the early stage of mammalian infection (176, 183); however, the mechanism for how OspC contributes to such a function had not been elucidated. In this dissertation, we provided evidence that spirochetes lacking OspC are cleared by phagocytes at the skin-site of inoculation in SCID mice, whereas wild-type spirochetes remain fully infectious *in vivo*, suggesting that OspC protects *B. burgdorferi* from being recognized by phagocytes during early infection in the murine host. We further showed that OspC reduced the phagocytosis of spirochetes by murine and human macrophages. Together, our *in vivo* and *in vitro* findings suggest that OspC protects spirochetes against skin phagocytes, as a potential immune evasion strategy to survive during early stages of mammalian infection. Findings from our studies could be used for future investigations to understand the interaction of other *B. burgdorferi* surface proteins with skin phagocytes as the mouse skin has been proposed as an important natural barrier that selects for *B. burgdorferi* populations with increased fitness in the host (106, 259).

The *ospC* mutant establishes infection in phagocyte depleted mice

   B. burgdorferi infection elicits both innate and adaptive immune responses to control spirochetal burden in the murine host (32, 39). Previous work has shown that the OspC-deficient spirochetes generated from different *B. burgdorferi* strain backgrounds cannot establish infection in both immunocompetent and SCID mice, indicating that adaptive immunity does not play a major role in eliminating the *ospC* mutant *in vivo* (49, 177). SCID mice have elevated levels of lytic complement activity and normal levels of NK cell activity (240). Thus, we further investigated NODSCIDg mice since they lack not only adaptive immunity, but also lytic complement, and NK cells, and also have impaired cytokine signaling due to the lack of interleukin 2 receptor common gamma chain (IL-2Rγ^{null}) (239). Our results showed that the *ospC* mutant also was not able to establish infection in NODSCIDg mice when inoculated at the standard dose (10^3 spirochetes per mouse). The same inoculum of *ospC* mutant spirochetes cannot cause infection in C3H/HeN and SCID mice, which is what we observed in our infectivity experiments using these mouse strains (49, 64, 65, 99). Our findings suggest that the lytic complement and NK cells do not play a major role in clearance of the *ospC* mutant *in vivo*. This data is consistent with a previous report by Bockenstedt et al. (112), showing that the fifth component of complement is not required for protection and disease progression of wild-type *B. burgdorferi* infection in C5-deficient mouse strains. Our results are also consistent with findings from a previous report showing that depletion of NK cells did not have a major effect on *B. burgdorferi* burden and dissemination in arthritis-resistant and -susceptible mouse strains (169). Another potential insight from our findings is that opsonic phagocytosis mediated by Fc receptors on phagocytes are not

involved in the clearance of the *ospC* mutant *in vivo*, as *ospC*-deficient spirochetes could not establish infection in 4-6 week old NODSCIDg and SCID mice that lack functional T and B cells and have no detectable immunoglobulins at this age (260).

We then focused on professional phagocytes as one of the primary target cells for our depletion studies, as mononuclear phagocytes were reported to infiltrate the skin-site of inoculation in mice (99) and neutrophils were elevated in circulation within the first week of *B. burgdorferi* infection in mice in our preliminary studies. Our result showed that the *ospC* mutant was cleared within the first 48 h post-challenge in mice treated with anti-Ly6G antibody, a method commonly used for neutrophil depletion. Although previous reports showed that neutrophils can effectively control spirochetal burden during infection (261, 262), our data suggest that the neutrophil is not the major factor in clearing the *ospC* mutant at the skin-site of inoculation. In contrast, we found that depletion of phagocytes at the skin site of inoculation in SCID mice allowed the *ospC* mutant to establish infection and dissemination, suggesting that phagocytes play an important role in clearing the *ospC* mutant. This finding suggest that *B. burgdorferi* employs OspC to evade phagocyte killing at the skin-site of infection. We also observed an increased spirochetal burden of wild-type *B. burgdorferi* in joints of clodronate-treated SCID mice. This observation is consistent with the notion that phagocytes such as F4/80$^+$ macrophages are important in controlling the wild-type *B. burgdorferi* burden in cardiac and joint tissue of infected mice (39, 181).

Although depletion of F4/80$^+$ phagocytes by clodronate liposome treatment is a widely used approach to study macrophage functions (263), our study did not rule out the possibility that other F4/80$^+$ phagocytes such as naïve epidermal Langerhans cells could

be affected by this treatment and subsequently contributed to the clearance of the *ospC* mutant (236, 264). It is also possible that macrophage apoptosis induced by clodronate liposome treatment may have altered the innate cell homeostasis (265, 266), and subsequently created a permissive environment which allowed the *ospC* mutant to survive at the skin-site of inoculation. However, our data showed that clodronate treatment did not alter leukocytes and neutrophil numbers in our experiments, suggesting that the survival of the *ospC* mutant upon clodronate treatment was unlikely due to a dramatic alteration of innate cell homeostasis.

B. burgdorferi OspC decreases macrophage phagocytosis

Previous studies have shown that human macrophages and murine peritoneal and bone marrow-derived macrophages can efficiently ingest and kill *B. burgdorferi* (155, 267). In our phagocytosis assays, we observed significantly higher phagocytosis of the *ospC* mutant than wild-type spirochetes by murine PMs or THP-1 macrophage-like cells, using two independent *B. burgdorferi* strains. This increased phagocytosis may result in the clearance of the *ospC* mutant at the skin-site of inoculation during the first 48 h post-infection as previously reported by other investigators (64, 268). Similarly to our findings, a previous report showed that another outer membrane lipoprotein such as OspB could have an antiphagocytic property against human neutrophils *in vitro* (269); however, the biological relevance of this finding is controversial, as this surface lipoprotein is rarely expressed by *B. burgdorferi* during mammalian infection (76, 171). In contrast, Lmp1, another outer membrane protein that is highly expressed during early mammalian infection, did not exhibit an antiphagocytic property in murine BMDM, as phagocytosis did not differ between wild-type and *lmp1* mutant spirochetes (270). Instead, *B.*

burgdorferi Lmp1 appeared to play a role in evasion of adaptive immunity in the murine host (270). Thus, our findings suggest that OspC could directly protect *B. burgdorferi* from phagocytosis by mouse and human macrophages.

Because OspC has been previously proposed to bind tick salivary proteins during early infection (89, 110), another possible interpretation of our findings is that spirochetes lacking OspC are more susceptible to killing by phagocytes at the skin-site of the tick bite because the *ospC* mutant may have a reduced ability to bind tick salivary proteins relative to the wild-type strain *in vivo*. It is well-accepted that tick salivary proteins provide a survival advantage for spirochetes in the murine host (89, 111, 178). *In vitro* studies also showed that tick salivary proteins decreased the ability of neutrophils to adhere to and kill spirochetes (271), suggesting tick proteins limit the interaction of spirochetes with neutrophils during early Lyme borreliosis. Future studies are needed to determine the contribution of OspC-specific tick ligands such as Salp15 in macrophage phagocytosis of wild-type and *ospC* mutant spirochetes.

Of note, we observed a high phagocytic activity of THP-1 cells against *B. burgdorferi*, which is somewhat different from a previous study showing that Vitamin D3-treated THP-1 cells have poor phagocytic capacity for *B. burgdorferi* (272). One possible explanation was that we used PMA to activate and differentiate THP-1 cells into macrophage-like cells (273, 274). PMA differentiated THP-1 cells have been demonstrated to exhibit higher phagocytic activity and adherence and different expression of surface receptors than Vitamin D3 differentiated THP-1 cells (222, 274).

Phagocytosis of *B. burgdorferi* by macrophages involves several phagocytic receptors that are known to increase the efficiency of internalization of spirochetes, as

well as Toll-like receptors that activate MyD88-dependent or -independent mechanisms to enhance phagocytosis (29, 30, 76). The scavenger receptor MARCO mediates phagocytosis of *B. burgdorferi* in mouse BMDM, and expression of this receptor was upregulated upon *Borrelia* stimulation in a MyD88-dependent manner (30). In our studies, we showed that nonselective CASR blockers and anti-MARCO antibody reduced the uptake of wild-type and *ospC* mutant spirochetes by murine PMs, suggesting that the class A family of scavenger receptors (including MARCO) plays a role in phagocytosis of *B. burgdorferi*. These results are in agreement with previous studies showing that blocking scavenger receptor-A I/II (SR-A I/II) and MARCO reduces phagocytosis of bacteria by murine PMs (47, 77), which are known to express CASR receptors. Although much is known about the structure of CASR and their ligands (60), the mechanisms for how CASR convey signals after microbial-ligand binding are not well understood (78). Recent studies proposed that SR-A/MARCO modulate TLR- and NOD-like receptors-signaling pathways in response to bacterial products or pathogenic bacteria (79-81). Establishing the potential interaction of *B. burgdorferi* lipoproteins with CASR-mediated activation will require further studies.

Although we did not measure the expression of CD36 on the PM surface after *Borrelia* challenge, our data suggest that anti-CD36 antibody interacts with this member of the scavenger receptor B family on murine PMs by reducing the uptake of wild-type and *ospC* mutant spirochetes. Furthermore, elicited murine PMs are known to express CD36 even under basal culture conditions and recognize diacylated microbial lipopeptides that signal via the TLR2/6 heterodimers (275). Thus, as shown with the scavenger receptor A family in a previous *B. burgdorferi* study (243), it is tempting to

speculate that CD36 expression is also upregulated during phagocytosis of spirochetes, perhaps via recognition of *Borrelia* diacylated antigens (275, 276). It will be important to determine the role of CD36-mediated recognition and uptake of *B. burgdorferi* by murine macrophages in the future, to better understand CD36-mediated responses in host defense and inflammation during Lyme borreliosis.

Cytokine expression of cells in response to the *ospC* mutant

Previous studies have investigated whether the *ospC* mutant elicits in human epidermal keratinocytes and dermal fibroblasts and murine BMDM a different pattern of cytokine and/or chemokine production when compared to these cells infected with the wild-type strain (99, 277, 278). In one report, secretion of IL-8, a chemotactic and inflammatory cytokine, was analyzed in human keratinocytes that were infected *in vitro* with either the wild-type, the *ospC* mutant, or the *ospC* complemented strain at an MOI of 100:1 for 24 h. This study proposed that secretion of IL-8 by keratinocytes is dependent on OspC as keratinocytes infected with the *ospC* mutant secreted less IL-8 when compared to keratinocytes infected with either the wild-type or the *ospC* complemented strain (277). Other reports showed that OspC did not have an effect on the production of IL-8 or KC (a murine IL-8 homolog) in human fibroblasts and murine BMDM after infection with wild-type, *ospC* mutant, or *ospC* complemented spirochetes (99, 278). In addition, OspC did not appear to have an effect on the expression and production of TNF-α and IL-10 in murine BMDM infected at an MOI of 10:1 for 3 h with either the wild-type, *ospC* mutant or *ospC* complemented strain. This finding is consistent with our results showing no differences in TNF-α and IL-10 expression in murine PMs infected with either the wild-type or the *ospC* mutant strain at an MOI of

100:1 for 2 h. Interestingly, the highest level of TNF-α expression in PMs infected with the *ospC* mutant occurred at 2 h post-challenge, which is when phagocytosis of the *ospC* mutant is significantly higher than the wild-type or the *ospC* complemented strains in our studies. This observation may be related to the quantity of spirochetes that are internalized by macrophages at a given point in time. In future studies, it would be valuable to determine if this relationship occurs by measuring TNF-α secretion in context of phagocytosis of spirochetes.

Phenotype of the *ospC* mutant in mice when inoculated with a high dose

We observed that the *ospC* mutant was capable of establishing infection and disseminating to multiple tissues in mice when inoculated with a high dose (10^6). This finding is in agreement with a recent report showing that the same *ospC* mutant (*ospC*K1) could establish infection in both wild-type C3H and SCID mice when inoculated at a high dose (107). However, Tilly et al. (107) did not report the contribution of the *ospC* mutant to disease development and persistence in mice when inoculated at a high dose. We observed that ear punch biopsies from SCID and C3H/HeN mice inoculated with the *ospC* mutant were culture positive 10 days later than ear punch biopsies collected from mice that were infected with the wild-type strain. In addition, we observed that the *ospC* mutant induced marked inflammation in the tibio-tarsal joints of infected SCID mice at 4 weeks post-challenge. Joint swelling or histological evidence of arthritis in tibio-tarsal joints was also present in NODSCIDg and C3H/HeN with active *ospC* mutant infection. Thus, although OspC is one of the major virulence factors of *B. burgdorferi* to infect mice (49, 64, 65), our data showed the requirement of OspC for establishing mammalian infection is not absolute and could be overcome by a large inoculum. The fact the *ospC*

mutant disseminates to multiple tissues distant from the site of inoculation also suggest that *ospC*-deficient spirochetes are motile during murine infection when using this large inoculum. Although the mechanism for this dose-dependent phenotype is not clear, our findings were consistent with the phenotype displayed by other *B. burgdorferi* mutants such as the *dbpAB* mutant. For example, the *dbpAB* mutant is not infectious when inoculated with doses ranging from 10^2-10^4 spirochetes per mouse (87) but is fully infectious when inoculated with a dose of 10^6 spirochetes per mouse (86, 87). In mice, low and intermediate doses (10^2-10^5) of the *dbpAB* mutant have been used to study dissemination, tissue colonization, persistence, tick acquisition and transmission (87, 279, 280); whereas, the high dose (10^6) of the *dbpAB* mutant have been used to study disease development and persistence in mice (86). Thus, the use of the high dose of the *ospC* mutant represents an alternative method to study the contribution of OspC in disease development, tissue tropism and/or persistence.

Part-II Role of *B. burgdorferi* EF-Tu during Lyme borreliosis

In recent years a growing number of highly conserved bacterial proteins that are commonly involved in metabolic regulation or cell stress responses have shown additional biological functions involved in bacterial adaptation, virulence, and/or immune modulation (196, 197). One such moonlighting protein is enolase that localizes on the surface of *B. burgdorferi* and has properties associated with spirochetal adhesion and immunogenicity. Previous studies with *B. burgdorferi* lysates have found that additional cytosolic proteins such as GroEL (*bb0649*), GAP (glyceraldehyde-3-phosphate-dehydrogenase, *bb0057*), and EF-Tu can be associated with the spirochetal membrane in variable amounts (192, 193, 281). In this dissertation, we found that rEF-TU was often

recognized by antibodies from sera from infected mice and patients diagnosed with Lyme disease, suggesting a potential role of EF-Tu as a serodiagnostic marker for Lyme disease. In addition, our results showed that EF-Tu does not appear to be exposed on the cell surface but indicates a subsurface localization in *B. burgdorferi* as EF-Tu was detected in protoplasmic cylinder fractions and in small quantities in OMVs.

EF-Tu is immunogenic during Lyme borreliosis

According to the CDC, serodiagnosis of Lyme disease should rely on the detection of class specific IgM and IgG antibodies individually or combined against diagnostically important purified antigens using a two-tiered approach consisting of ELISA followed by immunoblotting confirmation of results that are positive or equivocal (25). Immunoreactivity of these purified antigens appeared to be dependent on the duration of infection and the stage of Lyme disease. Of these proteins, surface lipoproteins OspC (22 kDa) and BmpA (39 kDa) and periplasmic FlaA (41 kDa) have been suggested as antigens that induce IgM responses during early Lyme borreliosis. Up to ten antigens have been suggested to elicit specific IgG responses for disseminated infection and late clinical manifestations of Lyme borreliosis (25, 26). Our immunoblotting results showed that rEF-Tu was recognized by antibodies from pooled mouse sera collected at the early and disseminated stages of infection. In addition, 7 out 10 patients with a history of prior tick exposure or infection and with early or late clinical manifestations were seroreactive to rEF-Tu. Thus, our findings suggest that rEF-Tu is recognized by IgM and IgG antibodies as this protein reacted with mouse and human sera collected at different stages of Lyme borreliosis.

Other *B. burgdorferi* periplasmic and cytoplasmic proteins have been shown to be immunogenic in human sera from Lyme disease patients (26, 193, 282, 283). Of these proteins, FlaB (33 kDa) and FlaA are highly reactive to IgM antibodies during the first 4 weeks of illness, and the protoplasmic protein p83/100 (83-100 kDa) is highly reactive to IgG antibodies in patients with late Lyme borreliosis (26, 284). Our data suggested that EF-Tu triggers an IgM-mediated response during early Lyme borreliosis as rEF-Tu exhibited reactivity with antibodies from infected mice within the first 4 weeks post-challenge. This finding suggests the role of *B. burgdorferi* EF-Tu as a potential early marker of Lyme borreliosis. In fact, this observation is consistent with a previous study showing that *Borrellia hermsii* EF-Tu was strongly reactive with IgM antibodies during early spirochetal infection in mice. However, because EF-Tu is a highly conserved protein among spirochetal species (285), this raises the possibility that this antigen may cross-react with IgM antibodies elicited from prior exposure to other spirochetal infections, as shown with FlaB that cross-reacts with antibodies from other spirochetal species (286, 287). In contrast, EF-Tu from other bacterial pathogens can elicit specific IgG-mediated responses during these bacterial infections (205, 249, 250). It is possible that the appearance of anti-EF-Tu IgG in mouse and human sera occurs after *B. burgdorferi* is killed by phagocytes, as our findings showed that *B. burgdorferi* EF-Tu was primarly localized in the cytoplasmic compartment. Further studies are needed to characterize the subclasses of immunoglobulins produced against *B. burgdorferi* EF-Tu at different stages of Lyme disease.

EF-Tu is not protective against *B. burgdorferi* challenge *in vivo*

Although *B. burgdorferi* EF-Tu appeared to elicit an antibody response *in vivo*, our active immunization experiments suggest that these anti-EF-Tu antibodies were not bactericidal during Lyme borreliosis as they were unable to reduce spirochetal burden in joints or in engorged tick larvae from immunized mice. One possible explanation of this lack of protection against spirochetal challenge could be because recombinant EF-Tu is not expressed in its native form in *E. coli*, which can lead to conformational changes in putative protective epitopes that may exist on EF-Tu. Given that our proteinase K and microscopy findings showed that EF-Tu was not on the cell surface, another possibility for this lack of protective phenotype could be attributed to changes in cytoplasmic EF-Tu after its degradation within antigen presenting cells. This biological process may lead to the generation of non-protective immunogenic soluble peptides that are presented via MHC-class II to naive $CD4^+$ T cells for a T cell-dependent B cell antibody response (103).

Localization of EF-Tu in *B. burgdorferi*

Our findings showed that *B. burgdorferi* EF-Tu predominantly localizes in PC fractions and is present in OMVs fractions in small quantities. Gram-negative bacteria naturally secretes outer membrane vesicles to deliver biologically active molecules and to interact with other cells in their environment (288). These vesicles are primarily composed of outer membrane proteins and periplasmic-associated proteins and enzymes (193, 289, 290). *B. burgdorferi* has shown to be able to produce OMVs when grown in BSK culture media without serum (291), a phenomenon that is also detected when spirochetes are co-culture with mammalian cells (292, 293) and during infection in Lyme

disease patients (293-295). It is thought that *B. burgdorferi* releases OMVs in response to physiological stress *in vivo* (296). These OMVs can serve as an adhesin on endothelial cells (297) and a mitogen for B cell responses *in vivo* (254). Thus, one might speculate from these observations that *B. burgdorferi* EF-Tu may have a function in OMVs, given that this protein appears to be immunogenic *in vivo*, and another highly conserved soluble enzyme such as enolase has been shown to be released in OMVs serving as an immunogenic plasminogen-binding protein (193). However, the biological function of OMVs biogenesis and constituents during *B. burgdorferi* infection is not completely understood.

CHAPTER VI: FUTURE DIRECTIONS

The data presented in this dissertation contribute to the current understanding of the biological function of OspC during mammalian infection and explore the role of EF-Tu during Lyme borreliosis. We demonstrated that depletion of phagocytes at the skin-site of inoculation in SCID mice allowed the *ospC* mutant to establish infection *in vivo*. In phagocyte-depleted SCID mice, the *ospC* mutant was capable of colonizing the tibio-tarsal joints and triggered neutrophilia during dissemination in a similar pattern as wild-type bacteria. Furthermore, *in vitro* studies showed that phagocytosis of the *ospC* mutant was significantly higher than the wild-type and *ospC* complemented strains, suggesting that OspC could have a protective role against macrophage phagocytosis. OspC was not involved in scavenger receptor A and B mediated phagocytosis of spirochetes by murine macrophages. Thus, these data reveal that OspC has an anti-phagocytic property, which may facilitate the evasion of spirochetes from phagocytes during early infection.

In addition, data from second part of this dissertation showed that *B. burgdorferi* EF-Tu triggered an antibody response during Lyme borreliosis. Our findings suggest that *B. burgdorferi* EF-Tu is an immunogenic antigen and may have epitopes that could be used to assist in the serodiagnosis of early Lyme borreliosis. These putative EF-Tu epitopes are likely not accessible to antibodies in intact *B. burgdorferi* during infection as we demonstrated that EF-Tu primarily localizes underneath the cell surface of spirochetes that were grown under favorable culture conditions.

Assess the interaction of *B. burgdorferi* OspC with macrophages in mice

Our findings suggest that OspC protects wild-type spirochetes when they encounter macrophages in the skin during early infection in SCID mice. To confirm the

111

contribution of these phagocytes to the clearance of the *ospC* mutant in mice, we will deplete these cells with clodronate liposome treatments in the skin of C3H/HeN mice as previously described in materials and methods for SCID mice. We will use the C3H/HeN mouse strain since this is the experimental mouse model for Lyme borreliosis (34). Infectivity of C3H mice will be analyzed by reisolation of the *ospC* mutant from different tissues 7 days post-challenge as described in infectivity studies conducted with SCID mice. If the *ospC* mutant disseminates in C3H mice treated with clodronate liposomes, this finding will support the notion that OspC plays a protective role for spirochetes against macrophages. Conversely, if the *ospC* mutant cannot establish infection in C3H mice treated with clodronate liposomes, this finding suggests that depletion of phagocytes along with B and T cells is needed for the *ospC* mutant to infect mice. This scenario implies that the *ospC* mutant has a reduced fitness and is less able to adapt in the mouse skin when compared to the wild-type strain.

Our IHC results showed that F4/80⁺ cells were depleted in the skin of SCID mice infected with wild-type or *ospC* mutant spirochetes. In the mouse skin, resident dermal macrophages and immature epidermal Langerhans cells can express the F4/80 glycoprotein on the cell surface (236, 264). To rule out the possibility that Langerhans cells are involved in the clearance of the *ospC* mutant, we can test this question by depleting these cells from the mouse epidermis prior to inoculation with either the wild-type or the *ospC* mutant strain. A suitable mouse model to test this question is the Langerin-DTR transgenic mouse strain, as treatment with diphteria toxin in this mouse strain selectively depletes epidermal Langerhans cells, dermal DC, and some lymphoid derived DC for at least 5 days (298), without causing an increase in neutrophils as shown

with other mouse strains used for DC depletion such as CD11b- or CD11c-DTR mice

(298, 299). A similar mouse strain has been used by Lyme disease investigators to test

whether a *B. burgdorferi p66* mutant could establish infection in mice depleted of DCs

and certain monocyte populations. This *B. burgdorferi* mutant had a similar pattern of

clearance *in vivo* as shown by the *ospC* mutant and could not establish infection in

dendritic cell-depleted, TLR2$^{-/-}$, and MyD88$^{-/-}$ mice (85). Thus, based on this evidence, it

is possible that depletion of DCs may not be sufficient for the *ospC* mutant to establish

infection in mice.

In addition, it will be important for this project to use additional approaches to

better understand how wild-type and *ospC* mutant spirochetes move in the skin of mice

and interact with phagocytes *in vivo*. To assess how these spirochetes move in the skin,

GFP-expressing spirochetes generated in this study could be used to assess whether the

ospC mutant exhibits different movements than the wild-type in the mouse skin, using

intravital microscopy. In the past 5 years, this technique has been employed to

characterize the movement of GFP-expressing *B. burgdorferi* wild-type and mutant

strains in the mouse skin and organs (79, 300), as most *in vitro* systems used to examine

the motility of *B. burgdorferi* do not resemble the tissue milieus that spirochetes

encounter *in vivo* (300). This technique has shown that *B. burgdorferi* exhibits at least

three different motility states in the mouse dermis and has been used to assess the

interaction of *B. burgdorferi* adhesins such as BBK32 with vascular endothelium (301,

302). By understanding the kinetics and movements of wild-type and *ospC* spirochetes in

the mouse dermis, we will be able to assess whether the *ospC* mutant has a defective

phenotype in migrating from connective tissue into the vasculature. If this defect occurs,

then *ospC* mutant spirochetes may be captured more efficiently by resident macrophages or Langerhans cells than wild-type spirochetes in the mouse skin. This phenotype could explain why the *ospC* mutant is rapidly cleared within 48 h from the skin-site of inoculation in mice, without a marked neutrophil recruitment into the mouse skin (64, 99). Alternatively, if the *ospC* mutant exhibits a similar pattern of motility to the wild-type *in vivo*, this finding would support the importance of OspC as a surface receptor for host cells or ligands in the mouse skin.

To evaluate the interaction of the wild-type and *ospC* mutant with phagocytes *in vivo*, we could test this by inoculating monomeric red fluorescent protein (mRFP)-expressing spirochetes in Macgreen transgenic mice and then image sections of the mouse skin using intravital microscopy. We will need to transform wild-type and the *ospC* mutant spirochetes with our construct that already contains the mRFP). The Macgreen mouse line express the enhanced green fluorescent protein (EGFP) reporter gene that is driven by the macrophage colony-stimulating factor receptor 1 (csf1r*)* promoter (303). Previous studies have shown that treatment of mice with the monoclonal anti-csfr1 antibody blocks csf1 signaling and efficiently depletes the number of F4/80$^+$ phagocyte populations in the skin (299). Thus, this approach will determine whether there are differences in the behavior between the *ospC* mutant and the wild-type strain when individual phagocyte populations are depleted in the mouse dermis and epidermis.

Identify the phagocytic receptor and mechanism involved in the uptake of the *ospC* mutant

Our results showed an enhanced uptake of the *ospC* mutant strain when compared to the wild-type using fluorometric based phagocytosis assays and flow cytometry. In

addition, we evaluated whether the scavenger receptor A and B were involved in this enhanced uptake of the *ospC* mutant and found scavenger receptor A and B mediated phagocytosis of spirochetes was independent of OspC. To evaluate the phagocytic receptor(s) that are involved during phagocytosis of the *ospC* mutant by murine macrophages, we could measure the cell surface expression of different phagocytic receptors in murine PMs before and after phagocytosis of the *ospC* mutant and the wild-type strain. Some phagocytic receptors involved in the binding and/or uptake of non-opsonized spirochetes include: MARCO, SRAI/II, CR3, CD14, and mannose (125, 138, 244). Other macrophage receptors that could be evaluated are those that have an inhibitory effect in phagocytosis (e.g. FcγIIB), as these receptors have motifs that recruit phosphatases that play an inhibitory function in phagocytosis (304). It will also be important to evaluate the expression of scavenger receptor CD36 in macrophages during *B. burgdorferi* challenge, as CD36 has been reported to mediate phagocytosis of different bacterial species (246). In addition, it is possible that CD36 could play a role in the pathogenesis of Lyme carditis or neuroborreliosis, as this pattern recognition receptor is expressed in several cell types (e.g. monocytes/macrophages, endothelial cells, cardiac myosites, platelets, and adiposytes) (305) and mediates several biological process, including inflammation of cardiovascular and neurodegenerative disorders, angiogenesis, thrombosis, oxidative stress, and metabolism (306). Thus, measuring the surface expression of different phagocytic receptors will allow us to obtain baseline data when murine PMs interact with either wild-type or *ospC* mutant spirochetes. This will allow us to determine whether OspC alters phagocytic receptor profiles in infected murine macrophages. One possible outcome of this experiment is that more than one phagocytic

receptor is involved in the higher uptake of the *ospC* mutant by PMs. Therefore, blocking multiple phagocytic receptors may be needed to show similar phagocytosis between the *ospC* mutant and the wild-type strain. Another possible scenario is that one phagocytic receptor mediates the recognition of OspC in spirochetes. If this occurs, research efforts will be directed to understand the interaction of OspC with their potential cognate receptor on macrophages. To further our understanding of this interaction, it will be important to ectopically express this phagocytic receptor on CHO cells to characterize the contribution of this receptor in binding OspC and phagocytizing spirochetes. For this experiment we would use CHO cells, as they stably express CR3 and have the ability to bind non-opsonized spirochetes and outer membrane lipoproteins such as OspA/B as well as phagocytose *B. burgdorferi* (138, 307). If OspC specifically interacts with one phagocytic receptor, we could then evaluate whether blocking this receptor would enhace the ability of macrophages to clear *B. burgdorferi* during early stages of infection *in vivo*.

Another possible outcome is that blocking phagocytic receptors do not restore phagocytosis of the *ospC* mutant to levels that are similar to those shown by wild-type spirohetes in PMs. This finding suggests that an additional mechanism such as coiling phagocytosis could mediate this enhanced uptake of the *ospC* mutant. To test this, murine PMs will be infected at an MOI of 100:1 with either wild-type or the *ospC* mutant strains expressing GFP, and coilining phagocytosis events will be enumerated by confocal laser scanning microscopy. To visualize the formation of actin-rich pseudopods that enwrap spirochetes in coiling phagocytosis, we could then use a probe such as phalloidin that binds with a high affinity to F-actin filaments in macrophages. In addition, we could employ an alternative method to block uptake of GFP-expressing spirochetes via coiling

phagocytosis. Murine macrophages will be transfected with small interfering RNA (siRNA) to knockdown formin FMNL1 and mDia1 which have shown to regulate coiling phagocytosis of *B. burgdorferi* (139). Phagocytosis of GFP-expressing spirochetes by siRNA-treated macrophages will be determined using a microplate fluorometer.

Our findings suggest that OspC could directly protect spirochetes against macrophage phagocytosis. Thus, another possibility is that OspC shields ligands on the spirochete's membrane from interacting with macrophages via conventional phagocytosis. For example, it is possible that macrophage receptors recognize ligands known as "eat me signals" (308) on the outer membrane of spirochetes lacking OspC, which lead to an enhanced uptake of the *ospC* mutant when compared to the wild-type strain. As mentioned above, it is known that macrophage phagocytosis of *B. burgdorferi* could be mediated by several phagocytic receptors and pattern-recognition receptors (125). It would be then important to evaluate whether OspC could have an effect on signaling via tyrosine kinases (e.g. PI3K) or serine/threonine kinases (e.g. RhoA kinase) that are known to regulate cytoskeletal activities during phagocytosis of bacteria (141, 309). To test this, we could measure the phosporylation of PI3K and RhoA kinases in cellular lysates from PMs infected (MOI of 100:1) with either wild-type or *ospC* mutant spirochetes. If OspC has an effect in the activation of these kinases, we can next confirm whether blocking PI3K or RhoA pathway inhibits the uptake of the *ospC* mutant to levels that are similar to those shown by the wild-type strain. Murine PMs will be then pretreated with pharmacological inhibitors specific for PI3K and/or RhoA kinases, and phagocytosis of GFP-expressing spirochetes could be determined using a microplate fluorometer.

Because *B. burgdorferi* encodes several outer surface proteins that can be expressed at specific stages of mammalian infection (76), it will also be important to evaluate whether other surface proteins exhibit a similar protective phenotype against macrophage phagocytosis *in vitro*. It is possible that this anti-phagocytic property of OspC is not unique, and perhaps, other surface lipoproteins important for mammalian infection may also protect against macrophage phagocytosis. To test this, non-opsonic phagocytosis could be assessed for several GFP-expressing *B. burgdorferi* single and double mutant strains that were generated in the lab. If other mutants showed an enhanced uptake by macrophages, this finding will suggest that *B. burgdorferi* employs certain surface proteins to protect from macrophage phagocytosis. Another possible outcome is that this protection against macrophage phagocytosis is restricted to OspC. This finding could be explained because OspC is an immunodominant antigen on the spirochetal membrane during the early course of infection (172, 173). It is well-known that *B. burgdorferi* upregulates the production of OspC as spirochetes are transmitted from ticks to mammals as a strategy to survive and adapt in the mammalian host environment (14, 171). However, OspC is downregulated in response to anti-OspC IgG antibodies within the first 2-3 weeks post-infection (174, 175). Therefore, this protective effect of OspC against macrophage phagocytosis could be specific to the early stage of mammalian infection. A proposed model of the functions of OspC during early Lyme borreliosis are represented in figure 33.

Characterize *B. burgdorferi* EF-Tu as a serodiagnostic marker of Lyme disease

Our data showed that rEF-Tu is recognized by antibodies in samples from infected mice and Lyme disease patients. To validate these findings and determine the

type of humoral responses, it will be then important to develop an ELISA to determine the frequency and duration of IgM and IgG specific antibodies from infectious sera from mice and humans collected at different stages of Lyme borreliosis. Then, immunoblotting can be used as a confirmatory tool for ELISA positive or equivocal results. These serological findings would be more meaningful if the sample size is increased for each group of Lyme disease patients to determine the sensitivity and specificity of each serological assay. To design this study, each stage of the illness and laboratory test results should be used to define an inclusion and exclusion criteria of the patient samples that will be analyzed by serology. It will also be important to evaluate how these results compare to current antigens that are used for the serodiagnosis of Lyme disease such as OspC and p83/100 for the early and late stages of illness, respectively (25, 26). Furthermore, as *B. burgdorferi* EF-Tu is a highly conserved antigen among *Borrelia* species (285), it will also be necessary to include other rEF-Tu antigens from other *Borrelia* species and bacterial species to assess cross-reactivity of IgM and IgG antibodies in samples tested by this newly developed ELISA. After performing these predicted experiments and if results demonstrate that EF-Tu could be used as a serodiagnostic marker for Lyme disease, it would then be appropriate to define the immunodominant epitopes that could be present in *B. burgdorferi* EF-Tu protein, which could be tested by this ELISA. We have preliminary performed sequence alignment of the full-length EF-Tu sequence among different pathogenic spirochetal species (e.g. *B. burgdorferi*, *Leptospira interrogans*, *Treponema pallidum*, *Treponema denticola*) and found that sequence homologies varied from 64% to 68% among these spirochetal species (data not shown). Therefore, we could start screening unique *B. burgdorferi* EF-

Tu peptides against serum panels from patients with early and late manifestations of Lyme disease.
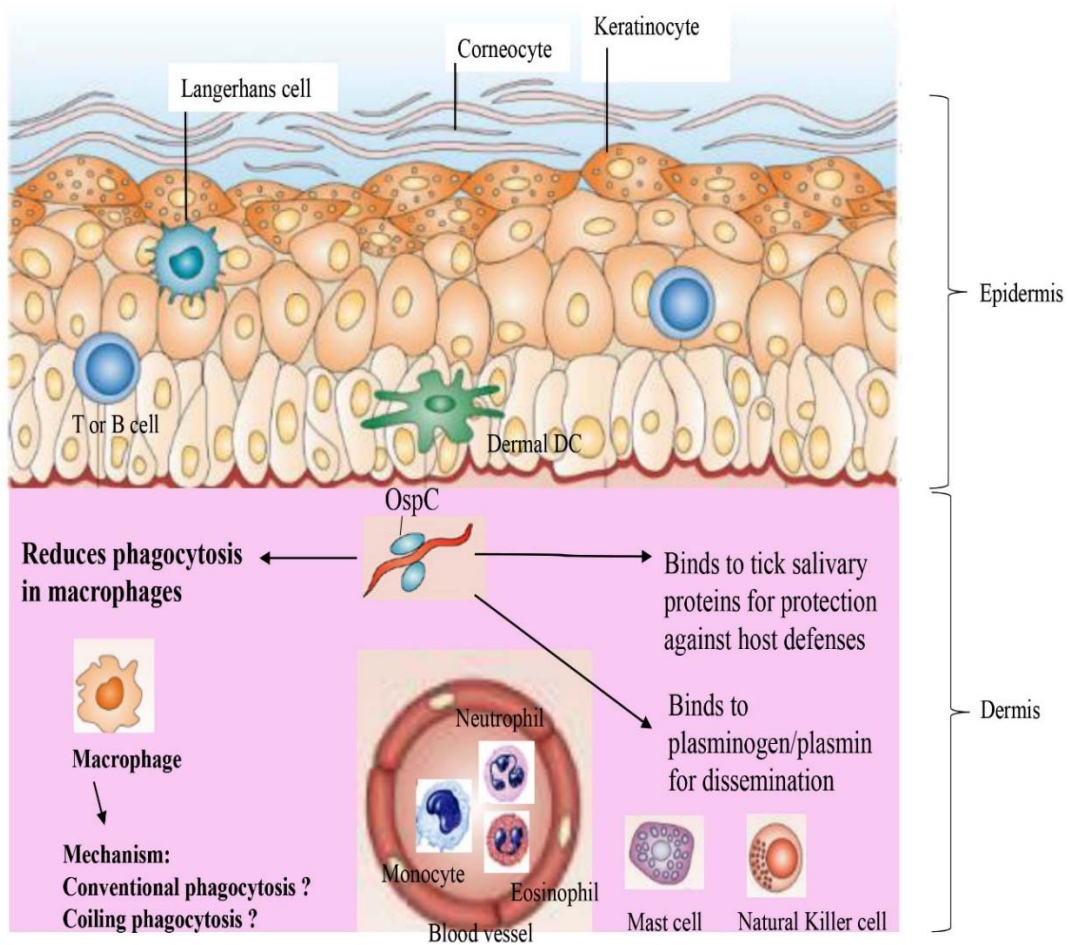
Figure 27. Proposed model of the functions of OspC during early Lyme borreliosis. Simplified illustration of the main cellular effectors involved in host defense during spirochetal infection within the murine epidermis and dermis (panel was adapted from (310)). Previous studies have shown that OspC binds to tick salivary proteins such as Salp15 which can protect spirochetes from complement- and antibody- mediated killing (111, 178). Alternatively, other studies have shown that OspC is a potent plasminogen receptors which may facilitate dissemination of spirochetes *in vivo.* Our studies show that

OspC could have anti-phagocytic property (bold font) that reduces phagocytosis of *B.burgdorferi* strains by murine and human macrophages. The mechanism for how phagocytosis is different between the wild-type and *ospC* mutant strains is under investigation. Conventional and coiling phagocytosis are the two major mechanisms that may be involved in the recognition and binding of spirochetal ligands. Our data demonstrate that B cells, T cells, NK cells, and neutrophils are not required for the clearance of the *ospC* mutant; however, F4/80$^+$ phagocytes such as macrophages and Langerhans cells play a role in the clearance of the *ospC* mutant *in vivo*. The role of keratinocytes, dermal dendritic cells (DC), eosinophils, and mast cells were not evaluated in our studies.

APPENDIX

Evaluation of Stat3 deficiency in endothelial cells and myeloid cells during Lyme borreliosis

The signal transducer and activator of transcription 3 (STAT3) has been shown to be important in several biological processes, including cell proliferation, migration, survival, and transformation, and angiogenesis (311). STAT3 is also an important regulator of inflammatory and immune responses in diverse pathological processes, including myocarditis, rheumatoid arthritis, and central nervous system autoimmune diseases (312-314), but its role in Lyme borreliosis is not well understood. Previously, a report from Behera et al. (315) showed that *B. burgdorferi* infection induced the phosphorylation and nuclear translocation of STAT3 in primary human chondrocytes. Another report indicated that STAT3 expression and phosphorylation was upregulated in cardiac tissues from C3H and Balb/c mice infected with *B. burgdorferi*, and this upregulation of STAT3 was associated with the progression of disease (316). *B. burgdorferi* lipoproteins also induce NF-κB nuclear translocation in myeloid and endothelial cells, resulting in cytokine and chemokine production and adhesion molecule expression (119). Because STAT3 inhibits the expression of NF-κB-regulated gene products involved in innate immunity and T helper 1 adaptive responses important for controlling microbial infections and inflammation (311), we then hypothesized that Stat3 deficiency in endothelial or myeloid cells exacerbates inflammation in joints during Lyme borreliosis. To test this hypothesis, we used endothelial cell- (**Figure 28A**) or myeloid cell-specific (**Figure 30A**) Stat3-deficient mice (Stat3$^{E-/-}$ or Stat3$^{B-/-}$) that were challenged with *B. burgdorferi* 5A4NP1 strain. Our preliminary results showed that all

three *B. burgdorferi* infected Stat3$^{E-/-}$ mice exhibited mild to moderate arthritis in tibio-tarsal joints at 4 weeks post-challenge. *B. burgdorferi* infected Stat3$^{F/F}$ (control, n = 5) mice exhibited minimal to mild arthritis in tibio-tarsal joints (**Figure 29**). No significant differences in spirochetal burden in tissues and granulocyte and mononuclear cell counts in blood were noted between Stat3$^{E-/-}$ and Stat3$^{F/F}$ mice at 4 weeks post-challenge (**Figure 28B-D**). *B. burgdorferi* infected Stat3$^{B-/-}$ mice (**Figure 31A,** n = 2) also exhibited mild arthritis in tibio-tarsal joints at day 10 post-challenge. *B. burgdorferi* infected Stat3$^{F/F}$ (control, n = 5) mice exhibited minimal to mild arthritis in tibio-tarsal joints (**Figure 31A**). Spirochetal burden in the heart and tibio-tarsal joint was similar between Stat3$^{B-/-}$ and Stat3$^{F/F}$ mice at day 10 post-challenge (**Figure 30B**). These preliminary findings suggest that Stat3 in endothelial cells may contribute to the resolution of arthritis in mice, as all three Stat3 $^{E-/-}$ mice appeared to have higher arthritis than the control group. Future studies should expand these preliminary findings to determine the role of Stat3 in endothelial cells in the development of arthritis in mice.
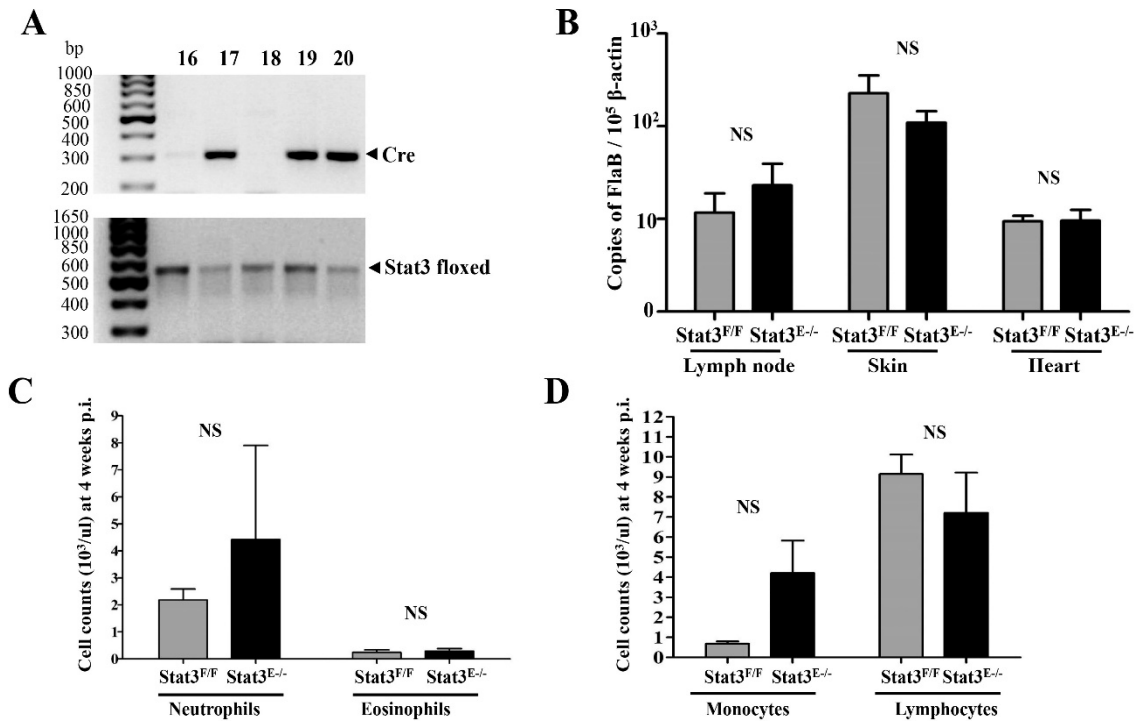
Figure 28. Spirochetal burden in tissues and leukocyte response in circulation of Stat3$^{E-/-}$ mice during disseminated *B. burgdorferi* infection. A) Demonstration of genotypes of *eTie2*-Cre (upper, Cre product = 300 bp) and Stat3 floxed alleles (lower, Stat3 floxed product = 520 bp) of mice used in this study. The *eTie2* gene promoter drives the expression of Cre recombinase for the deletion of loxP flanked Stat3 in endothelial cells. The genotype for mice 17, 19, and 20 was Stat3$^{F/F}$/*eTie2*-Cre, suggesting that *stat3* was deleted in endothelial cells in these mice (named as Stat3$^{E-/-}$). Mice 16 and 18 were littermate controls (named as Stat3$^{F/F}$). **B)** Spirochetal burden in inguinal lymph nodes, skin biopsies, and apex of hearts from mice (n = 2-3 per group) at 4 weeks (wk) post-challenge with *B. burgdorferi* 5A4NP1 strain (10^6 spirochetes inoculated per mouse via i.d.). *B. burgdorferi* was reisolated from all tissues tested by PCR. **C-D)** Granulocytes (left) and mononuclear cell (right) responses in peripheral blood of mice (n = 3-5 per group) infected with *B. burgdorferi* 4 weeks post-challenge.

124

Peripheral blood was analyzed with a HEMAVET 950 multispecies hematology cell counter as described in material and methods. Normal reference values for neutrophils, eosinophils, monocytes and lymphocytes in mice are ≤ 2.5, ≤ 0.2, ≤ 0.4, and 0.9 - 9.3 (x $10^3/\mu l$), respectively (NS = not significant).

A
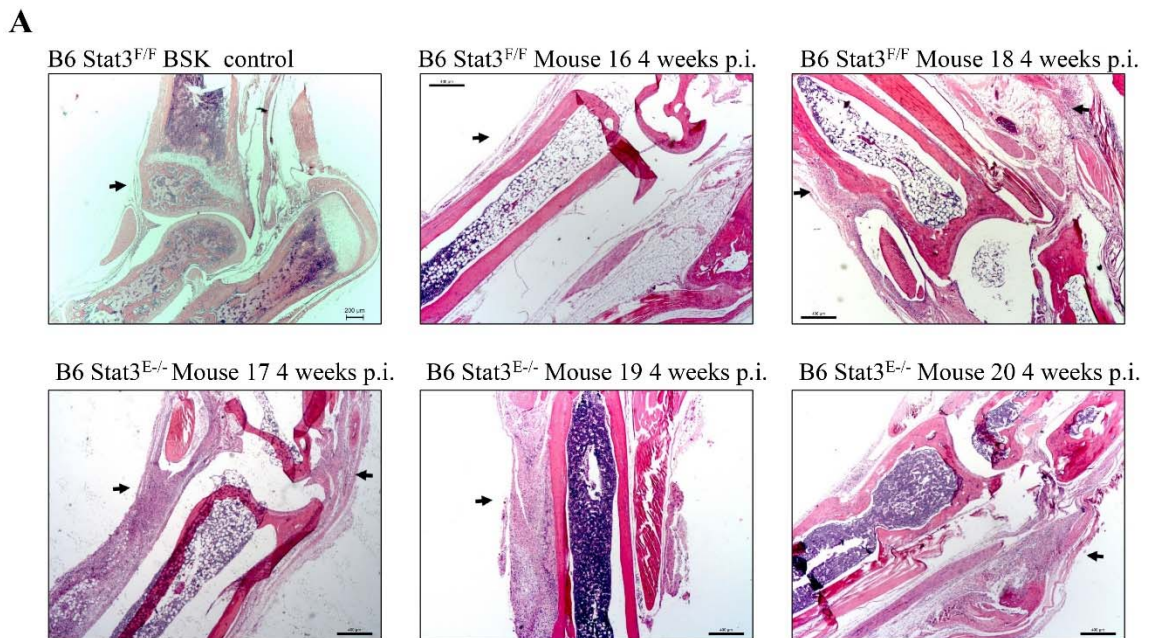
Figure 29. Arthritis severity in tibio-tarsal joints in *B. burgdorferi*-infected C57BL/6 (B6) Stat3^{F/F} and Stat3^{E-/-} mice at 4 weeks post-infection. Representative images (magnification, ×2.5, scale bar- 400 μm) of H&E-stained tibio-tarsal joints from BSK-injected (control) and 4 week-infected Stat3^{F/F} and Stat3^{E-/-} mice. Blinded histopathological evaluation of tibio-tarsal joints of mice was performed by a board certified veterinary pathologist. Stat3^{F/F} mice 16 and 18 exhibited minimal to mild inflammation of the ligament or tendon sheaths (herein collectively termed arthritis, black arrows) with cellular infiltrates primarily composed by macrophages, lymphocytes, and plasma cells and occasionally by neutrophils. Mouse 18 exhibited evidence of periosteal

inflammation and bone erosion and remodeling on random focal areas of the periosteum in the tibia (left black arrow). Stat3$^{E-/-}$ mice 17, 19, and 20 exhibited mild to moderate inflammation of the ligament or tendon sheaths (black arrows) as well as the periosteum, which had focal areas of bone erosion and remodeling. Cellular infiltrates of mice 17 and 19 were primarily composed of macrophages, lymphocytes, and plasma cells. Mouse 20 also exhibited moderate inflammation characterized by a mixture neutrophil and mononuclear cell (macrophages, lymphocytes, and plasma cells) infiltration in multiple areas throughout the fascia (black arrow) and muscle (collectively termed fasciitis and myositis, respectively).
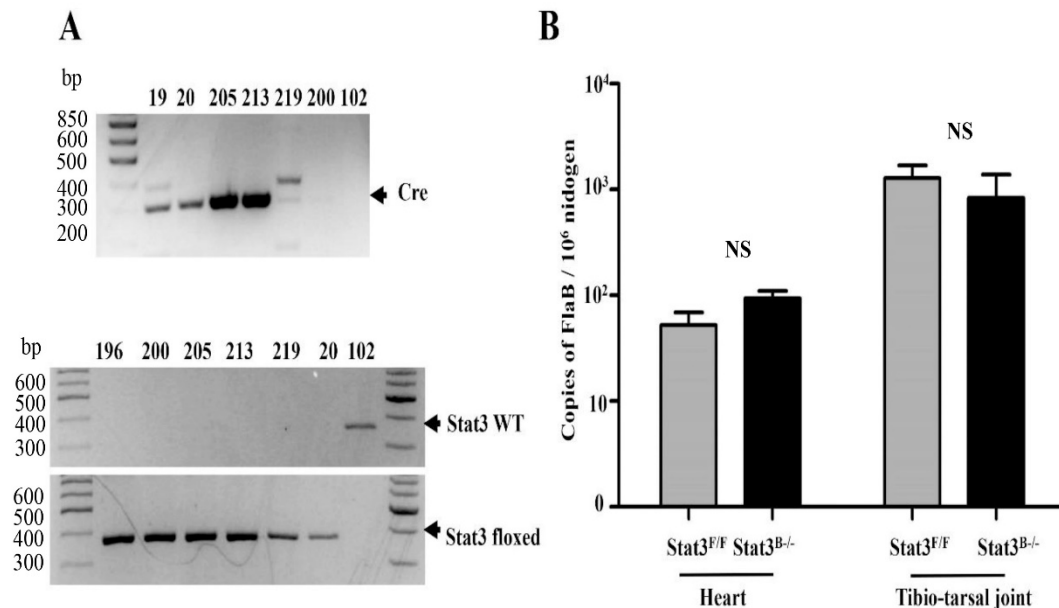
Figure 30. Spirochetal burden in tissues of mice deficient for Stat3 in myeloid cells infected with *B. burgdorferi* for 10 days. A) Demonstration of genotypes of *bTie2*-Cre (upper, Cre product = 300 bp) and Stat3 wild-type (WT) and Stat3 floxed alleles (lower, Stat3 WT = 361 bp and Stat3 floxed = 377 bp) of mice. The *bTie2* gene promoter drives

126

the expression of Cre recombinase for the deletion of loxP flanked *stat3* in myeloid cells.

The genotype for mice 205 and 213 was Stat3$^{F/F}$/*bTie2*-Cre, suggesting that *stat3* was

deleted in myeloid cells in these mice (named as Stat3$^{B-/-}$). Representative genotyping

results of Stat3$^{F/F}$ mice (200, and 219), Stat3 WT mice (102), and Cre$^+$ F/F mice (20) are

shown in this figure as controls from PCR reaction. **B)** Spirochetal burden in apex of

hearts and tibio-tarsal joints from mice (n = 2-5 per group, NS = not significant) at 10

days post-challenge with *B. burgdorferi* 5A4NP1 strain (10^5 spirochetes inoculated per

mouse via i.d.).

A
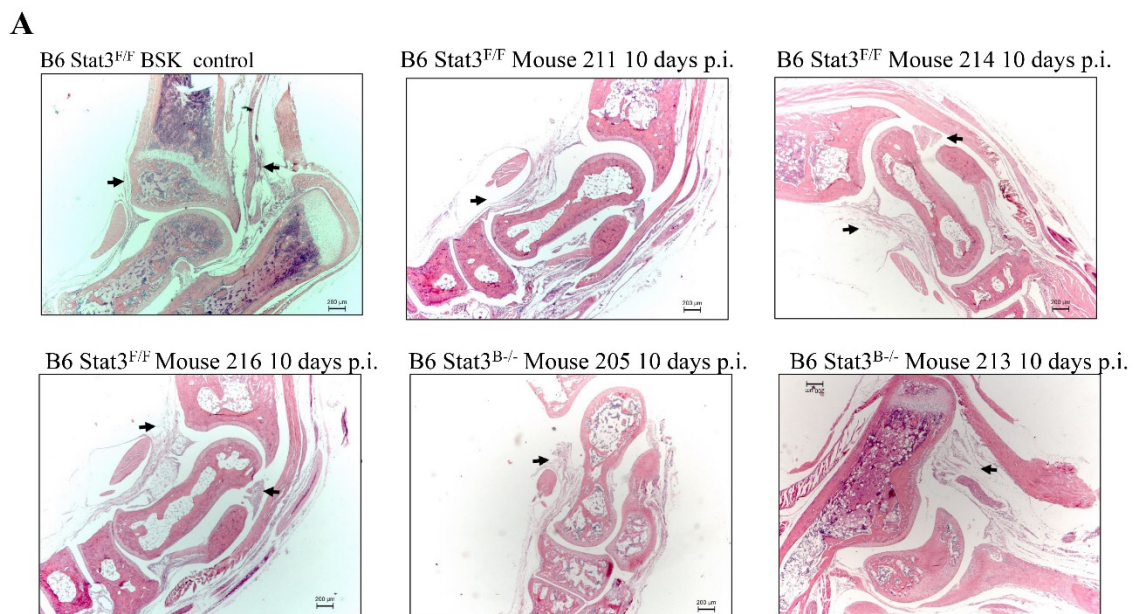
Figure 31. Arthritis severity in tibio-tarsal joints in *B. burgdorferi*-infected C57BL/6

(B6) Stat3$^{F/F}$ and Stat3$^{B-/-}$ mice at 10 days post-infection. Representative images

(magnification, ×2.5, scale bar- 200 μm) of H&E-stained tibio-tarsal joints from BSK-

injected (control) and 4 week-infected Stat3$^{F/F}$ and Stat3$^{B-/-}$ mice. Blinded

histopathological evaluation of tibio-tarsal joints of mice was performed by a board

certified veterinary pathologist. Stat3$^{F/F}$ mice 211, 214, and 216 exhibited minimal to mild inflammation of the synovial membrane and ligament or tendon sheaths (herein collectively termed arthritis, black arrows) with cellular infiltrates primarily composed of neutrophils and macrophages with few lymphocytes and plasma cells. Stat3$^{F/F}$ mice also exhibited evidence of mild fasciitis and myositis and periosteal inflammation. Stat3$^{B-/-}$ mice 205, and 213 exhibited mild inflammation of the synovial membrane (black arrows), the ligament or tendon sheaths and the fasciae and muscle. Cellular infiltrates of these mice were primarily composed by neutrophils and macrophages with some lymphocytes, and rare plasma cells.

Evaluation of Plac8 and nitric oxide deficiency in host defense and disease during Lyme borreliosis

Infection with the Lyme disease spirochete, *B. burgdorferi,* causes a debilitating inflammatory disorder in humans that primarily targets the skin, joints, heart, and nervous system. The outer surface lipoproteins of *B. burgdorferi* have shown to stimulate the production of inflammatory mediators such as cytokines and nitric oxide (NO) that can regulate the innate immune responses during Lyme borreliosis (170). *B. burgdorferi* also has shown to be highly susceptible to killing by NO donor compounds (152) and by iNOS-derived NO from macrophages (148, 155, 170). However, despite the sensitivity of *B. burgdorferi* to NO compounds *in vitro*, no critical differences in spirochetal burden and joint inflammation are observed between wild-type and iNOS-deficient mice (157, 317). These findings suggest that an additional compensatory antimicrobial mechanism is required to clear *B. burgdorferi* infection in tissues in mice. To determine if an additional mechanism is involved in killing *B. burgdorferi in vivo*, we then preliminary evaluated the role of Plac8 in host defense and disease during Lyme borreliosis. Plac8 is a cysteine-rich protein that is expressed by macrophages, neutrophils, lymphocytes, and epithelial cells and is involved in host defense against extracellular and intracellular bacterial infections in mice (318, 319). Two iNOS-deficient Plac8$^{-/-}$ mice and two Plac8$^{-/-}$ mice were challenged with *B. burgdorferi* B31-A3 strain. Nitric oxide production was inhibited by administration of 50 μM of the NO inhibitor (NOI), L-NMMA, to the drinking water on two days before infection through day 25 post-infection. Our preliminary results showed that iNOS-deficient Plac8$^{-/-}$ mice exhibited slightly higher spirochetal burden in inguinal lymph node, heart, and tibio-tarsal joint when compared to

129

Plac8$^{-/-}$ mice (**Figure 32A**). Both groups of infected-mice exhibited a similar pattern of inflammation in the tibio-tarsal joints at 3.5 weeks post-challenge (**Figure 33A**). These findings suggest that Plac8 deficiency may be involved in the clearance of spirochetes in tissues of mice. Future studies should expand these preliminary findings to determine the role of Plac8 in host defense during Lyme borreliosis.

A
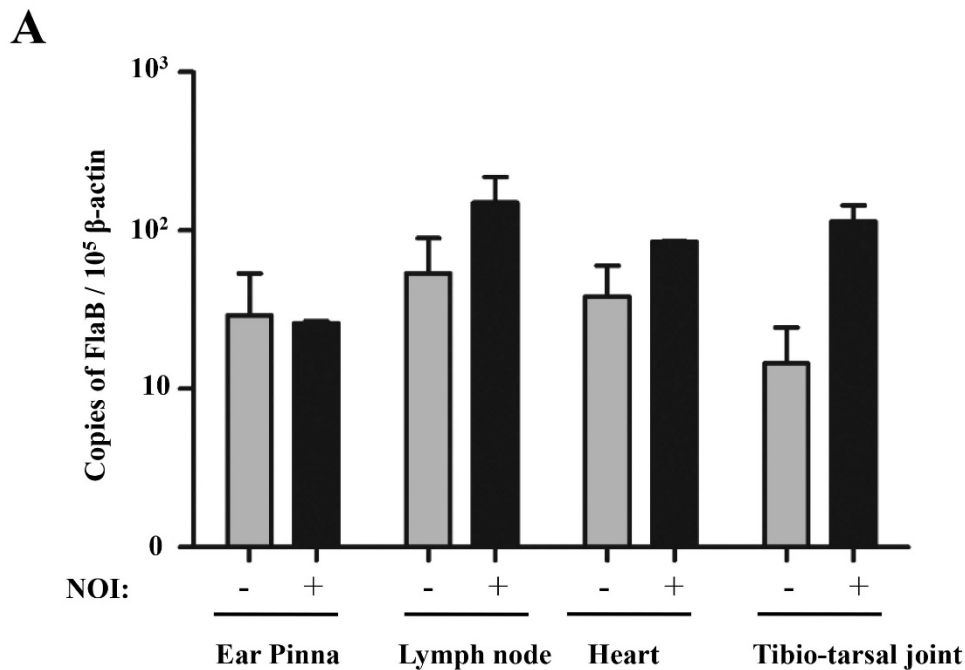
Figure 32. Spirochetal burden in tissues of Plac8$^{-/-}$ mice and Plac8$^{-/-}$ mice treated with nitric oxide inhibitor (NOI) at 3.5 weeks post-infection. A) Spirochetal burden in ear pinna, inguinal lymph node, apex of hearts, and tibio-tarsal joints from mice (n = 2 per group) at 3.5 weeks (wk) post-challenge with *B. burgdorferi* B31-A3 strain (10^6 spirochetes inoculated per mouse via i.d.). *B. burgdorferi* was reisolated from ear punch biopsies collected from all mice tested by PCR.

A
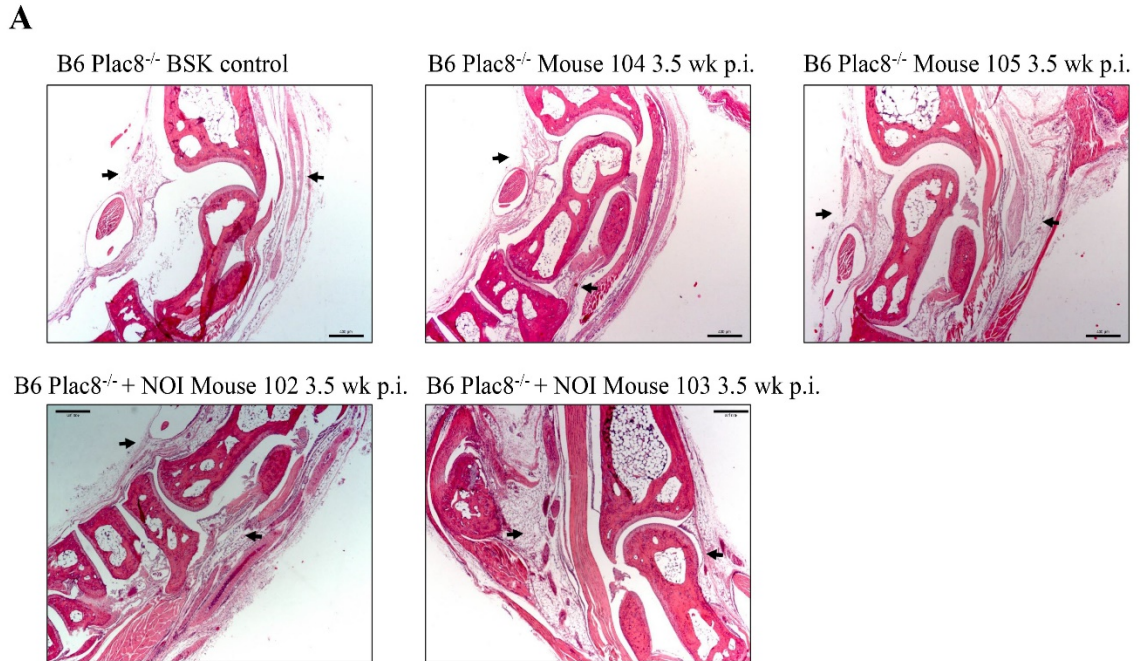
Figure 33. Arthritis severity in tibio-tarsal joints in *B. burgdorferi*-infected C57BL/6 (B6) Plac8-/- mice and Plac8-/- mice treated with nitric oxide inhibitor (NOI) at 3.5 weeks post-infection. A) Representative images (magnification, ×2.5, scale bar- 400 μm) of H&E-stained tibio-tarsal joints from BSK-injected (control) and 3.5 week-infected mice. Blinded histopathological evaluation of tibio-tarsal joints of mice was performed by a board certified veterinary pathologist. Plac8^{-/-} mice 104 and 105 exhibited mild inflammation of tibio-tarsal joints characterized by mild hyperplasia of the synovial membrane and thickening of ligament and tendon sheaths (black arrows). Cellular infiltrates were primarily composed of macrophages and lymphocytes and few plasma cells. Tibio-tarsal joints from NOI-treated Plac8^{-/-} mice 102 and 103 had mild inflammation of the synovial membrane, ligaments and tendon sheaths (black arrows) with cellular infiltrates primarily composed of macrophages, lymphocytes, and plasma cells.

REFERENCES

1. **Steere AC, Malawista SE, Snydman DR, Shope RE, Andiman WA, Ross MR, Steele FM.** 1977. Lyme arthritis: an epidemic of oligoarticular arthritis in children and adults in three connecticut communities. Arthritis Rheum **20:**7-17.
2. **Burgdorfer W, Barbour AG, Hayes SF, Benach JL, Grunwaldt E, Davis JP.** 1982. Lyme disease-a tick-borne spirochetosis? Science **216:**1317-1319.
3. **Johnson RC, Schmid GP, Hyde FW, Steigerwalt A, Brenner DJ.** 1984. *Borrelia burgdorferi* sp. nov.: etiologic agent of Lyme disease. Int J Syst Bacteriol **34:**496-497.
4. **Baranton G, Postic D, Saint Girons I, Boerlin P, Piffaretti JC, Assous M, Grimont PA.** 1992. Delineation of *Borrelia burgdorferi* sensu stricto, *Borrelia* garinii sp. nov., and group VS461 associated with Lyme borreliosis. Int J Syst Bacteriol **42:**378-383.
5. **Welsh J, Pretzman C, Postic D, Saint Girons I, Baranton G, McClelland M.** 1992. Genomic fingerprinting by arbitrarily primed polymerase chain reaction resolves *Borrelia burgdorferi* into three distinct phyletic groups. Int J Syst Bacteriol **42:**370-377.
6. **Centers for Disease Control and Prevention (CDC).** 2012. Summary of Notifiable Disease - United States 2011, p. 26, Morbidity and Mortality Weekly Report, vol. 60.
7. **Kuehn BM.** 2013. CDC estimates 300,000 US cases of Lyme disease annually. Jama **310:**1110.
8. **Centers for Disease Control and Prevention (CDC).** 2014. Reported cases of Lyme Disease-United States 2013. CDC Division of Vector-borne Infectious Diseases. In: http://www.cdc.gov/lyme/stats/maps/map2013.html.
9. **Burgdorfer W, Lane RS, Barbour AG, Gresbrink RA, Anderson JR.** 1985. The western black-legged tick, *Ixodes pacificus*: a vector of *Borrelia burgdorferi*. Am J Trop Med Hyg **34:**925-930.
10. **Doggett JS, Kohlhepp S, Gresbrink R, Metz P, Gleaves C, Gilbert D.** 2008. Lyme disease in Oregon. J Clin Microbiol **46:**2115-2118.
11. **Girard YA, Travinsky B, Schotthoefer A, Fedorova N, Eisen RJ, Eisen L, Barbour AG, Lane RS.** 2009. Population structure of the Lyme borreliosis spirochete *Borrelia burgdorferi* in the western black-legged tick (*Ixodes pacificus*) in Northern California. Appl Environ Microbiol **75:**7243-7252.
12. **Gray J.** 1998. Review The ecology of ticks transmitting Lyme borreliosis. Experimental & applied acarology **22:**249-258.
13. **Lane RS, Loye JE.** 1991. Lyme disease in California: interrelationship of ixodid ticks (*Acari*), rodents, and *Borrelia burgdorferi*. Journal of medical entomology **28:**719-725.
14. **Radolf JD, Caimano MJ, Stevenson B, Hu LT.** 2012. Of ticks, mice and men: understanding the dual-host lifestyle of Lyme disease spirochaetes. Nat Rev Micro **10:**87-99.
15. **Matuschka FR, Heiler M, Eiffert H, Fischer P, Lotter H, Spielman A.** 1993. Diversionary role of hoofed game in the transmission of Lyme disease spirochetes. Am J Trop Med Hyg **48:**693-699.

16. **Burgdorfer W, Hayes SF, Benach JL.** 1988. Development of *Borrelia burgdorferi* in ixodid tick vectors. Annals of the New York Academy of Sciences **539:**172-179.

17. **Magnarelli LA, Anderson JF.** 1988. Ticks and biting insects infected with the etiologic agent of Lyme disease, *Borrelia burgdorferi.* J Clin Microbiol **26:**1482-1486.

18. **Steere AC, Coburn J, Glickstein L.** 2004. The emergence of Lyme disease. J Clin Invest **113:**1093-1101.

19. **Steere AC, Bartenhagen NH, Craft JE, Hutchinson GJ, Newman JH, Rahn DW, Sigal LH, Spieler PN, Stenn KS, Malawista SE.** 1983. The early clinical manifestations of Lyme disease. Ann Intern Med **99:**76-82.

20. **Steere AC, Malawista SE, Hardin JA, Ruddy S, Askenase W, Andiman WA.** 1977. *Erythema chronicum migrans* and Lyme arthritis. The enlarging clinical spectrum. Ann Intern Med **86:**685-698.

21. **Halperin JJ, Logigian EL, Finkel MF, Pearl RA.** 1996. Practice parameters for the diagnosis of patients with nervous system Lyme borreliosis (Lyme disease). Neurology **46:**619-627.

22. **Steere AC.** 2001. Lyme Disease. New England Journal of Medicine **345:**115-125.

23. **Strle F, Stanek G.** 2009. Clinical manifestations and diagnosis of Lyme borreliosis. Current problems in dermatology **37:**51-110.

24. **Mullegger RR, McHugh G, Ruthazer R, Binder B, Kerl H, Steere AC.** 2000. Differential expression of cytokine mRNA in skin specimens from patients with *erythema migrans* or acrodermatitis chronica atrophicans. The Journal of investigative dermatology **115:**1115-1123.

25. **Johnson BJ.** 2011. 4 Laboratory Diagnostic Testing for *Borrelia burgdorferi* Infection1. Lyme Disease: An Evidence-Based Approach. Croydon, UK: CAB International**:**73-88.

26. **Aguero-Rosenfeld ME, Wang G, Schwartz I, Wormser GP.** 2005. Diagnosis of Lyme borreliosis. Clin Microbiol Rev **18:**484-509.

27. **Johnson BJ, Pilgard MA, Russell TM.** 2014. Assessment of new culture method for detection of *Borrelia* species from serum of Lyme disease patients. J Clin Microbiol **52:**721-724.

28. **Nadelman RB, Pavia CS, Magnarelli LA, Wormser GP.** 1990. Isolation of *Borrelia burgdorferi* from the blood of seven patients with Lyme disease. The American journal of medicine **88:**21-26.

29. **Sapi E, Pabbati N, Datar A, Davies EM, Rattelle A, Kuo BA.** 2013. Improved culture conditions for the growth and detection of *Borrelia* from human serum. International journal of medical sciences **10:**362-376.

30. **Berger BW, Johnson RC, Kodner C, Coleman L.** 1992. Cultivation of *Borrelia burgdorferi* from *erythema migrans* lesions and perilesional skin. J Clin Microbiol **30:**359-361.

31. **Barthold SW, Sidman CL, Smith AL.** 1992. Lyme borreliosis in genetically resistant and susceptible mice with severe combined immunodeficiency. Am J Trop Med Hyg **47:**605-613.

32. **Wooten RM, Weis JJ.** 2001. Host-pathogen interactions promoting inflammatory Lyme arthritis: use of mouse models for dissection of disease processes. Curr Opin Microbiol **4:**274-279.

33. **Barthold SW, Beck DS, Hansen GM, Terwilliger GA, Moody KD.** 1990. Lyme borreliosis in selected strains and ages of laboratory mice. J Infect Dis **162:**133-138.

34. **Moody KD, Barthold SW.** 1998. Lyme borreliosis in laboratory mice. Comparative Medicine **48:**168-171.

35. **Barthold SW, Cadavid, D., Philipp, M.** 2010. Animal Models of Borreliosis. S. Samuels and J Radolph, (ed), *Borrelia*: Molecular Biology, Host Interaction and Pathogenesis, Norfolk, UK.

36. **Yang L, Weis JH, Eichwald E, Kolbert CP, Persing DH, Weis JJ.** 1994. Heritable susceptibility to severe *Borrelia burgdorferi*-induced arthritis is dominant and is associated with persistence of large numbers of spirochetes in tissues. Infect Immun **62:**492-500.

37. **Ma Y, Seiler KP, Eichwald EJ, Weis JH, Teuscher C, Weis JJ.** 1998. Distinct characteristics of resistance to *Borrelia burgdorferi*-induced arthritis in C57BL/6N mice. Infect Immun **66:**161-168.

38. **Behera AK, Hildebrand E, Bronson RT, Perides G, Uematsu S, Akira S, Hu LT.** 2006. MyD88 deficiency results in tissue-specific changes in cytokine induction and inflammation in interleukin-18-independent mice infected with *Borrelia burgdorferi*. Infect Immun **74:**1462-1470.

39. **Bolz DD, Sundsbak RS, Ma Y, Akira S, Kirschning CJ, Zachary JF, Weis JH, Weis JJ.** 2004. MyD88 plays a unique role in host defense but not arthritis development in Lyme disease. J Immunol **173:**2003-2010.

40. **Liu N, Montgomery RR, Barthold SW, Bockenstedt LK.** 2004. Myeloid differentiation antigen 88 deficiency impairs pathogen clearance but does not alter inflammation in *Borrelia burgdorferi*-infected mice. Infect Immun **72:**3195-3203.

41. **Wooten RM, Ma Y, Yoder RA, Brown JP, Weis JH, Zachary JF, Kirschning CJ, Weis JJ.** 2002. Toll-like receptor 2 is required for innate, but not acquired, host defense to *Borrelia burgdorferi*. J Immunol **168:**348-355.

42. **Bockenstedt LK, Kang I, Chang C, Persing D, Hayday A, Barthold SW.** 2001. CD4$^+$ T helper 1 cells facilitate regression of murine Lyme carditis. Infect Immun **69:**5264-5269.

43. **McKisic MD, Redmond WL, Barthold SW.** 2000. Cutting edge: T cell-mediated pathology in murine Lyme borreliosis. J Immunol **164:**6096-6099.

44. **Schaible UE, Gay S, Museteanu C, Kramer MD, Zimmer G, Eichmann K, Museteanu U, Simon MM.** 1990. Lyme borreliosis in the severe combined immunodeficiency (scid) mouse manifests predominantly in the joints, heart, and liver. The American journal of pathology **137:**811-820.

45. **Schaible UE, Wallich R, Kramer MD, Nerz G, Stehle T, Museteanu C, Simon MM.** 1994. Protection against *Borrelia burgdorferi* infection in SCID mice is conferred by presensitized spleen cells and partially by B but not T cells alone. Int Immunol **6:**671-681.

46. **Purser JE, Norris SJ.** 2000. Correlation between plasmid content and infectivity in *Borrelia burgdorferi*. Proc Natl Acad Sci U S A **97:**13865-13870.

47. **Labandeira-Rey M, Skare JT.** 2001. Decreased infectivity in *Borrelia burgdorferi* strain B31 is associated with loss of linear plasmid 25 or 28-1. Infect Immun **69:**446-455.

48. **Barthold SW.** 1991. Infectivity of *Borrelia burgdorferi* relative to route of inoculation and genotype in laboratory mice. J Infect Dis **163:**419-420.

49. **Grimm D, Tilly K, Byram R, Stewart PE, Krum JG, Bueschel DM, Schwan TG, Policastro PF, Elias AF, Rosa PA.** 2004. Outer-surface protein C of the Lyme disease spirochete: a protein induced in ticks for infection of mammals. Proc Natl Acad Sci U S A **101:**3142-3147.

50. **Moriarty TJ, Norman MU, Colarusso P, Bankhead T, Kubes P, Chaconas G.** 2008. Real-time high resolution 3D imaging of the Lyme disease spirochete adhering to and escaping from the vasculature of a living host. PLoS Pathog **4:**e1000090.

51. **Gern L, Schaible UE, Simon MM.** 1993. Mode of inoculation of the Lyme disease agent *Borrelia burgdorferi* influences infection and immune responses in inbred strains of mice. J Infect Dis **167:**971-975.

52. **Piesman J, Dolan MC, Happ CM, Luft BJ, Rooney SE, Mather TN, Golde WT.** 1997. Duration of immunity to reinfection with tick-transmitted *Borrelia burgdorferi* in naturally infected mice. Infect Immun **65:**4043-4047.

53. **Motameni AR, Bates TC, Juncadella IJ, Petty C, Hedrick MN, Anguita J.** 2005. Distinct bacterial dissemination and disease outcome in mice subcutaneously infected with *Borrelia burgdorferi* in the midline of the back and the footpad. FEMS Immunol Med Microbiol **45:**279-284.

54. **Motaleb MA, Corum L, Bono JL, Elias AF, Rosa P, Samuels DS, Charon NW.** 2000. *Borrelia burgdorferi* periplasmic flagella have both skeletal and motility functions. Proc Natl Acad Sci U S A **97:**10899-10904.

55. **LaRocca TJ, Pathak P, Chiantia S, Toledo A, Silvius JR, Benach JL, London E.** 2013. Proving lipid rafts exist: membrane domains in the prokaryote *Borrelia burgdorferi* have the same properties as eukaryotic lipid rafts. PLoS Pathog **9:**e1003353.

56. **Radolf JD, Robinson EJ, Bourell KW, Akins DR, Porcella SF, Weigel LM, Jones JD, Norgard MV.** 1995. Characterization of outer membranes isolated from Treponema pallidum, the syphilis spirochete. Infect Immun **63:**4244-4252.

57. **Mursic VP, Wanner G, Reinhardt S, Wilske B, Busch U, Marget W.** 1996. Formation and cultivation of *Borrelia burgdorferi* spheroplast-L-form variants. Infection **24:**218-226.

58. **Rosa PA, Tilly K, Stewart PE.** 2005. The burgeoning molecular genetics of the Lyme disease spirochaete. Nat Rev Micro **3:**129-143.

59. **Casjens S, Palmer N, van Vugt R, Huang WM, Stevenson B, Rosa P, Lathigra R, Sutton G, Peterson J, Dodson RJ, Haft D, Hickey E, Gwinn M, White O, Fraser CM.** 2000. A bacterial genome in flux: the twelve linear and nine circular extrachromosomal DNAs in an infectious isolate of the Lyme disease spirochete *Borrelia burgdorferi*. Mol Microbiol **35:**490-516.

60. **Fraser CM, Casjens S, Huang WM, Sutton GG, Clayton R, Lathigra R, White O, Ketchum KA, Dodson R, Hickey EK, Gwinn M, Dougherty B, Tomb JF, Fleischmann RD, Richardson D, Peterson J, Kerlavage AR, Quackenbush J, Salzberg S, Hanson M, van Vugt R, Palmer N, Adams MD, Gocayne J, Weidman J, Utterback T, Watthey L, McDonald L, Artiach P, Bowman C, Garland S, Fuji C, Cotton MD, Horst K, Roberts K, Hatch B, Smith HO, Venter JC.** 1997. Genomic sequence of a Lyme disease spirochaete, *Borrelia burgdorferi*. Nature **390:**580-586.

61. **Casjens SR, Mongodin EF, Qiu WG, Luft BJ, Schutzer SE, Gilcrease EB, Huang WM, Vujadinovic M, Aron JK, Vargas LC, Freeman S, Radune D, Weidman JF, Dimitrov GI, Khouri HM, Sosa JE, Halpin RA, Dunn JJ, Fraser CM.** 2012. Genome stability of Lyme disease spirochetes: comparative genomics of *Borrelia burgdorferi* plasmids. PLoS One **7:**e33280.

62. **Jewett MW, Byram R, Bestor A, Tilly K, Lawrence K, Burtnick MN, Gherardini F, Rosa PA.** 2007. Genetic basis for retention of a critical virulence plasmid of *Borrelia burgdorferi*. Mol Microbiol **66:**975-990.

63. **Jain S, Sutchu S, Rosa PA, Byram R, Jewett MW.** 2012. *Borrelia burgdorferi* harbors a transport system essential for purine salvage and mammalian infection. Infect Immun **80:**3086-3093.

64. **Tilly K, Bestor A, Jewett MW, Rosa P.** 2007. Rapid clearance of Lyme disease spirochetes lacking OspC from skin. Infect Immun **75:**1517-1519.

65. **Tilly K, Krum JG, Bestor A, Jewett MW, Grimm D, Bueschel D, Byram R, Dorward D, VanRaden MJ, Stewart P, Rosa P.** 2006. *Borrelia burgdorferi* OspC protein required exclusively in a crucial early stage of mammalian infection. Infect Immun **74:**3554-3564.

66. **Hubner A, Yang X, Nolen DM, Popova TG, Cabello FC, Norgard MV.** 2001. Expression of *Borrelia burgdorferi* OspC and DbpA is controlled by a RpoN-RpoS regulatory pathway. Proc Natl Acad Sci U S A **98:**12724-12729.

67. **Samuels DS.** 2011. Gene regulation in *Borrelia burgdorferi*. Annu Rev Microbiol **65:**479-499.

68. **Yang XF, Alani SM, Norgard MV.** 2003. The response regulator Rrp2 is essential for the expression of major membrane lipoproteins in *Borrelia burgdorferi*. Proc Natl Acad Sci U S A **100:**11001-11006.

69. **Fisher MA, Grimm D, Henion AK, Elias AF, Stewart PE, Rosa PA, Gherardini FC.** 2005. *Borrelia burgdorferi* sigma54 is required for mammalian infection and vector transmission but not for tick colonization. Proc Natl Acad Sci U S A **102:**5162-5167.

70. **Caimano MJ, Iyer R, Eggers CH, Gonzalez C, Morton EA, Gilbert MA, Schwartz I, Radolf JD.** 2007. Analysis of the RpoS regulon in *Borrelia burgdorferi* in response to mammalian host signals provides insight into RpoS function during the enzootic cycle. Mol Microbiol **65:**1193-1217.

71. **Boardman BK, He M, Ouyang Z, Xu H, Pang X, Yang XF.** 2008. Essential role of the response regulator Rrp2 in the infectious cycle of *Borrelia burgdorferi*. Infect Immun **76:**3844-3853.

72. **Caimano MJ, Eggers CH, Hazlett KR, Radolf JD.** 2004. RpoS is not central to the general stress response in *Borrelia burgdorferi* but does control expression of one or more essential virulence determinants. Infect Immun **72:**6433-6445.

73. **Ouyang Z, Deka RK, Norgard MV.** 2011. BosR (BB0647) controls the RpoN-RpoS regulatory pathway and virulence expression in *Borrelia burgdorferi* by a novel DNA-binding mechanism. PLoS Pathog **7:**e1001272.

74. **Ouyang Z, Kumar M, Kariu T, Haq S, Goldberg M, Pal U, Norgard MV.** 2009. BosR (BB0647) governs virulence expression in *Borrelia burgdorferi*. Mol Microbiol **74:**1331-1343.

75. **Hyde JA, Shaw DK, Smith Iii R, Trzeciakowski JP, Skare JT.** 2009. The BosR regulatory protein of *Borrelia burgdorferi* interfaces with the RpoS regulatory pathway and modulates both the oxidative stress response and pathogenic properties of the Lyme disease spirochete. Mol Microbiol **74:**1344-1355.

76. **Norris SJ, Coburn, J., Leong, J. M., Hu, L.T., Hook, M.** 2010. Pathobiology of Lyme Disease *Borrelia*. S. Samuels and J Radolph, (ed), *Borrelia*: Molecular Biology, Host Interaction and Pathogenesis, Norfolk, UK.

77. **Barthold SW, Persing DH, Armstrong AL, Peeples RA.** 1991. Kinetics of *Borrelia burgdorferi* dissemination and evolution of disease after intradermal inoculation of mice. The American journal of pathology **139:**263-273.

78. **Shih CM, Pollack RJ, Telford SR, 3rd, Spielman A.** 1992. Delayed dissemination of Lyme disease spirochetes from the site of deposition in the skin of mice. J Infect Dis **166:**827-831.

79. **Coburn J, Leong J, Chaconas G.** 2013. Illuminating the roles of the *Borrelia burgdorferi* adhesins. Trends Microbiol **21:**372-379.

80. **Hastey CJ, Elsner RA, Barthold SW, Baumgarth N.** 2012. Delays and diversions mark the development of B cell responses to *Borrelia burgdorferi* infection. J Immunol **188:**5612-5622.

81. **Tunev SS, Hastey CJ, Hodzic E, Feng S, Barthold SW, Baumgarth N.** 2011. Lymphoadenopathy during Lyme borreliosis is caused by spirochete migration-induced specific B cell activation. PLoS Pathog **7:**e1002066.

82. **Sultan SZ, Manne A, Stewart PE, Bestor A, Rosa PA, Charon NW, Motaleb MA.** 2013. Motility is crucial for the infectious life cycle of *Borrelia burgdorferi*. Infect Immun **81:**2012-2021.

83. **Coburn J, Fischer JR, Leong JM.** 2005. Solving a sticky problem: new genetic approaches to host cell adhesion by the Lyme disease spirochete. Mol Microbiol **57:**1182-1195.

84. **Brissette CA, Gaultney RA.** 2014. That's my story, and I'm sticking to it--an update on *B. burgdorferi* adhesins. Frontiers in cellular and infection microbiology **4:**41.

85. **Ristow LC, Miller HE, Padmore LJ, Chettri R, Salzman N, Caimano MJ, Rosa PA, Coburn J.** 2012. The beta(3)-integrin ligand of *Borrelia burgdorferi* is critical for infection of mice but not ticks. Mol Microbiol **85:**1105-1118.

86. **Imai DM, Samuels DS, Feng S, Hodzic E, Olsen K, Barthold SW.** 2013. The early dissemination defect attributed to disruption of decorin-binding proteins is abolished in chronic murine Lyme borreliosis. Infect Immun **81:**1663-1673.

87. **Weening EH, Parveen N, Trzeciakowski JP, Leong JM, Hook M, Skare JT.** 2008. *Borrelia burgdorferi* lacking DbpBA exhibits an early survival defect during experimental infection. Infect Immun **76:**5694-5705.

88. **Parveen N, Cornell KA, Bono JL, Chamberland C, Rosa P, Leong JM.** 2006. Bgp, a secreted glycosaminoglycan-binding protein of *Borrelia burgdorferi* strain N40, displays nucleosidase activity and is not essential for infection of immunodeficient mice. Infect Immun **74:**3016-3020.

89. **Onder O, Humphrey PT, McOmber B, Korobova F, Francella N, Greenbaum DC, Brisson D.** 2012. OspC is potent plasminogen receptor on surface of *Borrelia burgdorferi*. J Biol Chem **287:**16860-16868.

90. **Grab DJ, Perides G, Dumler JS, Kim KJ, Park J, Kim YV, Nikolskaia O, Choi KS, Stins MF, Kim KS.** 2005. *Borrelia burgdorferi*, host-derived proteases, and the blood-brain barrier. Infect Immun **73:**1014-1022.

91. **Coleman JL, Sellati TJ, Testa JE, Kew RR, Furie MB, Benach JL.** 1995. *Borrelia burgdorferi* binds plasminogen, resulting in enhanced penetration of endothelial monolayers. Infect Immun **63:**2478-2484.

92. **Coleman JL, Gebbia JA, Piesman J, Degen JL, Bugge TH, Benach JL.** 1997. Plasminogen is required for efficient dissemination of *B. burgdorferi* in ticks and for enhancement of spirochetemia in mice. Cell **89:**1111-1119.

93. **Eicken C, Sharma V, Klabunde T, Owens RT, Pikas DS, Hook M, Sacchettini JC.** 2001. Crystal structure of Lyme disease antigen outer surface protein C from *Borrelia burgdorferi*. J Biol Chem **276:**10010-10015.

94. **Kumaran D, Eswaramoorthy S, Luft BJ, Koide S, Dunn JJ, Lawson CL, Swaminathan S.** 2001. Crystal structure of outer surface protein C (OspC) from the Lyme disease spirochete, *Borrelia burgdorferi*. EMBO J **20:**971-978.

95. **Marconi RT, Earnhart CG.** 2010. S. Samuels and J Radolph, (ed), *Borrelia*: Molecular Biology, Host Interaction and Pathogenesis, Norfolk, UK.

96. **Seinost G, Dykhuizen DE, Dattwyler RJ, Golde WT, Dunn JJ, Wang IN, Wormser GP, Schriefer ME, Luft BJ.** 1999. Four clones of *Borrelia burgdorferi* sensu stricto cause invasive infection in humans. Infect Immun **67:**3518-3524.

97. **Wang G, Ojaimi C, Wu H, Saksenberg V, Iyer R, Liveris D, McClain SA, Wormser GP, Schwartz I.** 2002. Disease severity in a murine model of lyme borreliosis is associated with the genotype of the infecting *Borrelia burgdorferi* sensu stricto strain. J Infect Dis **186:**782-791.

98. **Xu Q, McShan K, Liang FT.** 2007. Identification of an *ospC* operator critical for immune evasion of Borrelia burgdorferi. Mol Microbiol **64:**220-231.

99. **Antonara S, Ristow L, McCarthy J, Coburn J.** 2010. Effect of *Borrelia burgdorferi* OspC at the site of inoculation in mouse skin. Infect Immun **78:**4723-4733.

100. **Kurtenbach K, Sewell HS, Ogden NH, Randolph SE, Nuttall PA.** 1998. Serum complement sensitivity as a key factor in Lyme disease ecology. Infect Immun **66:**1248-1251.

101. **Preac Mursic V, Marget W, Busch U, Pleterski Rigler D, Hagl S.** 1996. Kill kinetics of *Borrelia burgdorferi* and bacterial findings in relation to the treatment of Lyme borreliosis. Infection **24:**9-16.

102. **Zhang JR, Norris SJ.** 1998. Genetic variation of the *Borrelia burgdorferi* gene *vlsE* involves cassette-specific, segmental gene conversion. Infect Immun **66:**3698-3704.
103. **Elsner RA, Hastey CJ, Baumgarth N.** 2015. CD4+ T cells promote antibody production but not sustained affinity maturation during *Borrelia burgdorferi* infection. Infect Immun **83:**48-56.
104. **Bunikis J, Tsao J, Luke CJ, Luna MG, Fish D, Barbour AG.** 2004. *Borrelia burgdorferi* infection in a natural population of *Peromyscus Leucopus* mice: a longitudinal study in an area where Lyme Borreliosis is highly endemic. J Infect Dis **189:**1515-1523.
105. **Bankhead T, Chaconas G.** 2007. The role of VlsE antigenic variation in the Lyme disease spirochete: persistence through a mechanism that differs from other pathogens. Mol Microbiol **65:**1547-1558.
106. **Rogovskyy AS, Bankhead T.** 2014. Bacterial heterogeneity is a requirement for host superinfection by the Lyme disease spirochete. Infect Immun **82:**4542-4552.
107. **Tilly K, Bestor A, Rosa PA.** 2013. Lipoprotein succession in *Borrelia burgdorferi*: similar but distinct roles for OspC and VlsE at different stages of mammalian infection. Mol Microbiol **89:**216-227.
108. **Dunkelberger JR, Song WC.** 2010. Complement and its role in innate and adaptive immune responses. Cell research **20:**34-50.
109. **de Taeye SW, Kreuk L, van Dam AP, Hovius JW, Schuijt TJ.** 2013. Complement evasion by *Borrelia burgdorferi*: it takes three to tango. Trends in parasitology **29:**119-128.
110. **Ramamoorthi N, Narasimhan S, Pal U, Bao F, Yang XF, Fish D, Anguita J, Norgard MV, Kantor FS, Anderson JF, Koski RA, Fikrig E.** 2005. The Lyme disease agent exploits a tick protein to infect the mammalian host. Nature **436:**573-577.
111. **Schuijt TJ, Hovius JW, van Burgel ND, Ramamoorthi N, Fikrig E, van Dam AP.** 2008. The tick salivary protein Salp15 inhibits the killing of serum-sensitive *Borrelia burgdorferi* sensu lato isolates. Infect Immun **76:**2888-2894.
112. **Bockenstedt LK, Barthold S, Deponte K, Marcantonio N, Kantor FS.** 1993. *Borrelia burgdorferi* infection and immunity in mice deficient in the fifth component of complement. Infect Immun **61:**2104-2107.
113. **Lawrenz MB, Wooten RM, Zachary JF, Drouin SM, Weis JJ, Wetsel RA, Norris SJ.** 2003. Effect of complement component C3 deficiency on experimental Lyme borreliosis in mice. Infect Immun **71:**4432-4440.
114. **Weis JJ, Bockenstedt, L.K.** 2010. Host Response. S. Samuels and J Radolph, (ed), *Borrelia*: Molecular Biology, Host Interaction and Pathogenesis, Norfolk, UK.
115. **Salazar JC, Pope CD, Sellati TJ, Feder HM, Jr., Kiely TG, Dardick KR, Buckman RL, Moore MW, Caimano MJ, Pope JG, Krause PJ, Radolf JD, Lyme Disease N.** 2003. Coevolution of markers of innate and adaptive immunity in skin and peripheral blood of patients with *erythema migrans*. J Immunol **171:**2660-2670.
116. **Chong-Cerrillo C, Shang ES, Blanco DR, Lovett MA, Miller JN.** 2001. Immunohistochemical analysis of Lyme disease in the skin of naive and infection-immune rabbits following challenge. Infect Immun **69:**4094-4102.

117. **Brandt ME, Riley BS, Radolf JD, Norgard MV.** 1990. Immunogenic integral membrane proteins of *Borrelia burgdorferi* are lipoproteins. Infect Immun **58:**983-991.

118. **Alexopoulou L, Thomas V, Schnare M, Lobet Y, Anguita J, Schoen RT, Medzhitov R, Fikrig E, Flavell RA.** 2002. Hyporesponsiveness to vaccination with *Borrelia burgdorferi* OspA in humans and in TLR1- and TLR2-deficient mice. Nat Med **8:**878-884.

119. **Hirschfeld M, Kirschning CJ, Schwandner R, Wesche H, Weis JH, Wooten RM, Weis JJ.** 1999. Cutting edge: inflammatory signaling by *Borrelia burgdorferi* lipoproteins is mediated by toll-like receptor 2. J Immunol **163:**2382-2386.

120. **Salazar JC, Duhnam-Ems S, La Vake C, Cruz AR, Moore MW, Caimano MJ, Velez-Climent L, Shupe J, Krueger W, Radolf JD.** 2009. Activation of human monocytes by live *Borrelia burgdorferi* generates TLR2-dependent and -independent responses which include induction of IFN-beta. PLoS Pathog **5:**e1000444.

121. **Kurt-Jones EA, Mandell L, Whitney C, Padgett A, Gosselin K, Newburger PE, Finberg RW.** 2002. Role of toll-like receptor 2 (TLR2) in neutrophil activation: GM-CSF enhances TLR2 expression and TLR2-mediated interleukin 8 responses in neutrophils. Blood **100:**1860-1868.

122. **Benhnia MR, Wroblewski D, Akhtar MN, Patel RA, Lavezzi W, Gangloff SC, Goyert SM, Caimano MJ, Radolf JD, Sellati TJ.** 2005. Signaling through CD14 attenuates the inflammatory response to *Borrelia burgdorferi*, the agent of Lyme disease. J Immunol **174:**1539-1548.

123. **Cabral ES, Gelderblom H, Hornung RL, Munson PJ, Martin R, Marques AR.** 2006. *Borrelia burgdorferi* lipoprotein-mediated TLR2 stimulation causes the down-regulation of TLR5 in human monocytes. J Infect Dis **193:**849-859.

124. **Shin OS, Isberg RR, Akira S, Uematsu S, Behera AK, Hu LT.** 2008. Distinct roles for MyD88 and Toll-like receptors 2, 5, and 9 in phagocytosis of *Borrelia burgdorferi* and cytokine induction. Infect Immun **76:**2341-2351.

125. **Cervantes JL, Hawley KL, Benjamin SJ, Weinerman B, Luu SM, Salazar JC.** 2014. Phagosomal TLR signaling upon *Borrelia burgdorferi* infection. Frontiers in cellular and infection microbiology **4:**55.

126. **Love AC, Schwartz I, Petzke MM.** 2014. *Borrelia burgdorferi* RNA induces type I and III interferons via Toll-like receptor 7 and contributes to production of NF-kappaB-dependent cytokines. Infect Immun **82:**2405-2416.

127. **Miller JC, Maylor-Hagen H, Ma Y, Weis JH, Weis JJ.** 2010. The Lyme disease spirochete *Borrelia burgdorferi* utilizes multiple ligands, including RNA, for interferon regulatory factor 3-dependent induction of type I interferon-responsive genes. Infect Immun **78:**3144-3153.

128. **Oosting M, Berende A, Sturm P, Ter Hofstede HJ, de Jong DJ, Kanneganti TD, van der Meer JW, Kullberg BJ, Netea MG, Joosten LA.** 2010. Recognition of *Borrelia burgdorferi* by NOD2 is central for the induction of an inflammatory reaction. J Infect Dis **201:**1849-1858.

129. **Petnicki-Ocwieja T, DeFrancesco AS, Chung E, Darcy CT, Bronson RT, Kobayashi KS, Hu LT.** 2011. Nod2 suppresses *Borrelia burgdorferi* mediated murine Lyme arthritis and carditis through the induction of tolerance. PLoS One **6:**e17414.

130. **Latz E, Xiao TS, Stutz A.** 2013. Activation and regulation of the inflammasomes. Nat Rev Immunol **13:**397-411.

131. **Oosting M, Buffen K, Malireddi SR, Sturm P, Verschueren I, Koenders MI, van de Veerdonk FL, van der Meer JW, Netea MG, Kanneganti TD, Joosten LA.** 2012. Murine *Borrelia* arthritis is highly dependent on ASC and caspase-1, but independent of NLRP3. Arthritis Res Ther **14:**R247.

132. **Montgomery RR, Nathanson MH, Malawista SE.** 1994. Fc- and non-Fc-mediated phagocytosis of *Borrelia burgdorferi* by macrophages. J Infect Dis **170:**890-893.

133. **Rittig MG, Krause A, Haupl T, Schaible UE, Modolell M, Kramer MD, Lutjen-Drecoll E, Simon MM, Burmester GR.** 1992. Coiling phagocytosis is the preferential phagocytic mechanism for *Borrelia burgdorferi*. Infect Immun **60:**4205-4212.

134. **Montgomery RR, Malawista SE.** 1996. Entry of *Borrelia burgdorferi* into macrophages is end-on and leads to degradation in lysosomes. Infect Immun **64:**2867-2872.

135. **Montgomery RR, Nathanson MH, Malawista SE.** 1993. The fate of *Borrelia burgdorferi*, the agent for Lyme disease, in mouse macrophages. Destruction, survival, recovery. J Immunol **150:**909-915.

136. **Benach JL, Fleit HB, Habicht GS, Coleman JL, Bosler EM, Lane BP.** 1984. Interactions of phagocytes with the Lyme disease spirochete: role of the Fc receptor. J Infect Dis **150:**497-507.

137. **Cinco M, Murgia R, Presani G, Perticarari S.** 1997. Integrin CR3 mediates the binding of nonspecifically opsonized *Borrelia burgdorferi* to human phagocytes and mammalian cells. Infect Immun **65:**4784-4789.

138. **Hawley KL, Olson CM, Jr., Iglesias-Pedraz JM, Navasa N, Cervantes JL, Caimano MJ, Izadi H, Ingalls RR, Pal U, Salazar JC, Radolf JD, Anguita J.** 2012. CD14 cooperates with complement receptor 3 to mediate MyD88-independent phagocytosis of *Borrelia burgdorferi*. Proc Natl Acad Sci U S A **109:**1228-1232.

139. **Naj X, Hoffmann AK, Himmel M, Linder S.** 2013. The formins FMNL1 and mDia1 regulate coiling phagocytosis of *Borrelia burgdorferi* by primary human macrophages. Infect Immun **81:**1683-1695.

140. **Hoffmann AK, Naj X, Linder S.** 2014. Daam1 is a regulator of filopodia formation and phagocytic uptake of *Borrelia burgdorferi* by primary human macrophages. FASEB journal : official publication of the Federation of American Societies for Experimental Biology **28:**3075-3089.

141. **Shin OS, Miller LS, Modlin RL, Akira S, Uematsu S, Hu LT.** 2009. Downstream signals for MyD88-mediated phagocytosis of *Borrelia burgdorferi* can be initiated by TRIF and are dependent on PI3K. J Immunol **183:**491-498.

142. **Benach JL, Habicht GS, Gocinski BL, Coleman JL.** 1984. Phagocytic cell responses to *in vivo* and *in vitro* exposure to the Lyme disease spirochete. Yale J Biol Med **57:**599-605.

143. **Montgomery RR, Lusitani D, de Boisfleury Chevance A, Malawista SE.** 2002. Human phagocytic cells in the early innate immune response to *Borrelia burgdorferi*. J Infect Dis **185:**1773-1779.

144. **Schutzer SE, Coyle PK, Reid P, Holland B.** 1999. *Borrelia burgdorferi*-specific immune complexes in acute Lyme disease. Jama **282:**1942-1946.

145. **Belperron AA, Liu N, Booth CJ, Bockenstedt LK.** 2014. Dual role for Fcgamma receptors in host defense and disease in *Borrelia burgdorferi*-infected mice. Frontiers in cellular and infection microbiology **4:**75.

146. **Takai T.** 2002. Roles of Fc receptors in autoimmunity. Nat Rev Immunol **2:**580-592.

147. **Cruz AR, Moore MW, La Vake CJ, Eggers CH, Salazar JC, Radolf JD.** 2008. Phagocytosis of *Borrelia burgdorferi*, the Lyme disease spirochete, potentiates innate immune activation and induces apoptosis in human monocytes. Infect Immun **76:**56-70.

148. **Lusitani D, Malawista SE, Montgomery RR.** 2002. *Borrelia burgdorferi* are susceptible to killing by a variety of human polymorphonuclear leukocyte components. J Infect Dis **185:**797-804.

149. **Menten-Dedoyart C, Faccinetto C, Golovchenko M, Dupiereux I, Van Lerberghe PB, Dubois S, Desmet C, Elmoualij B, Baron F, Rudenko N, Oury C, Heinen E, Couvreur B.** 2012. Neutrophil extracellular traps entrap and kill *Borrelia burgdorferi* sensu stricto spirochetes and are not affected by *Ixodes ricinus* tick saliva. J Immunol **189:**5393-5401.

150. **Morrison TB, Weis JH, Weis JJ.** 1997. *Borrelia burgdorferi* outer surface protein A (OspA) activates and primes human neutrophils. J Immunol **158:**4838-4845.

151. **Suhonen J, Hartiala K, Tuominen-Gustafsson H, Viljanen MK.** 2000. *Borrelia burgdorferi*--induced oxidative burst, calcium mobilization, and phagocytosis of human neutrophils are complement dependent. J Infect Dis **181:**195-202.

152. **Bourret TJ, Boylan JA, Lawrence KA, Gherardini FC.** 2011. Nitrosative damage to free and zinc-bound cysteine thiols underlies nitric oxide toxicity in wild-type *Borrelia burgdorferi*. Mol Microbiol **81:**259-273.

153. **Troxell B, Zhang JJ, Bourret TJ, Zeng MY, Blum J, Gherardini F, Hassan HM, Yang XF.** 2014. Pyruvate protects pathogenic spirochetes from H2O2 killing. PLoS One **9:**e84625.

154. **Garcia R, Gusmani L, Murgia R, Guarnaccia C, Cinco M, Rottini G.** 1998. Elastase is the only human neutrophil granule protein that alone is responsible for *in vitro* killing of *Borrelia burgdorferi*. Infect Immun **66:**1408-1412.

155. **Modolell M, Schaible UE, Rittig M, Simon MM.** 1994. Killing of *Borrelia burgdorferi* by macrophages is dependent on oxygen radicals and nitric oxide and can be enhanced by antibodies to outer surface proteins of the spirochete. Immunol Lett **40:**139-146.

156. **Crandall H, Ma Y, Dunn DM, Sundsbak RS, Zachary JF, Olofsson P, Holmdahl R, Weis JH, Weiss RB, Teuscher C, Weis JJ.** 2005. Bb2Bb3 regulation of murine Lyme arthritis is distinct from Ncf1 and independent of the phagocyte nicotinamide adenine dinucleotide phosphate oxidase. The American journal of pathology **167:**775-785.

157. **Brown CR, Reiner SL.** 1999. Development of Lyme arthritis in mice deficient in inducible nitric oxide synthase. J Infect Dis **179:**1573-1576.

158. **Malissen B, Tamoutounour S, Henri S.** 2014. The origins and functions of dendritic cells and macrophages in the skin. Nat Rev Immunol **14:**417-428.

159. **Hulinska D, Bartak P, Hercogova J, Hancil J, Basta J, Schramlova J.** 1994. Electron microscopy of Langerhans cells and *Borrelia burgdorferi* in Lyme disease patients. Zentralbl Bakteriol **280:**348-359.

160. **Filgueira L, Nestle FO, Rittig M, Joller HI, Groscurth P.** 1996. Human dendritic cells phagocytose and process *Borrelia burgdorferi*. J Immunol **157:**2998-3005.

161. **Mason LM, Veerman CC, Geijtenbeek TB, Hovius JW.** 2014. Menage a trois: *Borrelia*, dendritic cells, and tick saliva interactions. Trends in parasitology **30:**95-103.

162. **Mbow ML, Zeidner N, Panella N, Titus RG, Piesman J.** 1997. *Borrelia burgdorferi*-pulsed dendritic cells induce a protective immune response against tick-transmitted spirochetes. Infect Immun **65:**3386-3390.

163. **Yakimchuk K, Roura-Mir C, Magalhaes KG, de Jong A, Kasmar AG, Granter SR, Budd R, Steere A, Pena-Cruz V, Kirschning C, Cheng TY, Moody DB.** 2011. *Borrelia burgdorferi* infection regulates CD1 expression in human cells and tissues via IL1-beta. Eur J Immunol **41:**694-705.

164. **Kumar H, Belperron A, Barthold SW, Bockenstedt LK.** 2000. Cutting edge: CD1d deficiency impairs murine host defense against the spirochete, *Borrelia burgdorferi*. J Immunol **165:**4797-4801.

165. **Vivier E, Tomasello E, Baratin M, Walzer T, Ugolini S.** 2008. Functions of natural killer cells. Nat Immunol **9:**503-510.

166. **Katchar K, Drouin EE, Steere AC.** 2013. Natural killer cells and natural killer T cells in Lyme arthritis. Arthritis Res Ther **15:**R183.

167. **Golightly M, Thomas J, Volkman D, Dattwyler R.** 1988. Modulation of natural killer cell activity by *Borrelia burgdorferi*. Annals of the New York Academy of Sciences **539:**103-111.

168. **Barthold SW, de Souza M.** 1995. Exacerbation of Lyme arthritis in beige mice. J Infect Dis **172:**778-784.

169. **Brown CR, Reiner SL.** 1998. Activation of natural killer cells in arthritis-susceptible but not arthritis-resistant mouse strains following *Borrelia burgdorferi* infection. Infect Immun **66:**5208-5214.

170. **Ma Y, Seiler KP, Tai KF, Yang L, Woods M, Weis JJ.** 1994. Outer surface lipoproteins of *Borrelia burgdorferi* stimulate nitric oxide production by the cytokine-inducible pathway. Infect Immun **62:**3663-3671.

171. **Schwan TG, Piesman J, Golde WT, Dolan MC, Rosa PA.** 1995. Induction of an outer surface protein on *Borrelia burgdorferi* during tick feeding. Proc Natl Acad Sci U S A **92:**2909-2913.

172. **Bockenstedt LK, Hodzic E, Feng S, Bourrel KW, de Silva A, Montgomery RR, Fikrig E, Radolf JD, Barthold SW.** 1997. *Borrelia burgdorferi* strain-specific OspC-mediated immunity in mice. Infect Immun **65:**4661-4667.

173. **Gilmore RD, Jr., Kappel KJ, Dolan MC, Burkot TR, Johnson BJ.** 1996. Outer surface protein C (OspC), but not P39, is a protective immunogen against a tick-transmitted *Borrelia burgdorferi* challenge: evidence for a conformational protective epitope in OspC. Infect Immun **64:**2234-2239.

174. **Liang FT, Jacobs MB, Bowers LC, Philipp MT.** 2002. An immune evasion mechanism for spirochetal persistence in Lyme borreliosis. J Exp Med **195:**415-422.

175. **Liang FT, Yan J, Mbow ML, Sviat SL, Gilmore RD, Mamula M, Fikrig E.** 2004. *Borrelia burgdorferi* changes its surface antigenic expression in response to host immune responses. Infect Immun **72:**5759-5767.

176. **Radolf JD, Caimano MJ.** 2008. The long strange trip of *Borrelia burgdorferi* outer-surface protein C. Mol Microbiol **69:**1-4.

177. **Xu Q, McShan K, Liang FT.** 2008. Essential protective role attributed to the surface lipoproteins of *Borrelia burgdorferi* against innate defences. Mol Microbiol **69:**15-29.

178. **Hovius JW, Schuijt TJ, de Groot KA, Roelofs JJ, Oei GA, Marquart JA, de Beer R, van 't Veer C, van der Poll T, Ramamoorthi N, Fikrig E, van Dam AP.** 2008. Preferential protection of *Borrelia burgdorferi* sensu stricto by a Salp15 homologue in *Ixodes ricinus* saliva. J Infect Dis **198:**1189-1197.

179. **Earnhart CG, Leblanc DV, Alix KE, Desrosiers DC, Radolf JD, Marconi RT.** 2010. Identification of residues within ligand-binding domain 1 (LBD1) of the *Borrelia burgdorferi* OspC protein required for function in the mammalian environment. Mol Microbiol **76:**393-408.

180. **Lagal V, Portnoi D, Faure G, Postic D, Baranton G.** 2006. *Borrelia burgdorferi* sensu stricto invasiveness is correlated with OspC-plasminogen affinity. Microbes Infect **8:**645-652.

181. **Montgomery RR, Booth CJ, Wang X, Blaho VA, Malawista SE, Brown CR.** 2007. Recruitment of macrophages and polymorphonuclear leukocytes in L:yme carditis. Infect Immun **75:**613-620.

182. **Steere AC, Glickstein L.** 2004. Elucidation of Lyme arthritis. Nat Rev Immunol. **4:**143-152.

183. **Stewart PE, Wang X, Bueschel DM, Clifton DR, Grimm D, Tilly K, Carroll JA, Weis JJ, Rosa PA.** 2006. Delineating the requirement for the *Borrelia burgdorferi* virulence factor OspC in the mammalian host. Infect Immun **74:**3547-3553.

184. **Samuels DS.** 1995. Electrotransformation of the spirochete *Borrelia burgdorferi*. Methods Mol Biol **47:**253-259.

185. **Tokarz R, Anderton JM, Katona LI, Benach JL.** 2004. Combined effects of blood and temperature shift on *Borrelia burgdorferi* gene expression as determined by whole genome DNA array. Infect Immun **72:**5419-5432.

186. **Brooks CS, Hefty PS, Jolliff SE, Akins DR.** 2003. Global analysis of *Borrelia burgdorferi* genes regulated by mammalian host-specific signals. Infect Immun **71:**3371-3383.

187. **Schwan TG, Piesman J.** 2000. Temporal changes in outer surface proteins A and C of the Lyme disease-associated spirochete, *Borrelia burgdorferi*, during the chain of infection in ticks and mice. J Clin Microbiol **38:**382-388.

188. **Schwan TG.** 2003. Temporal regulation of outer surface proteins of the Lyme-disease spirochaete *Borrelia burgdorferi*. Biochem.Soc.Trans. **31:**108-112.

189. **Dressler F, Whalen JA, Reinhardt BN, Steere AC.** 1993. Western blotting in the serodiagnosis of Lyme disease. J Infect Dis **167:**392-400.

190. **Goettner G, Schulte-Spechtel U, Hillermann R, Liegl G, Wilske B, Fingerle V.** 2005. Improvement of Lyme borreliosis serodiagnosis by a newly developed recombinant immunoglobulin G (IgG) and IgM line immunoblot assay and addition of VlsE and DbpA homologues. J Clin Microbiol **43:**3602-3609.

191. **Kenedy MR, Lenhart TR, Akins DR.** 2012. The role of *Borrelia burgdorferi* outer surface proteins. FEMS Immunol Med Microbiol **66:**1-19.

192. **Nowalk AJ, Nolder C, Clifton DR, Carroll JA.** 2006. Comparative proteome analysis of subcellular fractions from *Borrelia burgdorferi* by NEPHGE and IPG. Proteomics **6:**2121-2134.

193. **Toledo A, Coleman JL, Kuhlow CJ, Crowley JT, Benach JL.** 2012. The enolase of *Borrelia burgdorferi* is a plasminogen receptor released in outer membrane vesicles. Infect Immun **80:**359-368.

194. **Floden AM, Watt JA, Brissette CA.** 2011. *Borrelia burgdorferi* enolase is a surface-exposed plasminogen binding protein. PLoS One **6:**e27502.

195. **Nogueira SV, Smith AA, Qin JH, Pal U.** 2012. A surface enolase participates in *Borrelia burgdorferi*-plasminogen interaction and contributes to pathogen survival within feeding ticks. Infect Immun **80:**82-90.

196. **Henderson B, Martin A.** 2011. Bacterial virulence in the moonlight: multitasking bacterial moonlighting proteins are virulence determinants in infectious disease. Infect Immun **79:**3476-3491.

197. **Wang G, Xia Y, Cui J, Gu Z, Song Y, Chen YQ, Chen H, Zhang H, Chen W.** 2013. The Roles of Moonlighting Proteins in Bacteria. Current issues in molecular biology **16:**15-22.

198. **Balasubramanian S, Kannan TR, Baseman JB.** 2008. The surface-exposed carboxyl region of *Mycoplasma pneumoniae* elongation factor Tu interacts with fibronectin. Infect Immun **76:**3116-3123.

199. **Kunert A, Losse J, Gruszin C, Huhn M, Kaendler K, Mikkat S, Volke D, Hoffmann R, Jokiranta TS, Seeberger H, Moellmann U, Hellwage J, Zipfel PF.** 2007. Immune evasion of the human pathogen *Pseudomonas aeruginosa*: elongation factor Tuf is a factor H and plasminogen binding protein. J Immunol **179:**2979-2988.

200. **Wolff DG, Castiblanco-Valencia MM, Abe CM, Monaris D, Morais ZM, Souza GO, Vasconcellos SA, Isaac L, Abreu PA, Barbosa AS.** 2013. Interaction of *Leptospira* elongation factor Tu with plasminogen and complement factor H: a metabolic leptospiral protein with moonlighting activities. PLoS One **8:**e81818.

201. **Mohan S, Hertweck C, Dudda A, Hammerschmidt S, Skerka C, Hallstrom T, Zipfel PF.** 2014. Tuf of *Streptococcus pneumoniae* is a surface displayed human complement regulator binding protein. Molecular immunology **62:**249-264.

202. **Barel M, Hovanessian AG, Meibom K, Briand JP, Dupuis M, Charbit A.** 2008. A novel receptor - ligand pathway for entry of *Francisella tularensis* in monocyte-like THP-1 cells: interaction between surface nucleolin and bacterial elongation factor Tu. BMC Microbiol **8:**145.

203. **Marques MA, Chitale S, Brennan PJ, Pessolani MC.** 1998. Mapping and identification of the major cell wall-associated components of *Mycobacterium leprae*. Infect Immun **66:**2625-2631.

204. **Vipond C, Suker J, Jones C, Tang C, Feavers IM, Wheeler JX.** 2006. Proteomic analysis of a meningococcal outer membrane vesicle vaccine prepared from the group B strain NZ98/254. Proteomics **6:**3400-3413.

205. **Nieves W, Heang J, Asakrah S, Honer zu Bentrup K, Roy CJ, Morici LA.** 2010. Immunospecific responses to bacterial elongation factor Tu during *Burkholderia* infection and immunization. PLoS One **5:**e14361.

206. **Schmeing TM, Voorhees RM, Kelley AC, Gao YG, Murphy FVt, Weir JR, Ramakrishnan V.** 2009. The crystal structure of the ribosome bound to EF-Tu and aminoacyl-tRNA. Science **326:**688-694.

207. **Hughes CA, Kodner CB, Johnson RC.** 1992. DNA analysis of *Borrelia burgdorferi* NCH-1, the first northcentral U.S. human Lyme disease isolate. J Clin Microbiol **30:**698-703.

208. **Pal U, Yang X, Chen M, Bockenstedt LK, Anderson JF, Flavell RA, Norgard MV, Fikrig E.** 2004. OspC facilitates *Borrelia burgdorferi* invasion of *Ixodes scapularis* salivary glands. J Clin Invest **113:**220-230.

209. **Kawabata H, Norris SJ, Watanabe H.** 2004. BBE02 disruption mutants of *Borrelia burgdorferi* B31 have a highly transformable, infectious phenotype. Infect Immun **72:**7147-7154.

210. **Yang XF, Pal U, Alani SM, Fikrig E, Norgard MV.** 2004. Essential role for OspA/B in the life cycle of the Lyme disease spirochete. J Exp Med **199:**641-648.

211. **Ye M, Zhang JJ, Fang X, Lawlis GB, Troxell B, Zhou Y, Gomelsky M, Lou Y, Yang XF.** 2014. DhhP, a cyclic di-AMP phosphodiesterase of *Borrelia burgdorferi*, is essential for cell growth and virulence. Infect Immun **82:**1840-1849.

212. **Yang X, Goldberg MS, Popova TG, Schoeler GB, Wikel SK, Hagman KE, Norgard MV.** 2000. Interdependence of environmental factors influencing reciprocal patterns of gene expression in virulent *Borrelia burgdorferi*. Mol Microbiol **37:**1470-1479.

213. **Fikrig E, Barthold SW, Sun W, Feng W, Telford SR, 3rd, Flavell RA.** 1997. *Borrelia burgdorferi* P35 and P37 proteins, expressed *in vivo*, elicit protective immunity. Immunity **6:**531-539.

214. **Cox DL, Akins DR, Bourell KW, Lahdenne P, Norgard MV, Radolf JD.** 1996. Limited surface exposure of *Borrelia burgdorferi* outer surface lipoproteins. Proc Natl Acad Sci U S A **93:**7973-7978.

215. **Sadziene A, Thomas DD, Barbour AG.** 1995. *Borrelia burgdorferi* mutant lacking Osp: biological and immunological characterization. Infect Immun **63:**1573-1580.

216. **Brooks CS, Vuppala SR, Jett AM, Akins DR.** 2006. Identification of *Borrelia burgdorferi* outer surface proteins. Infect Immun **74:**296-304.

217. **Xu H, He M, He JJ, Yang XF.** 2010. Role of the surface lipoprotein BBA07 in the enzootic cycle of *Borrelia burgdorferi*. Infect Immun **78:**2910-2918.

218. **Yang X, Lenhart TR, Kariu T, Anguita J, Akins DR, Pal U.** 2010. Characterization of unique regions of *Borrelia burgdorferi* surface-located membrane protein 1. Infect Immun **78:**4477-4487.

219. **Skare JT, Shang ES, Foley DM, Blanco DR, Champion CI, Mirzabekov T, Sokolov Y, Kagan BL, Miller JN, Lovett MA.** 1995. Virulent strain associated outer membrane proteins of *Borrelia burgdorferi*. J Clin Invest **96:**2380-2392.

220. **Yang X, Promnares K, Qin J, He M, Shroder DY, Kariu T, Wang Y, Pal U.** 2011. Characterization of multiprotein complexes of the *Borrelia burgdorferi* outer membrane vesicles. Journal of proteome research **10:**4556-4566.

221. **Zhou H, Imrich A, Kobzik L.** 2008. Characterization of immortalized MARCO and SR-AI/II-deficient murine alveolar macrophage cell lines. Particle and fibre toxicology **5:**7.

222. **Daigneault M, Preston JA, Marriott HM, Whyte MK, Dockrell DH.** 2010. The identification of markers of macrophage differentiation in PMA-stimulated THP-1 cells and monocyte-derived macrophages. PLoS One **5:**e8668.

223. **Birnie GD.** 1988. The HL60 cell line: a model system for studying human myeloid cell differentiation. The British journal of cancer. Supplement **9:**41-45.

224. **Serezani CH, Perrela JH, Russo M, Peters-Golden M, Jancar S.** 2006. Leukotrienes are essential for the control of *Leishmania amazonensis* infection and contribute to strain variation in susceptibility. J Immunol **177:**3201-3208.

225. **Welte T, Zhang SS, Wang T, Zhang Z, Hesslein DG, Yin Z, Kano A, Iwamoto Y, Li E, Craft JE, Bothwell AL, Fikrig E, Koni PA, Flavell RA, Fu XY.** 2003. STAT3 deletion during hematopoiesis causes Crohn's disease-like pathogenesis and lethality: a critical role of STAT3 in innate immunity. Proc Natl Acad Sci U S A **100:**1879-1884.

226. **Kano A, Wolfgang MJ, Gao Q, Jacoby J, Chai GX, Hansen W, Iwamoto Y, Pober JS, Flavell RA, Fu XY.** 2003. Endothelial cells require STAT3 for protection against endotoxin-induced inflammation. J Exp Med **198:**1517-1525.

227. **Saylor CA, Dadachova E, Casadevall A.** 2010. Murine IgG1 and IgG3 isotype switch variants promote phagocytosis of *Cryptococcus neoformans* through different receptors. J Immunol **184:**336-343.

228. **Aronoff DM, Canetti C, Peters-Golden M.** 2004. Prostaglandin E2 inhibits alveolar macrophage phagocytosis through an E-prostanoid 2 receptor-mediated increase in intracellular cyclic AMP. J Immunol **173:**559-565.

229. **Mishalian I, Ordan M, Peled A, Maly A, Eichenbaum MB, Ravins M, Aychek T, Jung S, Hanski E.** 2011. Recruited macrophages control dissemination of group A *Streptococcus* from infected soft tissues. J Immunol **187:**6022-6031.

230. **Daley JM, Thomay AA, Connolly MD, Reichner JS, Albina JE.** 2008. Use of Ly6G-specific monoclonal antibody to deplete neutrophils in mice. J Leukoc Biol **83:**64-70.

231. **Shi C, Hohl TM, Leiner I, Equinda MJ, Fan X, Pamer EG.** 2011. Ly6G^{+} neutrophils are dispensable for defense against systemic *Listeria monocytogenes* infection. J Immunol **187:**5293-5298.

232. **Morrison TB, Ma Y, Weis JH, Weis JJ.** 1999. Rapid and sensitive quantification of *Borrelia burgdorferi*-infected mouse tissues by continuous fluorescent monitoring of PCR. J Clin Microbiol **37:**987-992.

233. **Xu H, He M, Pang X, Xu ZC, Piesman J, Yang XF.** 2010. Characterization of the highly regulated antigen BBA05 in the enzootic cycle of *Borrelia burgdorferi*. Infect Immun **78:**100-107.

234. **Serezani CH, Lewis C, Jancar S, Peters-Golden M.** 2011. Leukotriene B4 amplifies NF-kappaB activation in mouse macrophages by reducing SOCS1 inhibition of MyD88 expression. J Clin Invest **121:**671-682.

235. **Austyn JM, Gordon S.** 1981. F4/80, a monoclonal antibody directed specifically against the mouse macrophage. Eur J Immunol **11:**805-815.

236. **Wang H, Peters T, Kess D, Sindrilaru A, Oreshkova T, Van Rooijen N, Stratis A, Renkl AC, Sunderkotter C, Wlaschek M, Haase I, Scharffetter-Kochanek K.** 2006. Activated macrophages are essential in a murine model for T cell-mediated chronic psoriasiform skin inflammation. J Clin Invest **116:**2105-2114.

237. **Barthold SW, Hodzic E, Tunev S, Feng S.** 2006. Antibody-mediated disease remission in the mouse model of Lyme borreliosis. Infect Immun **74:**4817-4825.

238. **Aberer E, Duray PH.** 1991. Morphology of *Borrelia burgdorferi*: structural patterns of cultured *Borrelia* in relation to staining methods. J Clin Microbiol **29:**764-772.

239. **Shultz LD, Lyons BL, Burzenski LM, Gott B, Chen X, Chaleff S, Kotb M, Gillies SD, King M, Mangada J, Greiner DL, Handgretinger R.** 2005. Human lymphoid and myeloid cell development in NOD/LtSz-scid IL2R gamma null mice engrafted with mobilized human hemopoietic stem cells. J Immunol **174:**6477-6489.

240. **Shultz LD, Schweitzer PA, Christianson SW, Gott B, Schweitzer IB, Tennent B, McKenna S, Mobraaten L, Rajan TV, Greiner DL, Leiter EH.** 1995. Multiple defects in innate and adaptive immunologic function in NOD/LtSz-scid mice. J Immunol **154:**180-191.

241. **Barbour AG.** 1984. Isolation and cultivation of Lyme disease spirochetes. Yale J Biol Med **57:**521-525.

242. **Wherry JC, Schreiber RD, Unanue ER.** 1991. Regulation of gamma interferon production by natural killer cells in scid mice: roles of tumor necrosis factor and bacterial stimuli. Infect Immun **59:**1709-1715.

243. **Petnicki-Ocwieja T, Chung E, Acosta DI, Ramos LT, Shin OS, Ghosh S, Kobzik L, Li X, Hu LT.** 2013. TRIF mediates Toll-like receptor 2-dependent inflammatory responses to *Borrelia burgdorferi*. Infect Immun **81:**402-410.

244. **Cinco M, Cini B, Murgia R, Presani G, Prodan M, Perticarari S.** 2001. Evidence of involvement of the mannose receptor in adhesion of *Borrelia burgdorferi* to monocyte/macrophages. Infect Immun **69:**2743-2747.

245. **Pearson AM.** 1996. Scavenger receptors in innate immunity. Curr Opin Immunol **8:**20-28.

246. **Baranova IN, Kurlander R, Bocharov AV, Vishnyakova TG, Chen Z, Remaley AT, Csako G, Patterson AP, Eggerman TL.** 2008. Role of human CD36 in bacterial recognition, phagocytosis, and pathogen-induced JNK-mediated signaling. J Immunol **181:**7147-7156.

247. **Shamsul HM, Hasebe A, Iyori M, Ohtani M, Kiura K, Zhang D, Totsuka Y, Shibata K.** 2010. The Toll-like receptor 2 (TLR2) ligand FSL-1 is internalized via the clathrin-dependent endocytic pathway triggered by CD14 and CD36 but not by TLR2. Immunology **130:**262-272.

248. **Cervantes JL, Dunham-Ems SM, La Vake CJ, Petzke MM, Sahay B, Sellati TJ, Radolf JD, Salazar JC.** 2011. Phagosomal signaling by *Borrelia burgdorferi* in human monocytes involves Toll-like receptor (TLR) 2 and TLR8 cooperativity and TLR8-mediated induction of IFN-beta. Proc Natl Acad Sci U S A **108:**3683-3688.

249. **Araujo FR, Costa CM, Ramos CA, Farias TA, Souza, II, Melo ES, Elisei C, Rosinha GM, Soares CO, Fragoso SP, Fonseca AH.** 2008. IgG and IgG2 antibodies from cattle naturally infected with *Anaplasma marginale* recognize the recombinant vaccine candidate antigens VirB9, VirB10, and elongation factor-Tu. Memorias do Instituto Oswaldo Cruz **103:**186-190.

250. **Bunk S, Susnea I, Rupp J, Summersgill JT, Maass M, Stegmann W, Schrattenholz A, Wendel A, Przybylski M, Hermann C.** 2008. Immunoproteomic identification and serological responses to novel *Chlamydia pneumoniae* antigens that are associated with persistent *C. pneumoniae* infections. J Immunol **180:**5490-5498.

251. **Viale MN, Echeverria-Valencia G, Romasanta P, Mon ML, Fernandez M, Malchiodi E, Romano MI, Gioffre AK, Santangelo Mde L.** 2014. Description of a novel adhesin of *Mycobacterium avium* subsp. *paratuberculosis*. BioMed research international **2014:**729618.

252. **Bunikis J, Barbour AG.** 1999. Access of antibody or trypsin to an integral outer membrane protein (P66) of *Borrelia burgdorferi* is hindered by Osp lipoproteins. Infect Immun **67:**2874-2883.

253. **Noppa L, Ostberg Y, Lavrinovicha M, Bergstrom S.** 2001. P13, an integral membrane protein of *Borrelia burgdorferi*, is C-terminally processed and contains surface-exposed domains. Infect Immun **69:**3323-3334.

254. **Whitmire WM, Garon CF.** 1993. Specific and nonspecific responses of murine B cells to membrane blebs of *Borrelia burgdorferi*. Infect Immun **61:**1460-1467.

255. **Earnhart CG, Rhodes DV, Smith AA, Yang X, Tegels B, Carlyon JA, Pal U, Marconi RT.** 2014. Assessment of the potential contribution of the highly conserved C-terminal motif (C10) of *Borrelia burgdorferi* outer surface protein C in transmission and infectivity. Pathogens and disease **70:**176-184.

256. **Anguita J, Ramamoorthi N, Hovius JW, Das S, Thomas V, Persinski R, Conze D, Askenase PW, Rincon M, Kantor FS, Fikrig E.** 2002. Salp15, an *Ixodes scapularis* salivary protein, inhibits CD4^{+} T cell activation. Immunity **16:**849-859.

257. **Dai J, Wang P, Adusumilli S, Booth CJ, Narasimhan S, Anguita J, Fikrig E.** 2009. Antibodies against a tick protein, Salp15, protect mice from the Lyme disease agent. Cell Host Microbe **6:**482-492.

258. **Hovius JW, de Jong MA, den Dunnen J, Litjens M, Fikrig E, van der Poll T, Gringhuis SI, Geijtenbeek TB.** 2008. Salp15 binding to DC-SIGN inhibits cytokine expression by impairing both nucleosome remodeling and mRNA stabilization. PLoS Pathog **4:**e31.

259. **Troy EB, Lin T, Gao L, Lazinski DW, Camilli A, Norris SJ, Hu LT.** 2013. Understanding barriers to *Borrelia burgdorferi* dissemination during infection using massively parallel sequencing. Infect Immun **81:**2347-2357.

260. **Bosma GC, Fried M, Custer RP, Carroll A, Gibson DM, Bosma MJ.** 1988. Evidence of functional lymphocytes in some (leaky) scid mice. J Exp Med **167:**1016-1033.

261. **Brown CR, Blaho VA, Loiacono CM.** 2004. Treatment of mice with the neutrophil-depleting antibody RB6-8C5 results in early development of experimental Lyme arthritis via the recruitment of Gr-1- polymorphonuclear leukocyte-like cells. Infect Immun **72:**4956-4965.

262. **Xu Q, Seemanapalli SV, Reif KE, Brown CR, Liang FT.** 2007. Increasing the recruitment of neutrophils to the site of infection dramatically attenuates *Borrelia burgdorferi* infectivity. J Immunol **178:**5109-5115.

263. **Van Rooijen N, Sanders A.** 1994. Liposome mediated depletion of macrophages: mechanism of action, preparation of liposomes and applications. Journal of immunological methods **174:**83-93.

264. **Lin HH, Faunce DE, Stacey M, Terajewicz A, Nakamura T, Zhang-Hoover J, Kerley M, Mucenski ML, Gordon S, Stein-Streilein J.** 2005. The macrophage F4/80 receptor is required for the induction of antigen-specific efferent regulatory T cells in peripheral tolerance. J Exp Med **201:**1615-1625.

265. **Birge RB, Ucker DS.** 2008. Innate apoptotic immunity: the calming touch of death. Cell death and differentiation **15:**1096-1102.

266. **Savill J, Dransfield I, Gregory C, Haslett C.** 2002. A blast from the past: clearance of apoptotic cells regulates immune responses. Nat Rev Immunol **2:**965-975.

267. **Linder S, Heimerl C, Fingerle V, Aepfelbacher M, Wilske B.** 2001. Coiling phagocytosis of *Borrelia burgdorferi* by primary human macrophages is controlled by CDC42Hs and Rac1 and involves recruitment of Wiskott-Aldrich syndrome protein and Arp2/3 complex. Infect Immun **69:**1739-1746.

268. **Seemanapalli SV, Xu Q, McShan K, Liang FT.** 2010. Outer surface protein C is a dissemination-facilitating factor of *Borrelia burgdorferi* during mammalian infection. PLoS One **5:**e15830.

269. **Hartiala P, Hytonen J, Suhonen J, Lepparanta O, Tuominen-Gustafsson H, Viljanen MK.** 2008. *Borrelia burgdorferi* inhibits human neutrophil functions. Microbes Infect **10:**60-68.

270. **Yang X, Coleman AS, Anguita J, Pal U.** 2009. A chromosomally encoded virulence factor protects the Lyme disease pathogen against host-adaptive immunity. PLoS Pathog **5:**e1000326.

271. **Montgomery RR, Lusitani D, De Boisfleury Chevance A, Malawista SE.** 2004. Tick saliva reduces adherence and area of human neutrophils. Infect Immun **72:**2989-2994.

272. **Moore MW, Cruz AR, LaVake CJ, Marzo AL, Eggers CH, Salazar JC, Radolf JD.** 2007. Phagocytosis of *Borrelia burgdorferi* and *Treponema pallidum* potentiates innate immune activation and induces gamma interferon production. Infect Immun **75:**2046-2062.

273. **Zhao JF, Chen HH, Ojcius DM, Zhao X, Sun D, Ge YM, Zheng LL, Lin X, Li LJ, Yan J.** 2013. Identification of *Leptospira interrogans* phospholipase C as a novel virulence factor responsible for intracellular free calcium ion elevation during macrophage death. PLoS One **8:**e75652.

274. **Schwende H, Fitzke E, Ambs P, Dieter P.** 1996. Differences in the state of differentiation of THP-1 cells induced by phorbol ester and 1,25-dihydroxyvitamin D3. J Leukoc Biol **59:**555-561.

275. **Hoebe K, Georgel P, Rutschmann S, Du X, Mudd S, Crozat K, Sovath S, Shamel L, Hartung T, Zahringer U, Beutler B.** 2005. CD36 is a sensor of diacylglycerides. Nature **433:**523-527.

276. **Kinjo Y, Tupin E, Wu D, Fujio M, Garcia-Navarro R, Benhnia MR, Zajonc DM, Ben-Menachem G, Ainge GD, Painter GF, Khurana A, Hoebe K, Behar SM, Beutler B, Wilson IA, Tsuji M, Sellati TJ, Wong CH, Kronenberg M.** 2006. Natural killer T cells recognize diacylglycerol antigens from pathogenic bacteria. Nat Immunol **7:**978-986.

277. **Marchal C, Schramm F, Kern A, Luft BJ, Yang X, Schuijt TJ, Hovius JW, Jaulhac B, Boulanger N.** 2011. Antialarmin effect of tick saliva during the transmission of Lyme disease. Infect Immun **79:**774-785.

278. **Schramm F, Kern A, Barthel C, Nadaud S, Meyer N, Jaulhac B, Boulanger N.** 2012. Microarray analyses of inflammation response of human dermal fibroblasts to different strains of *Borrelia burgdorferi* sensu stricto. PLoS One **7:**e40046.

279. **Blevins JS, Hagman KE, Norgard MV.** 2008. Assessment of decorin-binding protein A to the infectivity of *Borrelia burgdorferi* in the murine models of needle and tick infection. BMC Microbiol **8:**82.

280. **Shi Y, Xu Q, Seemanapalli SV, McShan K, Liang FT.** 2006. The *dbpBA* locus of *Borrelia burgdorferi* is not essential for infection of mice. Infect Immun **74:**6509-6512.

281. **Anda P, Gebbia JA, Backenson PB, Coleman JL, Benach JL.** 1996. A glyceraldehyde-3-phosphate dehydrogenase homolog in *Borrelia burgdorferi* and *Borrelia hermsii*. Infect Immun **64:**262-268.

282. **Jwang B, Dewing P, Fikrig E, Flavell RA.** 1995. The hook protein of *Borrelia burgdorferi*, encoded by the *flgE* gene, is serologically recognized in Lyme disease. Clinical and diagnostic laboratory immunology **2:**609-615.

283. **Coleman JL, Benach JL.** 1992. Characterization of antigenic determinants of *Borrelia burgdorferi* shared by other bacteria. J Infect Dis **165:**658-666.

284. **Rossler D, Eiffert H, Jauris-Heipke S, Lehnert G, Preac-Mursic V, Teepe J, Schlott T, Soutschek E, Wilske B.** 1995. Molecular and immunological characterization of the p83/100 protein of various *Borrelia burgdorferi* sensu lato strains. Med Microbiol Immunol **184:**23-32.

285. **Gupta RS, Mahmood S, Adeolu M.** 2013. Erratum: A phylogenomic and molecular signature based approach for characterization of the Phylum Spirochaetes and its major clades: proposal for a taxonomic revision of the phylum. Frontiers in microbiology **4:**322.

286. **Craft JE, Fischer DK, Shimamoto GT, Steere AC.** 1986. Antigens of *Borrelia burgdorferi* recognized during Lyme disease. Appearance of a new immunoglobulin M response and expansion of the immunoglobulin G response late in the illness. J Clin Invest **78:**934-939.

287. **Luft BJ, Dunn JJ, Dattwyler RJ, Gorgone G, Gorevic PD, Schubach WH.** 1993. Cross-reactive antigenic domains of the flagellin protein of *Borrelia burgdorferi*. Res Microbiol **144:**251-257.

288. **Kuehn MJ, Kesty NC.** 2005. Bacterial outer membrane vesicles and the host-pathogen interaction. Genes Dev **19:**2645-2655.

289. **Lee EY, Choi DS, Kim KP, Gho YS.** 2008. Proteomics in gram-negative bacterial outer membrane vesicles. Mass spectrometry reviews **27:**535-555.

290. **Porcella SF, Belland RJ, Judd RC.** 1996. Identification of an EF-Tu protein that is periplasm-associated and processed in *Neisseria gonorrhoeae*. Microbiology **142 (Pt 9):**2481-2489.

291. **Brorson O, Brorson SH.** 1997. Transformation of cystic forms of *Borrelia burgdorferi* to normal, mobile spirochetes. Infection **25:**240-246.

292. **Beermann C, Wunderli-Allenspach H, Groscurth P, Filgueira L.** 2000. Lipoproteins from *Borrelia burgdorferi* applied in liposomes and presented by dendritic cells induce CD8$^+$ T-lymphocytes *in vitro*. Cell Immunol **201:**124-131.

293. **Miklossy J, Kasas S, Zurn AD, McCall S, Yu S, McGeer PL.** 2008. Persisting atypical and cystic forms of *Borrelia burgdorferi* and local inflammation in Lyme neuroborreliosis. Journal of neuroinflammation **5:**40.

294. **Aberer E, Kersten A, Klade H, Poitschek C, Jurecka W.** 1996. Heterogeneity of *Borrelia burgdorferi* in the skin. Am J Dermatopathol **18:**571-579.

295. **Dorward DW, Schwan TG, Garon CF.** 1991. Immune capture and detection of *Borrelia burgdorferi* antigens in urine, blood, or tissues from infected ticks, mice, dogs, and humans. J Clin Microbiol **29:**1162-1170.

296. **Alban PS, Johnson PW, Nelson DR.** 2000. Serum-starvation-induced changes in protein synthesis and morphology of *Borrelia burgdorferi*. Microbiology **146 (Pt 1):**119-127.

297. **Shoberg RJ, Thomas DD.** 1993. Specific adherence of *Borrelia burgdorferi* extracellular vesicles to human endothelial cells in culture. Infect Immun **61:**3892-3900.

298. **van Blijswijk J, Schraml BU, Reis e Sousa C.** 2013. Advantages and limitations of mouse models to deplete dendritic cells. Eur J Immunol **43:**22-26.

299. **Chow A, Brown BD, Merad M.** 2011. Studying the mononuclear phagocyte system in the molecular age. Nat Rev Immunol **11:**788-798.

300. **Harman MW, Dunham-Ems SM, Caimano MJ, Belperron AA, Bockenstedt LK, Fu HC, Radolf JD, Wolgemuth CW.** 2012. The heterogeneous motility of the Lyme disease spirochete in gelatin mimics dissemination through tissue. Proc Natl Acad Sci U S A **109:**3059-3064.

301. **Moriarty TJ, Shi M, Lin YP, Ebady R, Zhou H, Odisho T, Hardy PO, Salman-Dilgimen A, Wu J, Weening EH, Skare JT, Kubes P, Leong J, Chaconas G.** 2012. Vascular binding of a pathogen under shear force through mechanistically distinct sequential interactions with host macromolecules. Mol Microbiol **86:**1116-1131.

302. **Norman MU, Moriarty TJ, Dresser AR, Millen B, Kubes P, Chaconas G.** 2008. Molecular mechanisms involved in vascular interactions of the Lyme disease pathogen in a living host. PLoS Pathog **4:**e1000169.

303. **MacDonald KP, Palmer JS, Cronau S, Seppanen E, Olver S, Raffelt NC, Kuns R, Pettit AR, Clouston A, Wainwright B, Branstetter D, Smith J, Paxton RJ, Cerretti DP, Bonham L, Hill GR, Hume DA.** 2010. An antibody against the colony-stimulating factor 1 receptor depletes the resident subset of monocytes and tissue- and tumor-associated macrophages but does not inhibit inflammation. Blood **116:**3955-3963.

304. **Flannagan RS, Jaumouille V, Grinstein S.** 2012. The cell biology of phagocytosis. Annual review of pathology **7:**61-98.

305. **Febbraio M, Hajjar DP, Silverstein RL.** 2001. CD36: a class B scavenger receptor involved in angiogenesis, atherosclerosis, inflammation, and lipid metabolism. J Clin Invest **108:**785-791.

306. **Silverstein RL, Febbraio M.** 2009. CD36, a scavenger receptor involved in immunity, metabolism, angiogenesis, and behavior. Sci Signal **2(72):**re3.

307. **Garcia RC, Murgia R, Cinco M.** 2005. Complement receptor 3 binds the *Borrelia burgdorferi* outer surface proteins OspA and OspB in an iC3b-independent manner. Infect Immun **73:**6138-6142.

308. **Hochreiter-Hufford A, Ravichandran KS.** 2013. Clearing the dead: apoptotic cell sensing, recognition, engulfment, and digestion. Cold Spring Harbor perspectives in biology **5:**a008748.

309. **Sarantis H, Grinstein S.** 2012. Subversion of phagocytosis for pathogen survival. Cell Host Microbe **12:**419-431.

310. **Nestle FO, Di Meglio P, Qin JZ, Nickoloff BJ.** 2009. Skin immune sentinels in health and disease. Nat Rev Immunol **9:**679-691.

311. **Yu H, Pardoll D, Jove R.** 2009. STATs in cancer inflammation and immunity: a leading role for STAT3. Nat Rev Cancer **9:**798-809.

312. **Camporeale A, Marino F, Papageorgiou A, Carai P, Fornero S, Fletcher S, Page BD, Gunning P, Forni M, Chiarle R, Morello M, Jensen O, Levi R, Heymans S, Poli V.** 2013. STAT3 activity is necessary and sufficient for the development of immune-mediated myocarditis in mice and promotes progression to dilated cardiomyopathy. EMBO molecular medicine **5:**572-590.

313. **Harris TJ, Grosso JF, Yen HR, Xin H, Kortylewski M, Albesiano E, Hipkiss EL, Getnet D, Goldberg MV, Maris CH, Housseau F, Yu H, Pardoll DM, Drake CG.** 2007. Cutting edge: An *in vivo* requirement for STAT3 signaling in TH17 development and TH17-dependent autoimmunity. J Immunol **179:**4313-4317.

314. **Krause A, Scaletta N, Ji JD, Ivashkiv LB.** 2002. Rheumatoid arthritis synoviocyte survival is dependent on Stat3. J Immunol **169:**6610-6616.

315. **Behera AK, Thorpe CM, Kidder JM, Smith W, Hildebrand E, Hu LT.** 2004. *Borrelia burgdorferi*-induced expression of matrix metalloproteinases from human chondrocytes requires mitogen-activated protein kinase and Janus kinase/signal transducer and activator of transcription signaling pathways. Infect Immun **72:**2864-2871.

316. **Zegarra-Moro OL, Vinasco J, Braga WU, Moro MH.** 2007. STAT3 mediates the initiation and progression of Lyme carditis. In Proceedings of The American Association of Immunologists Annual Meeting 2007. J Immunol**:**178. 96.29.

317. **Seiler KP, Vavrin Z, Eichwald E, Hibbs JB, Jr., Weis JJ.** 1995. Nitric oxide production during murine Lyme disease: lack of involvement in host resistance or pathology. Infect Immun **63:**3886-3895.

318. **Johnson RM, Kerr MS, Slaven JE.** 2012. Plac8-dependent and inducible NO synthase-dependent mechanisms clear Chlamydia muridarum infections from the genital tract. J Immunol **188:**1896-1904.

319. **Ledford JG, Kovarova M, Koller BH.** 2007. Impaired host defense in mice lacking ONZIN. J Immunol **178:**5132-5143.

<div align="center">

CURRICULUM VITAE

Sebastian Eduardo Carrasco

</div>

Education

Universidad Mayor, Santiago, Chile	DVM, Doctor of Veterinary Medicine 1995-2002
	BVS, Bachelor in Veterinary Sciences 1995-2000
University of California, Davis	MPVM, Master in Preventive Veterinary Medicine 2006-2007
University of California, Davis	M.S., Master in Comparative Pathology 2007-2012
Indiana University	Ph.D., Microbiology and Immunology 2011-2015

Honors, Awards, Fellowships

Honors and Awards:

2014	American Association of Immunologist Young Investigator Award. Best abstract in workshop Immune response to bacteria and parasites I. 43rd Annual Autumn Immunology Conference, Chicago, Illinois.
2014	John Wallace Diversity Scholarship. 43rd Annual Meeting of the Autumn Immunology Conference, Chicago, Illinois.
2011	Travel award, 18th Annual Midwest Microbial Pathogenesis Conference, University of Michigan, Ann Arbor, Michigan.
2008	Carl Storm Underrepresented Minority Travel award, Gordon Research Conference on Ocean and Human Health, Tilton, New Hampshire.
2007-08	Veterinary Graduate Academic Program (VGAP) Award, School of Veterinary Medicine, UC Davis, Davis, California.
2006	Travel and training course award, Fourth Biennial Foreign Animal Infectious Diseases Training course, School of Veterinary Medicine, The University of Wisconsin-Madison and the United States Department of Agriculture-APHIS-VS-PDS, Madison, Wisconsin.
1998-99	Vice-president of Veterinary Student Association, School of Veterinary Medicine, Universidad Mayor, Santiago, Chile.

Fellowships:

2015	President's Diversity Dissertation Year Fellowship Indiana University; and, Indiana University - Purdue University Indianapolis (IUPUI).
2013-14	National Institute of Health (NIH) T32 Fellowship in Immunology and Infectious Diseases, Department of Microbiology and Immunology, Indiana University School of Medicine
2008-10	Graduate Group of Comparative Pathology Student Block Fellowship, UC Davis.

2008-09   Graduate Student Fellowship. Pathogen Pollution Surveillance Using Marine Mammals as Sentinels of Oceanic Change. NOAA-UCAR Ocean and Human Health Initiative Graduate Trainee Program, UC Davis.

2008-09   Karen C. Drayer Wildlife Health Center Fellowship, UC Davis.

2007   Department of Homeland Security Scholarship, UC Davis.

Presentations

Carrasco SE, Troxell B, Yang Y, Brandt SL, Serezani CH, Yang XY. Outer surface lipoprotein OspC protects *Borrelia burgdorferi* from macrophage phagocytosis", **Oral and Poster presentation**, 43rd Annual Meeting of the Autumn Immunology Conference, Chicago, IL, Nov 21-24, 2014.

Brandt S, Wang S, Blank S, Delafield N, **Carrasco SE**, Serezani CH. "Topical leukotriene B4 improves methicillin-resistant *Staphylococcus aureus* skin infection", 43rd Annual Meeting of the Autumn Immunology Conference, Chicago, IL, Nov 21-24, 2014.

Carrasco SE. "*Borrelia burgdorferi* Outer Surface Protein OspC impairs macrophage phagocytosis". **Oral Presentation**, Research in progress seminar series at the Department of Microbiology and Immunology, Indiana University - School of Medicine, September 16, 2014.

Carrasco SE, Troxell B, Yang Y, Brandt SL, Sandusky GE, Condon KW, Serezani CH, Yang XY. The Role of OspC of *Borrelia burgdorferi* in Avoiding Clearance by Innate Host Factors", Poster presentation, 114th General meeting American Society of Microbiology, Boston, MA, May 17-20, 2014.

Brandt S, Wang S, Delafield N, **Carrasco SE**, Serezani CH. "Leukotriene B4 controls methicillin-resistant *Staphylococcus aureus* skin infection". Poster presentation, American Association of Immunologists Annual Meeting, Pittsburgh, PA, May 2-6, 2014.

Carrasco SE, Troxell B, Yang Y, Sandusky GE, Condon KW, Serezani CH, Yang XY. Examining the role of *Borrelia burgdorferi* outer surface protein C in avoiding clearance by murine innate immune factors". Poster presentation. The Indiana University School of Medicine Biomedical Gateway Program - campus visit. February 27, 2014.

Carrasco SE, Troxell B, Yang Y, Sandusky GE, Condon KW, Serezani CH, Yang XY. Examining the role of *Borrelia burgdorferi* outer surface protein C in avoiding clearance by murine innate immune factors", Poster presentation, Gordon Research Conference in Biology of Spirochetes, Ventura, California, January 19-24, 2014.

Carrasco SE, Troxell B, Yang Y, Sandusky GE, Condon KW, Serezani CH, Yang XY. Examining the role of *Borrelia burgdorferi* outer surface protein C in avoiding clearance by murine innate immune factors". Poster presentation. The Indiana University School of Medicine Biomedical Gateway Program - campus visit. January 30, 2014.

Carrasco SE. "Examining the role of *Borrelia burgdorferi* outer surface protein C in avoiding clearance by innate host factors". **Oral Presentation**, Research in progress seminar series at the Department of Microbiology and Immunology, Indiana University - School of Medicine, November 26, 2013.

Carrasco SE. "Spirochete - host interaction: Roles of EF-TU and OspC during Lyme borreliosis". **Oral Presentation**, Research in progress seminar series at the Department of Microbiology and Immunology, Indiana University - School of Medicine, April 2, 2013.

Carrasco SE. "Role of the outer surface lipoprotein C in the establishment of infection caused by the Lyme disease spirochete". **Oral Presentation**, Research in progress seminar series at the Department of Microbiology and Immunology, Indiana University - School of Medicine, March 20, 2012.

Carrasco SE, He M, Troxell B, Yang Y, Yang XF. Characterization of surface localized enolase and elongation factor-tu (EF-TU) in the enzootic cycle of Lyme disease spirochete. Poster Presentation. Gordon research conference in Biology of Spirochetes, Ventura, CA, January, 2012.

Carrasco SE, He M, Troxell B, Yang Y, Yang XF. Characterization of surface localized enolase and elongation factor-tu (EF-TU) in the enzootic cycle of Lyme disease spirochete. Poster Presentation. 18th Annual Midwest Microbial Pathogenesis Conference, University of Michigan, Ann Arbor, MI, October, 2011.

Carrasco SE, Chomel BB, Maggi RG, Breitschwerdt EB, Gill VA, Byrne BA, Kasten RW, Burek KA, Miller MA, Goldstein T. Mazet JK. Role of infectious diseases in mortality of Alaskan sea otters (*Enhydra lutris kenyoni*). **Oral Presentation**. NOAA/Oceans and Human Health Initiative Trainees meeting, The Marine Mammal Center, Sausalito, CA, February, 2010.

Carrasco SE, Chomel BB, Maggi RG, Breitschwerdt EB, Gill VA, Byrne BA, Kasten RW, Burek KA, Miller MA, Goldstein T. Mazet JK. Role of infectious diseases in mortality of Alaskan sea otters (*Enhydra lutris kenyoni*). **Oral Presentation**. NOAA/Oceans and Human Health Initiative principal investigators meeting Seattle, WA, October, 2009.

Carrasco SE, Chomel BB, Maggi RG, Breitschwerdt EB, Gill VA, Byrne BA, Kasten RW, Burek KA, Miller MA, Goldstein T. Mazet JK. Identify zoonotic diseases of northern sea otter in the Pacific Northwest and Alaska. **Oral Presentation**. NOAA/Oceans and Human Health Initiative Trainees meeting, NOAA West Coast Center**,** Seattle, WA, October, 2008.

Carrasco SE, Chomel BB, Maggi RG, Breitschwerdt EB, Gill VA, Byrne BA, Kasten RW, Burek KA, Miller MA, Goldstein T. Mazet JK. Investigation of infectious diseases in northern sea otters (*Enhydra lutris kenyoni*) in Alaska. Invited **Oral Presentation** opened to the general public, The U.S. Fish and Wildlife Service's Marine Mammals Management Division, Island and Ocean Visitor Center, Homer, AK, August, 2008.

Carrasco SE, Burek KA, Oaks JL, Beckmen KB, Davis MA, Baker KNK, Mazet JK. Potential zoonotic bacteria in endangered Steller sea lions (*Eumetopias jubatus*) in Alaska. Poster Presentation. Gordon research conference in Oceans and Human Health / graduate research seminar in Oceans and Human Health. New London, NH, July, 2008.

Carrasco SE, Highland MA, Pesavento PA. Hypereosinophilic paraneoplastic syndrome secondary to intestinal mast cell tumor in a 10 year old cat. **Oral Presentation**. CL Davis Foundation 25th Annual West Coast Subdivision Meeting. Pacific Grove, CA, April, 2008.

Carrasco SE, Chomel BB, Mazet JK, Maggi RG, Kasten RW, Byrne BA, Miller MA, , Gill VA, Doroff AM, Burek KA, Breitschwerdt EB. Investigation of *Bartonella* spp. in northern sea otters (*Enhydra lutris kenyoni*) with vegetative valvular endocarditis in Alaska. Poster Presentation. 5th International conference on rickettsiae and ricketsial diseases. Marseilles, France, May, 2008.

Publications

Carrasco SE, Troxell B, Yang Y, Brandt SL, Li H, Sandusky GE, Condon KW, Serezani CH, Yang XY. Outer surface protein OspC is an anti-phagocytic factor that protects *Borrelia burgdorferi* from phagocytosis by macrophages. **Infection and Immunity** (*Submitted*).

Carrasco SE, Troxell B, Yang Y, Yang X, Pal U, Yang XY. *Borrelia burgdorferi* elongation factor EF-Tu is an immunogenic antigen during Lyme borreliosis. **Emerging Microbes and Infection** (*In review*).

Hu S[#], **Carrasco SE**[#], Sandusky GE, Roberts CS, Derbigny WA**.** TLR3 elicits a protective immune response to genital tract infections with *Chlamydia muridarum.* **Journal of Immunology** (*In review,* [#] equal contribution).

Ye M, Caimano M, Yang Y, Zhang JJ, **Carrasco SE**, Lou Y, Yang XF. Cyclic di-AMP is essential for the mammalian infection of *Borrelia burgdorferi* (*In preparation*).

Zhang JJ, Corona A, Yang Y, Li H, Troxell, B, **Carrasco SE**, He M, Schwartz I, Yang XF*. Cyclic di-GMP regulates glycerol uptake and metabolism through the effector PlzA and the repressor BadR in *Borrelia burgdorferi* (*In preparation*).

Troxell B, Ye M, Yang Y, **Carrasco SE**, Lou Y, Yang XF. Manganese and Zinc Regulate Virulence Determinants in *Borrelia burgdorferi*. **Infection and Immunity**, 2013; 81:8 2743-2752.

Carrasco SE*, Chomel BB, Gill VA, Doroff AM, Miller MA, Burek KA, Kasten RW, Byrne BA, Goldstein T, Mazet JK. Exposure to *Bartonella* spp. is common in Alaskan Sea Otters. **Vector-Borne and Zoonotic Diseases**. 2014; 14(12):831-7. PMID: 25514118 PMCID: PMC4270147.

Carrasco SE*, Chomel BB, Kasten RW, Maggi RG, Breitschwerdt EB, Byrne BA, Gill VA, Burek KA, Miller MA, Goldstein T, Mazet JK. Novel *Bartonella* Infection in Northern and Southern Sea Otters (*Enhydra lutris kenyoni* and *Enhydra lutris nereis*), **Veterinary Microbiology**, 2014; 170 (3-4):325-34. PMID: 24629902.

Carrasco SE*, Burek KA, Beckmen KB, Oaks JL, Davis MA, Baker KNK, Mazet JK. Aerobic oral and rectal bacteria of free-ranging Steller sea lion pups and juveniles (*Eumetopias jubatus*) in Alaska, **Journal of Wildlife Diseases**, 2011 47(4), 807-820.

Chomel BB, Kasten RK, Williams C, Wey AC, Henn JB, Maggi R, **Carrasco SE**, Mazet JK, Boulouis HJ, Maillard R, Breitschwerdt EB. *Bartonella* endocarditis: a pathology shared by animal reservoirs and patients. **Annals of the NY Academy of Sciences**, 2009; 1166:120-126.

Carrasco SE, Moreira R. Gonzalez CG, Vidal M. Epidemiologic Basis for the international recognition of Chile as country free of *Brucella melitensis*. Universidad Mayor, Servicio Agricola Ganadero (SAG), Department of Agriculture, Santiago, Chile, **Technical Bulletin**, 2002; 1-30.